

Extracellular matrix regulation of GABA-ergic interneurons and
schizophrenia

Thesis

for the degree of

doctor rerum naturalium (Dr. rer. nat.)

approved by the Faculty of Natural Sciences of
Otto von Guericke University Magdeburg

by Mag. Gabriela Aleksandra Matuszko

born on 30.09.1987 in Łódź (Poland)

Examiner: Prof. Dr. Alexander Dityatev
Prof. MD Sabina Berretta

Submitted on: 16.11.2021

Defended on: 05.09.2022

“A PhD is like a bus trip to Azerbaijan.
It is long, challenging and full of surprises.
But, the most important question
the PhD candidates need to ask themselves is:
do I want to be in Azerbaijan?”

Prof. Leszek Kaczmarek PhD

I Summary

Gabriela Matuszko, M.Sc.

“Extracellular matrix regulation of GABA-ergic interneurons and schizophrenia”

The extracellular matrix (ECM) of the brain plays a crucial role in regulating healthy neuronal development including neuronal migration, maturation and synaptic transmission. Those mechanisms affect higher cortical functions such as cognition, attendance, memory and language and their alteration are associated with numerous brain diseases including schizophrenia. Schizophrenia affects excitatory-inhibitory balance, and gamma oscillation in the brain as well as the special form of ECM - perineuronal net (PNN), which enwraps cell bodies of a subset of GABA-ergic interneurons. Although deficits in both ECM and GABA-ergic interneurons are well documented in schizophrenia, the mechanisms leading to those abnormalities are still ambiguous. Investigating those mechanisms in schizophrenia patients is challenging due to the limited amount of postmortem brain samples, various medication histories and nonhomogeneous background of the disease. Therefore there is a strong need for animal models of schizophrenia. To this aim, I examined ECM alterations and parvalbumin-expressing (PV⁺) GABA-ergic interneurons in two animal models. First, I used the well-established model of rats sub-chronic treated with ketamine. Administration of the glutamate N-methyl-D-aspartate receptor (NMDAR) antagonist ketamine mimics the deficits in excitatory input onto PV⁺ interneurons reported in schizophrenia. The immunohistochemistry analysis of the model shows that the sub-chronic ketamine treatment induces a significant reduction of parvalbumin expression in interneurons and a loss of PNN-coated cells in the medial prefrontal cortex (mPFC) but not in the hippocampal CA1 area. Interestingly sub-chronic treatment with antipsychotics haloperidol and risperidone shows no effects on PNN density in the mPFC. Additionally, the analysis of the CS56⁺ glia-related form of ECM shows no effect of ketamine treatment in the density of the aggregates in mPFC however it induces upregulation of total CS56⁺ ECM. The sub-chronic treatment with ketamine also shows no effect on human natural killer 1 carbohydrate in mPFC. In the second part of the thesis, I developed a mouse model injected with adeno-associated virus encoding shRNA against the hyaluronan and proteoglycan link protein 1 (AAV_HAPLN1_shRNA) to PFC. The AAV_HAPLN1_shRNA treated mice show normal PPI. The immunohistochemistry analysis reveals no effect of AAV_HAPLN1_shRNA treatment on the density of excitatory synapses and surrounding brevican in the neuropil. However, perisomatic analysis of excitatory CAMK2CaMK2 positive cells shows the decreased density of inhibitory puncta after the treatment. Similarly, perisomatic analysis of PV interneurons shows the reduced density of inhibitory puncta after treatment. Altogether those findings suggest that the ketamine-treated rat model of schizophrenia can be used to investigate both PV interneurons and ECM deficits in this disorder. Additionally, the acute HAPLN1 knockdown mice model results imply that the acute local deficits of HAPLN1 protein and followed ECM alteration may lead to inhibitory input deficits on both excitatory and inhibitory cells.

II Zusammenfassung

Gabriela Matuszko, M.Sc.

"Regulierung der extrazellulären Matrix von GABA-ergen Interneuronen und Schizophrenie"

Die extrazelluläre Matrix (EZM, engl. ECM) des Gehirns spielt eine entscheidende Rolle bei der Regulierung der gesunden neuronalen Entwicklung sowie der neuronalen Migration, Reifung und synaptische Übertragung. Diese Mechanismen wirken sich auf höhere kortikale Funktionen wie Kognition, Aufmerksamkeit, Gedächtnis und Sprache aus. Ihre Veränderung wird mit zahlreichen Hirnerkrankungen einschließlich Schizophrenie in Verbindung gebracht. Schizophrenie beeinträchtigt das Gleichgewicht zwischen Erregung und Hemmung und die Gamma-Oszillation im Gehirn sowie die spezielle Form der EZM - das perineuronale Netz (PNN), das die Zellkörper der GABA-ergen Interneuronen umhüllt. Obwohl Defizite sowohl der ECM als auch der GABA-ergen Interneuronen bei Schizophrenie gut dokumentiert sind, sind die Mechanismen, die zu diesen Anomalien führen, noch unklar. Die Untersuchung dieser Mechanismen bei Schizophrenie-Patienten ist aufgrund der begrenzten Anzahl von postmortalen Hirnproben, der unterschiedlichen Medikation und des inhomogenen Krankheitsverlaufs eine Herausforderung. Daher besteht ein großer Bedarf an Tiermodellen für Schizophrenie. Zu diesem Zweck habe ich ECM-Veränderungen und Parvalbumin-exprimierende (PV+) GABA-erge Interneuronen in zwei Tiermodellen untersucht. Zunächst verwendete ich das gut etablierte, mit Ketamin subchronisch behandelte Rattenmodell. Durch die Verwendung von Ketamin, eines Glutamat-N-Methyl-D-Aspartat-Rezeptor (NMDAR)-Antagonisten, wird der bei der Schizophrenie berichtete Defizit in dem erregenden Input auf PV+-Interneuronen imitiert. Die immunhistochemische Analyse des Modells zeigt, dass die subchronische Behandlung mit Ketamin eine signifikante Verringerung der Expression des Parvalbumins in Interneuronen und eine Verringerung der PNN-umhüllte Zellen im medialen präfrontalen Kortex (mPFC) bewirkt. Jedoch nicht aber im CA1-Bereich des Hippocampus. Interessanterweise zeigt die subchronische Behandlung mit den Antipsychotika Haloperidol und Risperidon keine Auswirkungen auf die PNN-Dichte im mPFC. Darüber hinaus zeigt die Analyse der CS56+ Glia-verwandten Form der ECM keine Auswirkungen der Ketamin-Behandlung auf die Dichte der Aggregate im mPFC, führt jedoch zu einer Hochregulierung der gesamten CS56+ ECM. Die subchronische Behandlung mit Ketamin zeigt auch keine Wirkung auf das menschliche natürliche Killer-1-Kohlenhydrat im mPFC. Im zweiten Teil der Arbeit entwickelte ich ein Mausemodell, bei dem adeno-assoziierte Viren, welche die shRNA des Hyaluronan- und Proteoglykan-Link-Proteins 1 (AAV_HAPLN1_shRNA) beinhalten, in das PFC injiziert wurden. Die mit AAV_HAPLN1_shRNA behandelten Mäuse zeigen eine normale Präpulsinhibition (PPI). Die immunhistochemische Analyse zeigt keine Auswirkung der AAV_HAPLN1_shRNA-Behandlung auf die Dichte der exzitatorischen Puncta, die Dichte der exzitatorischen Synapsen und das umgebende Brevikan im Neuropil. Die perisomatische Analyse der exzitatorischen CAMK2CaMK2-positiven Zellen zeigt jedoch, dass die Dichte der

inhibitorischen Puncta nach der Behandlung abnahm. Ebenso zeigt die perisomatische Analyse von PV-Interneuronen eine verringerte Dichte von hemmenden Puncta nach der Behandlung. Insgesamt deuten diese Ergebnisse darauf hin, dass das mit Ketamin behandelte Rattenmodell der Schizophrenie verwendet werden kann, um sowohl PV-Interneuronen als auch ECM-Defizite bei dieser Störung zu untersuchen. Darüber hinaus deuten die Ergebnisse des akuten HAPLN1-Knockdown-Modells bei Mäusen darauf hin, dass die akuten lokalen Defizite des HAPLN1-Proteins und die anschließende Veränderung der ECM zu Defiziten bei der hemmenden Wirkung sowohl auf erregende als auch auf hemmende Zellen führen können.

III List of abbreviations

AAV	adeno-associated virus
ASR	acoustic startle reflex
B3GAT2	b -1,3-glucuronyltransferase 2
BCAN	brevican
BRAL	brain link protein
CaMK2	calcium/calmodulin dependent protein kinase 2
cDNA	complementary DNA
COMT	catechol-O-methyl transferase
CSPG	chondroitin sulfate proteoglycans
CS56	chondroitin sulfate 56
DACS	Dandelion Clock-like Structure
DIV	day <i>in vitro</i>
DMEM	Dulbecco's Modified Eagle Medium
ECM	extracellular matrix
GABA	γ -aminobutyric acid
GAPDH	glyceraldehyde 3-phosphate dehydrogenase
GFP	green fluorescence protein
GWAS	genome-wide association studies
HAPLN1	hyaluronan and proteoglycan link protein 1
HAS 1-3	hyaluronan synthases
HBSS	Hanks' Balanced Salt solution
HEK 293T	human embryonic kidney cell line 293T
hGH	human growth hormone
HLA	human leukocyte antigen
HNK1	human natural killer 1 carbohydrate

IMDM	Iscove's modified Dulbecco's medium
ITR	inverted terminal repeats
MHC	major histocompatibility complex
MCS	multicistronic site
MMP	matrix metalloprotease
ML	mediolateral
mPFC	medial prefrontal cortex
NGS	normal goat serum
NMDAR	N-methyl-D-aspartate receptor
ori	origins of replication
PB	phosphate buffer
PBS	phosphate buffer solution
PEI	polyethylenimine
PFA	perfluoroether
PGK	phosphoglycerate kinase
PFC	prefrontal cortex
PNN	perineuronal net
polyA	polyadenylation
PPI	pre-pulse inhibition
PSD 95	postsynaptic density protein 95
PV	parvalbumin
ROI	region of interest
S100 β	S100 calcium binding protein β
SNP	single nucleotide polymorphism
shRNA	small hairpin RNA
sss	superior sagittal sinus
U6	ubiquitin promotor 6
WFA	Wisteria Floribunda agglutinin

VGAT	vesicular GABA transporter
VGLUT1	vesicular glutamate transport
qPCR	quantitative polymerase chain reaction

IV Contents

I	Summary	I
II	Zusammenfassung	II
III	List of abbreviations	IV
IV	Contents	VII
1	Introduction	1
1.1	Brain plasticity	1
1.2	Neuronal extracellular matrix.....	2
1.2.1	Perineuronal net.....	2
1.2.2	Perisynaptic ECM	5
1.3	Schizophrenia disease	14
1.3.1	Definition and diagnosis.....	14
1.3.2	Genetic origins	14
1.3.3	Environmental factors	17
1.3.4	Neurobiology.....	18
1.3.5	The ECM alteration in schizophrenia.....	26
1.3.6	Treatment - typical and atypical antipsychotics	28
1.4	The ketamine model of schizophrenia.....	29
1.5	The HAPLN1 protein.....	31
2	Objectives of the thesis	33
3	Materials and methods	34
3.1	Animals	34
3.2	Hippocampal primary cell culture	34
3.2.1	Astrocyte conditioned medium	35
3.2.2	AAV infection of hippocampal primary cell culture	35
3.3	AAV preparation and injection.....	36
3.3.1	Construct preparation	36
3.3.2	HEK 293T culture	37
3.3.3	Polyethylenimine Transfection.....	37
3.3.4	Viral particle purification	38
3.3.5	Viral titration	38
3.3.6	Viral validation.....	39
3.3.7	Viral injection.....	40
3.4	Ketamin treatment	42
3.5	Social interaction test	42
3.6	Acoustic startle reflex and pre-pulse inhibition	42
3.7	Immunohistochemistry.....	43

3.7.1	Immunohistochemistry of ketamine-treated rats	43
3.7.2	Immunohistochemistry of AAV-treated mice	45
3.8	Acquisition and image processing	48
3.8.1	Acquisition and image processing of rats samples	48
3.8.2	Acquisition and image processing of AAV treated mice samples	49
3.9	Statistics	50
4	Results	51
4.1	Results for ketamine-treated rats	51
4.1.1	Social interaction test	51
4.1.2	Densities of PV and WFA positive cells in the hippocampal CA1 area of ketamine-treated rats	51
4.1.3	Expression of dendritic ECM in the hippocampal CA1 area of ketamine-treated rats	53
4.1.4	Densities of PV and WFA positive cells in the mPFC of ketamine-treated rats ..	54
4.1.5	Expression of PV, PNN marker and HNK-1 in the mPFC of ketamine-treated rats	56
4.1.6	Dandelion Clock-like Structure (DACs) of glial ECM in the mPFC of ketamine-treated rats	59
4.1.7	PNN fine structure analysis in the mPFC of ketamine-treated rats	60
4.1.8	Densities of PV- and WFA-positive cells in the mPFC of antipsychotics-treated rats	61
4.1.9	Glial ECM in the mPFC of antipsychotic-treated rats	64
4.2	Results for AAV treated mice	64
4.2.1	HAPLN1 shRNA constructs validation	64
4.2.2	Acoustic startle reflex and pre-pulse inhibition	68
4.2.3	Excitatory synaptic puncta and BCAN in the neuropil area	71
4.2.4	Inhibitory presynaptic puncta and BCAN in perisomatic area of CaMK2 positive cells	75
4.2.5	Inhibitory presynaptic puncta and WFA in perisomatic area of PV positive interneurons	77
5	Discussion	80
5.1	Sub-chronic treatment with ketamine induces the reduction of WFA ⁺ cells in rat mPFC	80
5.2	Sub-chronic treatment with haloperidol and risperidone show no effects on the density of WFA ⁺ cells in mPFC	81
5.3	Sub-chronic ketamine treatment show no effect on WFA ⁺ cells in the hippocampal CA1 area	82
5.4	Sub-chronic ketamine treatment induces a significant reduction of parvalbumin expression in mPFC	82
5.5	Sub-chronic ketamine treatment shows no effect on HNK-1 expression in PFC	83

5.6	The decrease of WFA ⁺ cells in PFC is accompanied by the upregulation of total CS56 ⁺ ECM.....	83
5.7	The AAV-induced reduction of HAPLN1 protein in mouse mPFC	84
5.8	Normal PPI in the AAV_HAPLN1_shRNA treated mice	85
5.9	The AAV_HAPLN1_shRNA treatment does not affect neuropil density of excitatory puncta, synapses and surrounding BCAN.....	86
5.10	The inhibitory perisomatic input on CaMK2 ⁺ cells is decreased in mPFC of AAV_HAPLN1_shRNA treated mice.....	86
5.11	The inhibitory perisomatic input on PV ⁺ cells is decreased in mPFC of AAV_HAPLN1_shRNA treated mice.....	87
6	Conclusions	88
	References	i
	Declaration of Honour	xix

1 Introduction

1.1 Brain plasticity

The brain is the most complex part of the human body. To perform its functions, it needs the ability to change and adapt to constantly new challenges in human life. This ability of the nervous system to change its activity in response to intrinsic and extrinsic stimuli is called brain plasticity or neural plasticity and it results in reorganizing the brain structure, functions, or connections (Mateos-Aparicio and Rodríguez-Moreno, 2019).

The origins of research on brain plasticity can be found in the works of Santiago Ramon y Cajal who first defined the neuron as the anatomical, genetic and metabolic unit of the nervous system as well as constructed the cerebral gymnastic hypothesis suggesting that brain capacity can be improved with an increased number of neuronal connections (review by Mateos-Aparicio and Rodríguez-Moreno, 2019). Later works of Eugenio Tanzi and Ernesto Lugaro, suggesting that repetitive learning can strengthen neuronal connections, and Jerzy Konorski and Donald Hebb postulating that morphological changes in synapses are the substrate of learning, brought the focus on synapse formation and maturation in the context of brain plasticity (review by Berlucchi and Buchtel, 2009; Bijoch, Borczyk and Czajkowski, 2020).

During brain development, we can observe periods of increased brain plasticity called critical periods. Those periods occur mostly in an early postnatal age when first experiences shape behaviour and respective brain areas of human and other vertebrae. As a result of these intensive learning phases, a massive number of synapses are formed. During those periods rodents learn how to use their whiskers for navigation, kittens open their eyes and learn how to see and human exposed to language learn it as a native tongue. It is estimated that a human child is born with 2500 synaptic connection per one neuron in the cerebral cortex and, at the age of three, the number increases up to 15 000 synapses per one neuron (Gopnik, Meltzoff and Kuhl, 2001). During critical periods, the brain is fragile and stress factors causing an imbalance of undergoing processes may lead to severe mental disorders including schizophrenia.

Several lines of evidence suggest that GABA-ergic interneurons and the extracellular matrix surrounding them, play important role in the regulation of brain plasticity during critical periods (Dityatev *et al.*, 2007; McRae *et al.*, 2007; Frischknecht *et al.*, 2009). However, the exact

mechanism of these regulations is not completely understood and there is a need for good animal models of the disease to further investigate those mechanisms.

1.2 Neuronal extracellular matrix

Neural extracellular matrix (ECM) is a complex and dynamic structure, which occupies space between cells and blood vessels in the brain. It plays an important role in regulating synaptic functions, such as synaptogenesis, synaptic maturation, plasticity and regulation efficacy of synaptic transmission. Those processes are critical for main brain functions, such as memory and learning. Moreover, alteration of ECM has been reported in numerous mental disorders including schizophrenia (Impagnatiello *et al.*, 1998; Pantazopoulos *et al.*, 2010, 2013). The main components of ECM are hyaluronic acid, chondroitin sulfate proteoglycans (CSPG) such as brevican, aggrecan, versican and neurocan, glycoproteins tenascin - C and Tenascin – R and link proteins: hyaluronan and proteoglycan link protein 1 (HAPLN1) and brain link protein (BRAL). Those components can be organized in the brain in two main forms of ECM: perineuronal net (PNN) and perisynaptic ECM (Yamaguchi, 2000).

1.2.1 Perineuronal net

PNN is a mesh-like form of ECM surrounding somata and proximal dendrites of specific subclasses of neurons, which was first described by Camillo Golgi at the end of the 19th century (Celio *et al.*, 1998). The backbone of the structure is constituted by linear glycosaminoglycan - hyaluronic acid, which is anchored in the cell membrane by three transmembrane hyaluronan synthases (HAS1–3), and linked with N- terminus site of CSPGs. The bound between hyaluronan and CSPGs are stabilized by linked proteins, whereas C-terminus CSPGs are connected with tenascins (Fig. 1).

PNN functions

PNNs form a physical barrier around the cell soma of specific subclasses of neurons including parvalbumin-expressing, fast-spiking, GABA-ergic interneurons, and create separate microenvironment surrounding the perisomatic synapses. The sulphate groups attached to glycosaminoglycan (GAG) side chains of CSPGs and the negatively charged hyaluronic acid, building PNN, generate a highly polyanionic microenvironment. The negatively charged structure might interact with calcium, potassium and sodium ions, providing a local ‘buffer reservoir’ for

physiologically relevant cations (Brückner *et al.*, 1993). Accessibility of physiologically relevant ions might be particularly important for fast-spiking interneurons due to their high activity.

Another important function of PNNs is protection against oxidative stress. A study on Alzheimer's disease patient brain samples has shown that parvalbumin cortical interneurons enwrapped in PNNs are less frequently affected by lipofuscin accumulation, suggesting a PNN protective role against oxidative stress (Morawski *et al.*, 2004). An animal study using mice carrying a genetic redox imbalance has shown an inverse relationship between the robustness of PNNs and the intracellular level of oxidative stress in parvalbumin interneurons. Moreover, the study suggested that PNNs act like a protective shield against oxidative stress but also undergo oxidative stress-induced degradation (Cabungcal *et al.*, 2013). Another animal study using aggrecan-, brevican-, tenascin-R- and HAPLN1-deficient mice has shown that aggrecan, HAPLN1 and tenascin-R are essential PNN components to protect neurons against iron-induced oxidative stress (Suttkus *et al.*, 2014).

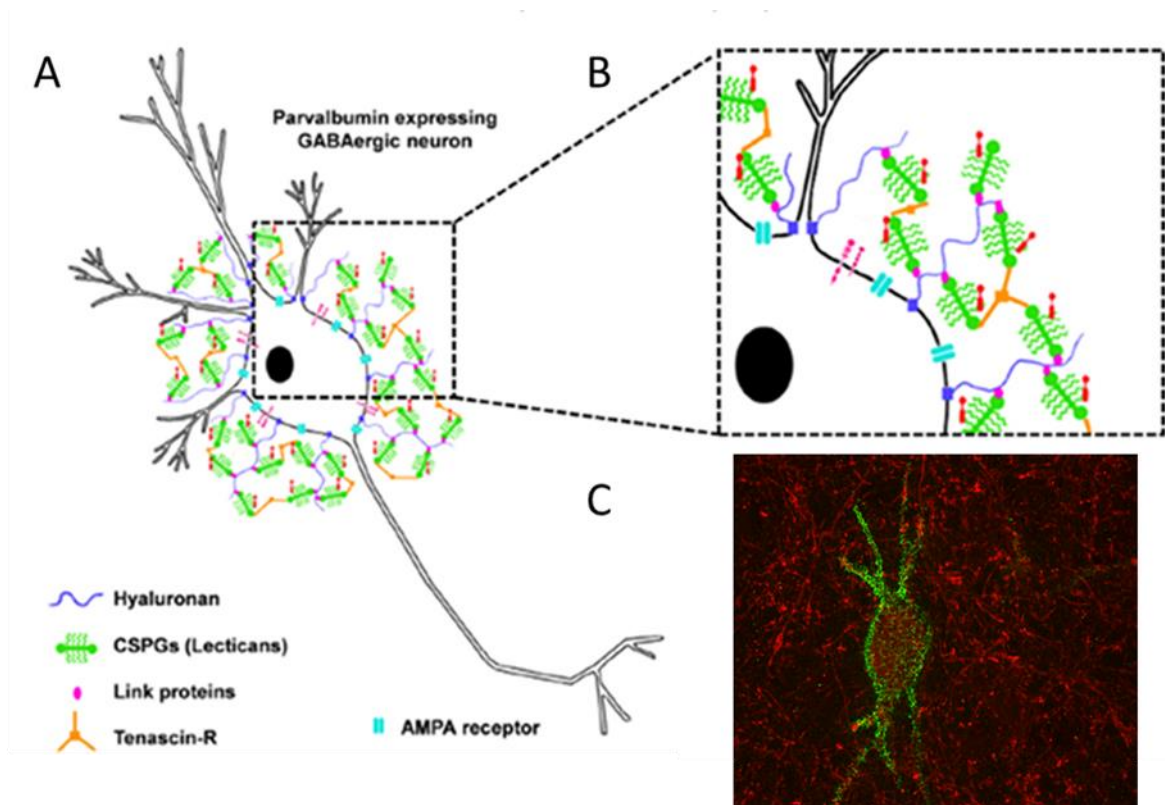


Fig. 1 PNN around parvalbumin-positive interneuron. (A) PNN ensheathing cell body and proximal dendrites of parvalbumin-positive interneuron. (B) Zoom in of PNN structure: backbone hyaluronan represents in dark blue, connected with N - terminus site CSPG shown in green and stabilized by link protein in pink. N-terminus site of CSPGs connected by tenascin - R in orange

(C) Confocal microscopy picture of PNN visualized using Wisteria floribunda agglutinin (WFA) Adapted with modifications from (Soleman *et al.*, 2013).

The PNNs formation coincides with the closure of critical periods sealing the activity-dependent brain plasticity (Carulli *et al.*, 2010) (Mauney *et al.*, 2013)(Rogers *et al.*, 2018). The exact time points of PNNs formation differ in different brain areas supporting the hypothesis that PNNs maturation is related to the closure of critical periods for the acquisition of specific functions (Horii-Hayashi *et al.*, 2015). The animal study done by Pizzorusso and colleagues has shown that enzymatic degradation of PNN by chondroitinase ABC leads to reactivation of ocular dominance plasticity in the adult rat visual cortex (Pizzorusso *et al.*, 2002). Moreover, sensory deprivation by the dark rearing, whisker removal or song deprivation in birds delays PNN formation in respective brain areas (review by Carulli *et al.*, 2010). Altogether, those findings suggest that the formation of PNNs is necessary for the regulation of critical period brain plasticity.

There are several mechanisms involved in executing PNNs regulatory functions of brain plasticity. The CSPGs composition of PNN is changing during a lifetime. Versican and neurocan are highly expressed during development (Yamaguchi, 2000) whereas aggrecan and brevican are major CSPG in the adult brain (Zimmermann and Dours-Zimmermann, 2008). Furthermore, the animal study using adult rats has shown that the majority of PNNs express aggrecan whereas brevican is highly expressed in the neuropil and show brain region differences in expression of those two CSPGs (Dauth *et al.*, 2016).

The structural maturation of PNNs occurs parallel to the closure of the critical period and manifests as a change in sulphation motifs of glycosaminoglycan side chains of CSPGs. The immature PNNs pattern is 6-sulphated glycosaminoglycans reach and was reported stable till post-natal day 21 in the rat visual cortex. Between postnatal day 21 and adulthood, the sulphation pattern changes by decreasing the number of 6-sulphated glycosaminoglycans and increasing the number of 4-sulphated glycosaminoglycans affecting binding properties of CSPGs (Carulli *et al.*, 2010). In addition, tenascins composition is changed over time. Development is characterized by highly expressed tenascin C whereas adult tissue is reach of tenascin R.

Recent animal studies suggest that also geometrical structure of PNN is dynamic and might regulate synapse formation (Arnst *et al.*, 2016).

1.2.2 Perisynaptic ECM

The definition of a chemical synapse is continuously changing reflecting our increasing understanding of the synaptic transmission mechanism. The primary definition includes two components: presynaptic site, sending the signal by releasing neurotransmitters into the synaptic cleft, and postsynaptic site, containing a variety of neurotransmitter receptors that initiate an action potential in a secondary neuron due to excessive ion influx.

This definition was extended by Araque and colleagues to the tripartite synapse, which includes astrocytes in synaptic transmission (Araque *et al.*, 1999). Several lines of evidence showing transient calcium waves in the astrocytic cytoplasm point to an astrocytic excitability mechanism, which can be triggered by neuron-released neurotransmitters and lead to a release of astrocytic gliotransmitters such as glutamate, D-serine, ATP and GABA. The release of gliotransmitters may lead to a modulation of excitatory and inhibitory postsynaptic currents (reviewed by Perea, Navarrete and Araque, 2009). Moreover, astrocytes clear glutamate from the synaptic cleft through glutamate uptake by the astrocytic excitatory amino acid transporter 1 and 2 proteins (EAAT1,2). Then, it is converted to glutamine, which is further relocated to the presynaptic neuron allowing a fast recycling of glutamate and protecting against its accumulation-dependent toxic effect (Schousboe *et al.*, 2014).

Several studies reported that extracellular matrix molecules secreted by neurons and astrocytes regulate synaptic functions in multiple manners (Dityatev and Schachner, 2003; Galtrey and Fawcett, 2007; Faissner *et al.*, 2010; Gundelfinger *et al.*, 2010). Based on those reports a new synapse model was theorized – the tetrapartite synapse (Dityatev and Rusakov, 2011). This definition includes presynaptic site, postsynaptic site, astrocyte end-foot and ECM molecules and describes multiple interactions between those synaptic components.

ECM regulation of synaptic formation, maturation and plasticity

The tetrapartite synapse gives a better overlook of the dynamic environment surrounding synapses. Several ECM proteins support their formation, maturation and stabilization (review by Ferrer-Ferrer and Dityatev, 2018) and the alteration of the expression levels of those proteins may lead to synaptic deficits associated with schizophrenia disorder.

Thrombospondins

Thrombospondins are part of these ECM proteins and are secreted by astrocytes. They are glycoproteins with an oligomeric and multidomain structure that allows them to bind to numerous receptors and regulate cell-cell and cell-matrix interactions. Among them, trimeric thrombospondin 1 and 2 (TSP 1/2) trigger the formation of glutamatergic synapses by the activation of the postsynaptic neuronal receptor $\alpha 2\delta$ -1 (Cacna2d1) via their type 2 EGF-like repeats (Christopherson *et al.*, 2005; Eroglu *et al.*, 2009). Both *in vitro* studies using purified rat retinal ganglion cell culture from wild type rats and animal studies using thrombospondin 1 and 2 knockout mice, have shown a strong reduction of excitatory synapse density in absence of thrombospondin 1 and 2. Although thrombospondin-induced synapses are presynaptic active, they are primarily postsynaptic silent due to the lack of postsynaptic AMPA receptors and require a second astrocytic signal for functional maturation (Christopherson *et al.*, 2005). Moreover, two single nucleotide polymorphisms in thrombospondin 1 gene rs2228261 (TT) and rs2292305 (GG) were associated with schizophrenia risk in the Korean population and the SNP rs2292305 (GG) showed a weak association with poor concentration symptoms in schizophrenic patients (Park *et al.*, 2012). Additionally, human postmortem studies have shown a reduction in the expression of thrombospondin mRNA in the anterior cingulate gyrus of schizophrenic patients (Katsel *et al.*, 2011). Altogether, these data suggest that thrombospondins may play a role in schizophrenia pathophysiology related to excitatory synapse formation.

Pentraxins

Another group of proteins related to ECM regulation of synapses are pentraxins. The neuronal pentraxins family includes calcium-dependent lectins such as neuronal pentraxin 1, neuronal pentraxin 2 (known also as neuronal activity-regulated pentraxin Narp) and neuronal pentraxin receptor. The presynaptic released neuronal pentraxins and transmembrane neuronal pentraxin receptor co-aggregate with the GluA4 subunit-containing AMPA receptor. The neuronal pentraxin 1 and neuronal pentraxin receptor recruit AMPA receptor to the synaptic cleft in both native and artificial synapses and its knock-down results in reduced clustering ability for GluA4 AMPA receptor (Sia *et al.*, 2007).

The neuronal pentraxin 2 clusters GluA4 subunit containing-AMPA receptor in excitatory synapses on parvalbumin-expressing interneurons and potentiates excitatory synapses in these neurons. Interestingly, the extracellular perineuronal nets enhance pentraxin 2 accumulation in those synapses (Chang *et al.*, 2010). On the contrary, the matrix metalloproteinase tumour

necrosis factor- α converting enzyme (TACE) cuts the neuronal pentraxin receptor, triggering endocytosis of connected AMPA receptors and leading to a downregulation of those synapses (Cho *et al.*, 2008).

Additionally, a recent meta-analysis study performed by Manchia and colleagues shows that neuronal pentraxin 2 gene expression is consistently downregulated in hiPSC-derived neurons and post-mortem brain from schizophrenic patients (Manchia *et al.*, 2017).

Cerebellins

Cerebellins are extracellular glycoproteins that organize excitatory synapses. Four types of cerebellins are expressed (Cbln 1-4) in vertebrae brains. Three types of them (Cbln1, Cbln2 and Cbln4) form homohexamers, while Cbln3 needs the presence of Cbln1 to form a functional protein. The N-terminal stalk of Cbln1 and Cbln2 binds strongly to α and β neuroligins, whereas Cbln4 binds strongly to deleted in colorectal cancer (DCC) protein. The C-terminal C1q-domain of Cbln1, Cbln2 and Cbln4 binds to glutamate receptor-related proteins GluD1 and GluD2. These three components synaptic bridge seems to regulate synapse formation.

Animal studies using Cbln1 knockout (KO) animals have shown the decreased density of excitatory synapses in the cerebellum and the increased density of excitatory synapses on thalamic axons projecting to the striatum. Moreover, animals lacking Cbln1 show impairment in motor skills as well as in hippocampal-dependent learning. A recent animal study using multiple cerebellins knockouts shows that different cerebellins act as synaptic organizers in specific subsets of neurons and likely contribute to many different brain functions. The study also suggests a cerebellins role in the specification and long-term synapse maintenance rather than in synapse formation. The Cbln1/2 double KO mice show no alteration in synapse density in young mice hippocampus but have a 50% reduction in excitatory synapses in the CA1 hippocampal area and in the dentate gyrus of ageing mice. Furthermore, Cbln1/2 ablation results in a delayed loss of synapses also in the striatum and retrosplenial cortex (Seigneur and Südhof, 2018).

Reelin

Reelin is an extracellular glycoprotein that regulates cell migration and glutamatergic synapse maturation. During early brain development, reelin regulates neuronal guidance through binding to very-low-density lipoprotein receptor (VLDLR) and apolipoprotein E receptor type 2 (ApoER2). Animal studies using reelin KO mice have shown disrupted architecture of cortical

layers and distorted dendritic arborisation in many brain areas, including cerebral cortex, cerebellar cortex and hippocampus (Lambert de Rouvroit and Goffinet, 1998). Additionally, mice with double KO of reelin binding partners VLDLR and ApoER2 show the same architecture distortion pattern (Trommsdorff *et al.*, 1999).

During development, GABAergic interneurons secrete reelin into extracellular space affecting neighbouring cortical pyramidal cells. The released reelin binds to the ApoER2 receptor, which leads to phosphorylation of Dab 1 protein and activation of PI3K kinase and, in consequence, promotes neurites outgrowth. Animal studies have shown that both acute and chronic application of reelin can enhance this process in mouse cortex. The reelin protein also supports LTP via ApoER2 and VLDR-mediated phosphorylation of GluN2-containing NMDA receptor, which enhances their conductance. Moreover, the developmental switch of NMDA receptor subunits from high conductance GluN2B to low conductance GluN2A can be blocked by reelin application.

Reelin is also strongly associated with schizophrenia. A 50% reduction of its mRNA and protein levels was found in several brain areas of schizophrenia patients, including PFC and hippocampus (Impagnatiello *et al.*, 1998; Fatemi *et al.*, 1999; Guidotti *et al.*, 2000). The reelin deficits were proposed to be mediated as a result of methylation of the reelin promotor induced by prenatal stress (Costa *et al.*, 2002). Moreover, human reelin null patients have shown lissencephaly associated with a profound cognition deficit, a loss of muscle tone and a radiologically evident brain deformation that is less severe but still abundantly present in heterozygous RELN persons (Hong *et al.*, 2000).

Matrix metalloproteinases

The matrix metalloproteinases (MMPs) are a large group of over twenty proteins, which cleave components of ECM, cell adhesion molecules, cytokines and growth factors. Their calcium-dependent-multilevel-regulated activity contributes to the structural and functional reorganization of excitatory synapses and modulates immune responses (review by Beroun *et al.*, 2019). The MMPs are composed of N-terminal signal peptide followed by propeptide, a catalytic domain and in most cases hinge region and hemopexin domain on the C-terminal end of the protease. The sixteen of MMPs expressed in the brain are secreted into extracellular space, or anchored to the cell membrane, as non-active pro-MMPs. In order to activate the pro-MMP, the propeptide needs to be cleaved by other proteases (Sternlicht and Werb, 2001) or modified by S-nitrosylation (Gu *et al.*, 2002). Once activated, tissue inhibitors of metalloproteinases (TIMPs) can inhibit MMPs

binding to (i) their catalytic site, and blocking its enzymatic ability, or to (ii) the hemoplexin domain, blocking its interactions with substrate or membrane docking proteins.

The MMP-1, known also as collagenase 1, is expressed in the human brain mostly by glia but also by a subset of neurons (Jerusalimsky and Balaban, 2013; Allen *et al.*, 2016). At the same time, *in vitro* studies using adult neural progenitor cells from hippocampi of MMP-1-overexpressing mice have indicated that MMP-1 enhances proliferation and increases differentiation of the progenitor cells towards neurons (Valente *et al.*, 2015). Additionally, another animal study using mice overexpressing MMP-1 showed MMP1-enhanced dendritic complexity which resulted in deficits in learning and memory abilities (Allen *et al.*, 2016).

MMP-2, also named gelatinase A, is mostly expressed in the human brain by astrocytes and a subset of neurons in numerous brain areas, including the schizophrenia-related cortex and hippocampus (Beroun *et al.*, 2019). The expression of MMP-2 is increased during early postnatal development and it was shown to affect cell migration (Ogier *et al.*, 2006; Aujla and Huntley, 2014). Additionally, an increased level of MMP-2 was reported in response to kainate treatment in rats (Zhang, Deb and Gottschall, 1998). Recent studies, that investigated cerebrospinal fluid of major depression and schizophrenic patients, show an increased level of MMP-2 linked to brain inflammation in comparison to healthy individuals (Omori *et al.*, 2020).

MMP-3, also known as stromelysin 1, is expressed during the early development of the central nervous system by both neurons and glia (Van Hove *et al.*, 2012). In the adult brain, MMP-3 levels are very low. However, increased MMP-3 levels were reported in mice hippocampus during learning (Wiera *et al.*, 2017). Besides, MMP-3 digests numerous chondroitin sulfate proteoglycans including: neural/glial antigen 2, brevican, versican, neurocan, phosphacan (Muir *et al.*, 2002). Also, transient MMP-3 activation was shown to be necessary for NMDAR-dependents EPSP-to spike potentiation (Wójtowicz and Mozrzymas, 2014). Moreover, *in vitro* studies have shown that MMP-3 cleaves NR-1 subunit and MMP-3-deficient mice have shown an increased number of matured spines and disrupted open-eye potentiation in the visual cortex (Pauly *et al.*, 2008; Aerts *et al.*, 2015).

The 1171 5A/6A polymorphism in position rs3025058 in MMP-3 gene was associated with the risk of schizophrenia in the Turkish population. The 5A5A genotype and 5A allele distributions of the MMP3 gene were significantly more frequent in patients with schizophrenia (Kucukali *et al.*, 2009).

The MMP-7, known also as matrilysin, is similarly expressed to MMP-3 during early development and barely detectable in the healthy, adult brain (Ulrich *et al.*, 2005; Roberts *et al.*, 2013). Animal studies using extracts from rat cortical slice preparation have shown that MMP-7 cleaves NR1 and NR2A subunits of the NMDA receptor but not AMPA receptor subunits, increasing AMPAR/NMDAR ratio in the postsynaptic site of glutamatergic synapses. Those modifications lead to a reduction of NMDAR-induced calcium influx (Szklarczyk *et al.*, 2008). Another study in mice hippocampal primary neuronal culture shows MMP-7-induced changes of mature mushroom-shaped spines into immature filopodia, suggesting a role in memory loss or motor coordination. The reported MMP-7-induced spines alterations were NMDAR-dependent and were abolished by application of NMDAR inhibitor MK-801 (Bilousova *et al.*, 2006). Interestingly, recent human studies show no alteration of MMP-7 level in cerebrospinal fluid of schizophrenia patients (Omori *et al.*, 2020).

MMP-9, also known as gelatinase B, peaks during early brain development. Nonetheless, increased expression was also reported after activity-induced neuroplasticity. MMP-9 is released postsynaptically from excitatory neurons in an activity-dependent manner. Upon activation, MMP-9 cleaves several extracellular matrix molecules, including neuroligin-1, nectin-3, β -dystroglycan, collapsin response mediator protein-2 and intercellular adhesion molecule-5 (ICAM-5) (Beroun *et al.*, 2019). MMP-9's trimming of ICAM-5 results in an increased ratio of GluA1/GluA2 AMPAR subunits and increased glutamatergic transmission (Lonskaya *et al.*, 2013). *In vitro* studies using rat hippocampal primary cell culture have shown MMP-9-dependent dendritic spine enlargement, accompanied by an accumulation of AMPAR in the synapse and an increase in burst frequency's spike count after chemically induced LTP (Niedringhaus *et al.*, 2013; Szepesi *et al.*, 2014).

Moreover, MMP-9 enzymatic activity increases NR-1 NMDAR subunit lateral mobility and the application of integrin β -1 Ab abolishes this effect, suggesting that MMP-9-induced increase of NMDAR mobility is mediated by integrin signalling (Michaluk *et al.*, 2009). MMP-9-induced increased mobility of the NMDAR receptor was reported to change its synaptic functions, namely to accelerate desensitization onset and deactivation kinetics of NMDA-evoked currents (Gorkiewicz *et al.*, 2010).

Interestingly, three SNPs in the MMP-9 gene were associated with schizophrenia disease. The C/T SNP in position rs20544 is strongly linked with delusional symptoms in schizophrenic patients. The carriers of C variants tend to suffer more chronic severe delusional symptoms. *In silico* analysis show that the C variant changes the 3-D structure of the MMP-9 mRNA region

binding to fragile X mental retardation protein (FMRP). Stronger binding of FMRP to MMP-9 mRNA in C variants results in a decrease of synaptic availability of the MMP-9 protein. Rat hippocampal primary cell culture transfected with MMP-9 C variants show to have a higher percentage on mature mushroom-shaped spines in comparison to T variant, but do not show an increase of spine head area after chemically induced LTP in contrary to T variants (Lepeta *et al.*, 2017). Altogether those findings show that MMP-9 might play a role in schizophrenia disease pathophysiology related to the alteration of excitatory synapses.

The functional polymorphism in the MMP-9 promotor region 1562 C/T was associated with schizophrenia. The carriers of CC variants were over-represented in schizophrenic patients in comparison to healthy individuals (Rybakowski *et al.*, 2009; Han *et al.*, 2011).

The SNP in position rs 13925 of the MMP-9 gene was shown to be involved in the severity of childhood trauma and further antipsychotic treatment response in a study of South African first-episode schizophrenia patients. The recessive genotype was associated with a reduced risk of developing treatment-refractory schizophrenia. (McGregor *et al.*, 2018).

Leucine-rich and glioma-inactivated protein 1

The leucine-rich and glioma-inactivated protein 1 (LGI1) forms a trans-synaptic complex, which regulates the glutamatergic transmission and its several mutations are associated with autosomal dominant partial epilepsy with auditory features (ADPEAF). The extracellular LGI1 protein is secreted by presynaptic terminals and binds to the presynaptic disintegrin and metalloproteinase domain-containing protein 23 (ADAM 23). The ADAM 23 protein is coupled with voltage-gated potassium channel Kv1.1, which regulates glutamate release. The complex of Kv 1.1, ADAM 23 and LGI1 protein protects the Kv 1.1. channel against Kv β 1-induced inactivation (Schulte *et al.*, 2006). Furthermore, mice treated with autoimmune encephalitis patients-derived anti-LGI1 antibodies showed reduced synaptic levels of Kv1.1 and AMPAR protein as well as pyramidal neurons hyperexcitability and increased presynaptic glutamate release probability (Petit-Pedrol *et al.*, 2018).

The postsynaptic partner of LGI1 protein is the ADAM 22 protein, which forms a complex with the postsynaptic density protein 95 (PSD-95), stargazin and AMPA receptor. Adding LGI1 protein into hippocampal rat slices increases the AMPA/NMDAR ratio in glutamatergic synapses and AMPA-mediated synaptic currents (Fukata *et al.*, 2006). Mice treated with anti-LGI1 antibodies have shown impaired long-term potentiation and severe memory deficits due to suggested

corrupted LGI1-mediated AMPAR recruitment into the postsynaptic site of glutamatergic synapses (Petit-Pedrol *et al.*, 2018).

An animal study using LGI1 truncated protein has suggested that LGI1 protein regulates NMDA receptor maturation. The peak of NGI1 expression coexists with developmental NR2B to NR2A shift and mice expressing a truncated form of the NGI1 protein seem to suffer arrested NMDAR maturation (Zhou *et al.*, 2009).

Tenascin C

Tenascin C (TN-C) is an ECM oligomeric glycoprotein of modular structure. Each monomer of the human TN-C protein consists of a TA domain, followed by a cysteine-rich domain, fourteen epidermal-growth factor (EGF)-like domains, eight to seventeen fibronectin (FN)-type III domains, depending on splicing variant, and a single fibrinogen (FG)-like carboxy-terminal part. Additional FN-type III domains, termed A1, A2, A3, A4, B, AD2, AD1, C and D, can be inserted between domains 5 and 6 in the largest TN-C spliced variant. The functional TN-C protein forms a hexamer, binding each monomer through the TA domain.

TN-C is highly expressed in CNS during critical stages of neural development, as well as during regeneration and synaptic plasticity in the adult brain. It can play a dual role in cell adhesion and migration. The FN-type III region exhibits pro-adhesive characteristics and is responsible for the TN-C role in neuronal outgrowth enhancement (Götz *et al.*, 1997; Zhang *et al.*, 1997). Whereas, the EGF-like domains are associated with anti-adhesive properties of TN-C and are responsible for the protein's role as a barrier inhibiting neuronal outgrowth, cell proliferation and migration. Phases of intensive axonal outgrowth were associated with the large splice variant of TN-C protein-containing seventeen FN-type3 domains *in vitro* (Meiners and Geller, 1997; Meiners *et al.*, 1999). Moreover, *in vivo* studies have shown that the mRNA of TN-C FN-type3 domain repeats B and D are highly upregulated in rats cortical lesion promoting local neurite outgrowth (Dobbertin *et al.*, 2010).

Increased TN-C mRNA and protein levels were also reported in the rat dentate gyrus and hippocampus within hours after neuronal stimulation (Nakic *et al.*, 1998). TN-C-deficient mice have shown impaired hippocampal CA1 LTP and abolished LTD after stimulation of Schaffer collaterals. Moreover, blocking of L-type voltage-gated calcium channels (VDCCs) has reduced the LTP in the wild type but not in TN-C- KO mice, suggesting that TN-C modulation of synaptic transmission is linked with the VDCCs (Evers *et al.*, 2002). The intrahippocampal injection of TN-C fibronectin like repeats FN-type III repeats 5-6 fragment, but not FN-type III repeats 3-5

fragment, reduces CA1 LTP and impaired mice memory recall in step down passive avoidance task in TN-C deficient and wild type mice, suggesting that the first fragment of the protein might play a role in binding to the channel (Strekalova *et al.*, 2002).

Tenascin R

The tenascin R (TN-R) ECM glycoprotein is similar to TN-C modular oligomeric protein. Contrary to TN-C, the TN-R forms trimers, not hexamers. Each monomer of TN-R consists of an amino-terminal TA domain, a cysteine-rich domain, 4.5 EGF-like repeats, eight or nine FN-type III domains and an FG carboxy-terminal part. During development, TN-R promotes cell adhesion, migration and neuronal outgrowth.

In the adult brain, TN-R regulates GABA-ergic transmission by decorating PNN of a subset of interneurons and carrying human natural killer 1 (HNK-1) carbohydrate. Two animal studies using TN-R-deficient mice and anti-HNK-1 carbohydrate antibodies respectively have shown that lack of TN-R or HNK-1 carbohydrate in the synaptic cleft resulted in impaired LTP in hippocampal CA1 and increased basal synaptic transmission. Both the GIRK channel and GABAB receptor agonist abolished the HNK-1 Ab-induced effect on perisomatic inhibition (Saghatelian *et al.*, 2000, 2001). Altogether these findings suggested a mechanism of TN-R-dependent metaplasticity regulation of synaptic transmission. In this mechanism, TN-R carries HNK-1 carbohydrate into perisomatic inhibitory synapses. The HNK-1 carbohydrate interacts directly with the GABAB receptor on the cell body of a pyramidal neuron and inhibits the receptor activation by GABA. Therefore, the presynaptic release of GABA from an inhibitory interneuron activates only the GABAA receptor. In TN-R-deficient mice, the HNK-1 carbohydrate is not delivered into the postsynaptic GABAB receptor, which is activated upon tonic GABA release. Activation of both GABAA and GABAB receptors results in increased potassium concentration in the synaptic cleft, which might lead to depolarization of the presynaptic membrane and increase the spontaneous release of GABA and a decrease of the evoke GABA release (Saghatelian *et al.*, 2003).

Moreover, TN-R deficient mice have shown an abnormal structure of PNN, a strong reduction in density and altered architecture of active zones in perisomatic inhibitory synapses in the CA1 pyramidal layer and anxiety and motor impairments (Freitag, Schachner and Morellini, 2003; Nikonenko *et al.*, 2003)

1.3 Schizophrenia disease

1.3.1 Definition and diagnosis

Schizophrenia is a heterogeneous mental disorder which, according to the World Health Organization, affects one percent of the human population. It strikes individuals in late adolescence and early adulthood in ages between 16 and 30 years old (Mueser and McGurk, 2004). This chronic mental disorder increases patient's lifetime risk of suicide to 5% (Palmer, Pankratz and Bostwick, 2005; Hor and Taylor, 2010), and corrupts patient's productivity and self-organization skills leading to a high rate of unemployment, homelessness and poverty (Knapp, Mangalore and Simon, 2004).

Due to a lack of molecular markers, schizophrenia is diagnosed based on a clinical interview. The diagnosis of this disorder is built on three groups of symptoms. Positive symptoms include hallucinations, delusions, disorganized speech and disorganized or catatonic behaviour. Negative symptoms involve social withdraw, reduced face expression - flat affect, poor speech - alogia, lack of motivation - avolition and reduced perception of pleasure – anhedonia. Cognitive symptoms represent disrupted memory, learning and understanding. However, not all those symptoms occur in every schizophrenia case. According to the current classification (International Classification of Diseases – ICD-10 and American norm DSM5), two patients suffering from only a certain number of different symptoms can have the same diagnosis.

1.3.2 Genetic origins

Several genetic and environmental factors have been reported to be associated with the disease. Family and twins studies show a 13 % increased risk of developing schizophrenia in offspring of a schizophrenic parent and a 50 % risk for identical twins when one of them was diagnosed with the disease (Gottesman and Erlenmeyer-Kimling, 2001). This data might suggest that schizophrenia is not a genetically determined disease but a multifactorial and polygenic disorder, which aggregates in families. Genome-wide association studies (GWAS), identified over 100 loci implicating about 600 genes significant for schizophrenia (Schizophrenia Working Group of the Psychiatric Genomics Consortium, 2014).

Three of the most investigated gene pathways associated with the disease are: the COMT gene encoding catechol-O-methyl transferase (COMT) involved in catabolic clearance of excitatory

neurotransmitter dopamine (Axelrod and Tomchik, 1958), glutamate transmission-related single nucleotides polymorphism (SNP), and Human Leukocyte Antigen (HLA) or Major Histocompatibility Complex (MHC) locus. The first of them contains common G>A SNP in position rs4680, which produces a valine-to-methionine substitution in COMT protein (Lachman *et al.*, 1996). This substitution leads to a decrease in enzymatic activity of COMT protein (Chen *et al.*, 2004) and, consequently, an increase of dopamine levels in the synaptic cleft. Gene association studies of this SNP and schizophrenia show conflicting results reporting significant relevance of valine variant, methionine variant, or no relevance of the SNP with the disease. Those differences might be partially explained by the sample biased caused by gender- and ethnicity-driven differences in Valine variant frequency. Nevertheless, the low activity, methionine COMT variant was suggested to be associated with early-onset of schizophrenia in recent meta-analysis studies (Taylor *et al.*, 2017). Moreover, the schizophrenic carriers of this variant were reported to better respond to antipsychotic - olanzapine treatment compared to the high activity COMT variant (Percovic *et al.*, 2020).

The second group of SNPs affects glutamate receptors and glutamate transmission. The genes which are associated with schizophrenia and affect glutamate receptors code subunits of ionotropic receptors such as N-methyl-D-aspartate receptor (NMDAR), α -amino-3-hydroxy-5-methyl-4-isoxazolepropionic acid receptor (AMPA) and kainate receptor, as well as metabolic glutamate receptor 5 (mGluR5). The simultaneous mutations in two genes GRIN1A and GRIN2A coding NMDAR subunits NR1 and NR2 lead to hypofunction of the receptor and were reported to be a strong schizophrenia risk factor (Qin *et al.*, 2005).

The SNPs in gene GRIA1 coding AMPA receptor subunit GluR1 were linked with schizophrenia in independent genome-wide scans (Ripke *et al.*, 2013) as well as in a case-control association study on the Italian population with eight polymorphisms spanning the whole GRIA1 gene (Magri *et al.*, 2006). Lee and colleagues also have shown that modification of the GluR1 subunit results in impaired synaptic plasticity (Lee *et al.*, 2003).

The functional polymorphism in the kainite receptor gene GRIK3 coding the serine substitution with alanine in the GRIK3 subunit of the kainite receptor results in lower protein stability and was linked with higher schizophrenia risk (Begni *et al.*, 2002). The mutation in the metabotropic glutamate receptor GRM5 gene was linked with schizophrenia in humans (Devon *et al.*, 2001) and the lack of the protein was reported to disrupt learning and hippocampal LTP in the mice model (Lu *et al.*, 1997).

Moreover, the SRR gene coding serine racemase and NOS1 gene coding nitric oxide synthase-I regulating glutamate receptors were also associated with the disease. The serine racemase converts l-serine to d-serine. The d-serine is an agonist of the NMDA receptor and facilitates its firing. The genetic variant in the SRR gene linked with reduced activity of serine racemase and possibly NMDA receptor hypofunction was associated with schizophrenia (Morita *et al.*, 2007; Ripke *et al.*, 2013).

A functional promoter polymorphism of neuronal nitric oxide synthase AA/AG in position rs41279104 is associated with schizophrenia (Reif *et al.*, 2006). The risk allele influences expression of the NOS1 gene and may decrease NO-dependent GABA release upon glutamatergic neurons causing impaired inhibition and as a result an excessive glutamate release. Increased glutamate release may lead to glutamate excitotoxic effect and result in neuronal cell death in the frontal cortex; as a proposed mechanism explaining slower dorsolateral cortical functioning reported in schizophrenic patients functional imaging studies (Reif *et al.*, 2011).

Third, MHC is primarily involved in the processing and presentation of antigens, and the recognition of self-versus non-self antigens (Janeway *et al.*, 2001). MHC alteration could be linked with an increased risk of schizophrenia disease in offspring of mothers suffering viral or parasitic infection during pregnancy. Moreover, MHC genes also have functions in schizophrenia etiopathogenesis processes such as neurogenesis, neuronal differentiation, migration, and in glutamate receptor signalling (Goddard, Butts and Shatz, 2007; Shatz, 2009; Glynn *et al.*, 2011; Elmer and McAllister, 2012).

Genetic studies also show ECM-related genes associated with the disease. A common variation of the neurocan gene was linked with schizophrenia and bipolar disorder (Mühleisen *et al.*, 2012; Ripke *et al.*, 2013). The neurocan is a proteoglycan extensively expressed in the human brain and according to animal studies its expression peaks during late embryogenesis followed by an expression decrease within the first month after birth, suggesting that it may play a role in early brain development (Meyer-Puttlitz *et al.*, 1996). In “*in vitro*” studies in chicken retina neurons show that neurocan inhibits neuronal adhesion and neuronal growth due to its binding with cadherin (Li *et al.*, 2000). Additionally, mice lacking this proteoglycan showed impaired maintaining of LTP, suggesting a role in neuroplasticity (Zhou *et al.*, 2001). The A allele in SNP rs 1064395 in the neurocan gene was proposed to be a schizophrenia risk factor. Functional magnetic resonance studies with healthy individuals and schizophrenic patients associate it with a lack of task-related deactivation during semantic verbal fluency in the left lateral temporal cortex and poorer performance in verbal memory tasks (Mühleisen *et al.*, 2012). Altogether those

findings show a role of neurocan in the pathophysiology of schizophrenia disease during early development and adulthood neuroplasticity.

An SNP of β -1,3-glucuronyltransferase 2 (B3GAT2), HNK-1 biosynthesis enzyme was reported as a schizophrenia risk factor, correlated with decreased cortex volume in schizophrenic patients (Kahler *et al.*, 2011). A decrease in the enzyme activity may lead to a decrease in the HNK-1 carbohydrate level in the brain. The lack of HNK-1 carbohydrate was reported to compromise GABAergic transmission due to a decrease of GABA-mediated perisomatic inhibitory postsynaptic currents (IPSCs) in animal studies (Saghatelian *et al.*, 2000, 2001). Altogether these findings may link the decrease of HNK-1 carbohydrate synthesis with impairment of GABA-mediated gamma oscillation observed in schizophrenic patients.

An SNP rs7004633 in matrix metalloprotease MMP-16 gene was also associated with schizophrenia with GA allele as a risk factor (Consortium, 2011). The MMP-16 belongs to type I transmembrane proteins and degrades several ECM components, including fibrin, syndecan-1, collagen III, aggrecan, gelatin and vitronectin. It is also activating proMMP2 to active matrix metalloprotease 2 (MMP-2) (Sbardella *et al.*, 2012), which is necessary for proper blood-brain barrier formation (Kanda *et al.*, 2019).

1.3.3 Environmental factors

Although there are many genetic factors involved in schizophrenia, they do not fully explain the mechanism of developing the disease. Environmental factors seem to play a crucial role in triggering this process. During pregnancy, maternal stress (Yang *et al.*, 2017), malnutrition (Brown and Susser, 2008) and viral infection with influenza (Brown *et al.*, 2004), rubella (Brown *et al.*, 2001), varicella-zoster (Torrey, Rawlings and Waldman, 1988) and polio (Suvisaari *et al.*, 1999), as well as parasitic toxoplasmosis (Brown *et al.*, 2005), have been associated with schizophrenia. Additionally, birth complications (Rosso *et al.*, 2000) and early childhood trauma were shown to be positively correlated with the risk of developing this mental disorder (Cannon *et al.*, 2003). During adulthood, the main risk factors are substance abuse (Andreasson *et al.*, 1987), urbanization (Freeman, 1994) and migration (Sharpley *et al.*, 2001; Zolkowska, Cantor-Graae and McNeil, 2001).

1.3.4 Neurobiology

This combination of complex genetic variation and multiple environmental factors leads to severe neurobiological deficits. Human *post mortem* brain studies revealed enlarged ventricles and decreased volume of several brain areas including the PFC and hippocampus of schizophrenia patients (Brown *et al.*, 1986; Selemon and Goldman-Rakic, 1999; Schmitt *et al.*, 2009). This result was confirmed by more recent studies using the MRI technique, which allows avoiding artefacts caused by tissue handling and fixation time (Anvari *et al.*, 2015; Godwin *et al.*, 2018).

Parvalbumin (PV) -expressing fast-spiking GABA-ergic interneurons provide inhibitory control of cortical and subcortical circuits and seem to play a crucial role in the pathophysiology of schizophrenia. The density of PV interneurons in human *post mortem* PFC was intensively examined in the context of the disease throughout the last decade. However, the outcome of the studies gives conflicted results, as they reported both the reduced density of PV interneurons (Beasley and Reynolds, 1997; Reynolds, Beasley and Zhang, 2002; Sakai *et al.*, 2008; Bitanirwe and Woo, 2014) as well as the unaltered density of PV interneurons, but reduced expression of parvalbumin in interneurons (Woo, Miller and Lewis, 1997; Hashimoto *et al.*, 2003; Tooney and Chahl, 2004; Enwright *et al.*, 2016; Alcaide *et al.*, 2019). Despite the differences, all the studies seem to agree that the hypofunction of PV interneurons is a feature of the disease and plays an important role in its pathology. A recent meta-analysis study confirmed the reduction of parvalbumin-expressing interneurons in schizophrenic patient's PFC (Kaar *et al.*, 2019). Moreover, loss of PV interneurons was associated with gamma oscillation deficits in an animal model of schizophrenia (Lodge, Behrens and Grace, 2009).

Interestingly, also excitatory neurons are compromised in PFC in human *post mortem* brain studies of schizophrenic patients. For example, there is a decreased dendritic spine density in pyramidal neurons of mPFC layer 3 in schizophrenia samples (Glantz and Lewis, 2000). Those deficits may be linked with compromised working memory and cognitive deficits in schizophrenic patients.

The clinical symptoms and cognitive and functional deficits of schizophrenia typically begin and emerge gradually during late adolescence and early adulthood. This period is an important maturation time for such high-cognitive functions as reasoning, abstract thinking and planning (Andersen, 2003). This process is associated with the maturation of PFC neurons via intensive pruning of excitatory synapses (Goldman-Rakic, 1987; Bourgeois, Goldman-Rakic and Rakic, 1994), which is correlated with the capacity of PFC pyramidal neurons networks to synchronize

and oscillate in gamma frequency (Uhlhaas *et al.*, 2010). Interestingly gamma oscillation is reported to be compromised in schizophrenia patients (Spencer, Niznikiewicz, *et al.*, 2008; Spencer, Salisbury, *et al.*, 2008), suggesting a pivotal role of PFC maturation in triggering symptoms of the disease. Numerous animal studies indicated the maturation of intracortical inhibition subserved by the PV neurons and the formation of extracellular matrix environment as two important mechanisms that regulate the time course of the critical period for developmental synaptic plasticity in the cerebral cortex (Hensch *et al.*, 1998; Fagiolini and Hensch, 2000; Pizzorusso *et al.*, 2002; Ye and Miao, 2013; Murase, Lantz and Quinlan, 2017).

The dopamine hypothesis of schizophrenia

The dopamine hypothesis is the most enduring and well-studied neurotransmitter-based hypothesis in schizophrenia research. It results in three generations of antipsychotic drugs, which are the majority of drugs currently used in schizophrenia treatment (Howes and Kapur, 2009). The hypothesis proposes that the hyperactive dopamine transmission in the mesolimbic brain area and the hypoactive dopamine transmission in the prefrontal cortex result in schizophrenic symptoms. The hypothesis is based on two facts: that activation of D2 dopamine receptor by agonist like amphetamine causes positive symptoms, such as hallucination and psychosis, in healthy individuals; and blocking of D2 dopamine receptor by antipsychotic drugs inhibits positive symptoms of schizophrenia (Creese, Burt and Snyder, 1976; Seeman *et al.*, 1976).

There are four major dopamine pathways in the human brain illustrated in Fig. 2. The mesolimbic pathway starts in the ventral tangmental area and projects to the nucleus accumbens, amygdala and hippocampus. The nucleus accumbens key function is to control reward and motivation, pleasure, fatigue, libido and euphoria. In the context of the disease, its hyperactivity is responsible for delusion and hallucination. The activation of the amygdala triggers fears, anxiety and panic. Whereas, the main function of the hippocampus is working memory formation. Altogether, is thought to be responsible for psychosis.

The mesocortical pathway also originates in the ventral tangmental area but projects to the cerebral cortex, including the prefrontal cortex. The prefrontal cortex is responsible for executive function, planning and concentration. The dopamine hypoactive transmission in this pathway leads to negative symptoms and cognitive deficits in schizophrenia. Moreover, typical antipsychotic drugs used in antipsychotic treatment in schizophrenia often increase the negative symptoms.

The nigrostriatal pathway originates in substantia nigra and projects to striatum, which facilitates movement. Blocking of dopamine receptors in this pathway leads to extrapyramidal disorders like

tarditive dyskinesia and Parkinson-like symptoms, which are common side effects of antipsychotic drugs used in schizophrenia treatment.

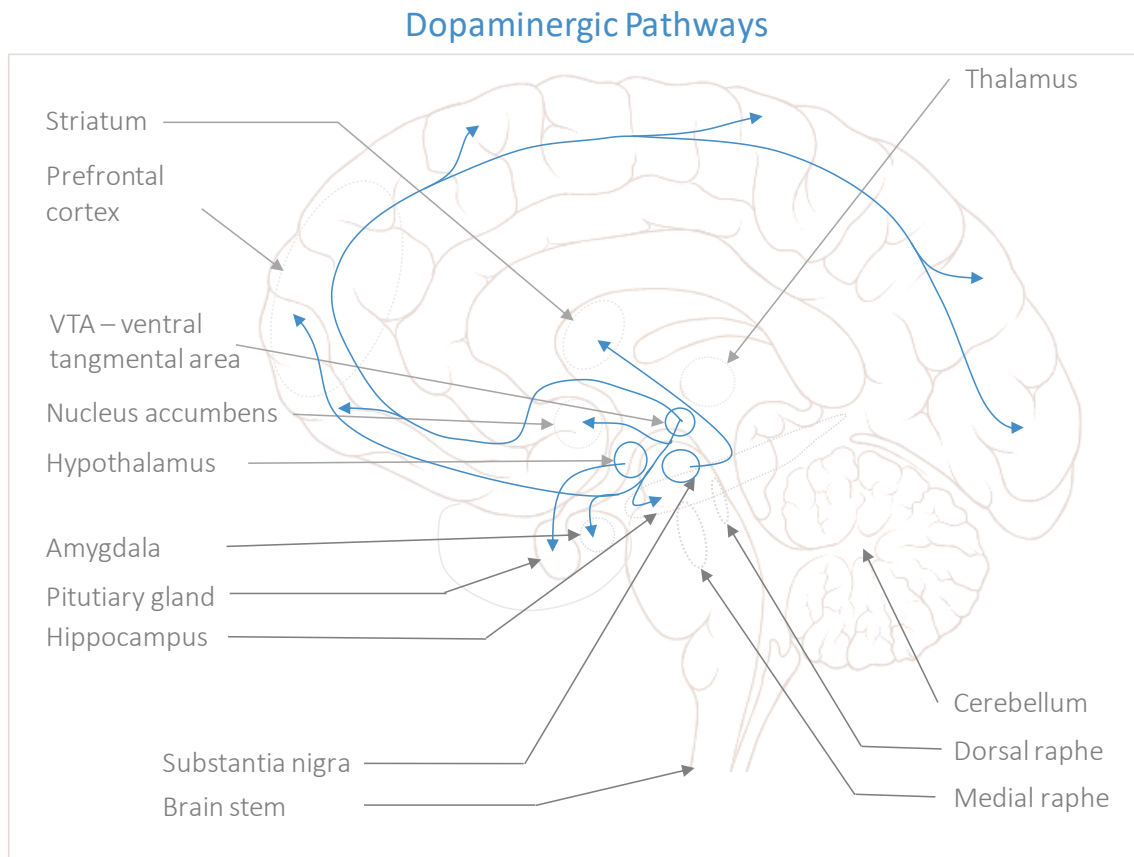


Fig. 2 The four major dopaminergic pathways in the human brain. The mesolimbic pathway originates in the ventral tangmental area marked with a blue circle and projects limbic areas such as nucleus accumbens, amygdala, hippocampus and PFC marked in grey. The mesocortical pathway originates in the ventral tangmental area marked with a blue circle and projects to the cerebral cortex. The nigrostriatal pathway originates in substantia nigra marked with blue circle and projects to striatum marked in grey. The tuberinfundibular pathway originates in the hypothalamus marked in a blue circle and projects to the pituitary gland. The direction of projections marked with blue arrows. Adapted from (Barth, Villringer and Sacher, 2015).

The tuberoinfundibular dopamine pathway originates in the hypothalamus and projects to the pituitary gland, which regulates prolactin secretion. Blocking of dopamine receptors in this pathway cause prolactin release and might leads to galactorrhea, gynecomastia and sexual dysfunction, also known side effect of antipsychotic treatment. Although the dopamine hypothesis helps to describe the brain alteration behind positive symptoms, it is not explaining the origins of the disease.

The serotonin hypothesis

The serotonin hypothesis was a chronological first neurotransmitter-based hypothesis in schizophrenia research. It lost its popularity with increased interest in dopamine role in the disease but the discovery of the second generation of antipsychotic drugs targeting not only dopamine but also serotonin receptors brought new interest into serotonin research in schizophrenia. The hypothesis was formed in 1954 by Woodley and Shaw who proposed that the positive symptoms of schizophrenia are a result of serotonin deficits in the human brain (Woolley and Shaw, 1954). They built their hypothesis based on two scientific observations. First, in 1943 Albert Hofmann reported that D-lysergic acid (LSD) administration causes schizophrenia-like symptoms. And second, Gaddum and Hammed showed that D-lysergic acid antagonized the vasoconstrictor effect of serotonin in smooth muscles (GADDUM and HAMEED, 1954). Those two observations led to the conclusion that D-lysergic acid is a serotonin receptor antagonist. Later radioligand binding studies confirmed that D-lysergic acid binds to serotonin 5HT_{2A} receptor (Titeler, Lyon and Glennon, 1988).

Serotonin is a neurotransmitter, which is widely distributed in the human brain. Although the number of serotonergic neurons is relatively low, its numerous projections originating from dorsal and medial raphe intervene through the complete central nervous system (Fig. 3). The serotonin release and can lead to depolarization, hyperpolarization as well as no effect on cortical pyramidal neurons. The effect depends on serotonin excitatory 5HT_{2A} and inhibitory 5HT_{1A} receptor expression balance in pyramidal neurons. In the PFC, stimulation of the 5HT_{2A} receptor not only blocks dopamine release but also increases the release of glutamate, increasing the frequency of excitatory postsynaptic currents (EPSCs). This effect can be blocked by stimulation of presynaptic inhibitory metabolic glutamate (mGluR) II and III receptors as well as antagonists of postsynaptic non-NMDA, AMPA or kainite glutamate receptors.

Moreover, human *post mortem* studies have shown decreased density of 5HT_{2A} receptor in schizophrenic brain tissue as well as increased density of 5HT_{1A} receptor in PFC, suggesting that serotonin receptor alterations play important role in the disease aetiology (Hashimoto *et al.*, 1991; Laruelle *et al.*, 1993).

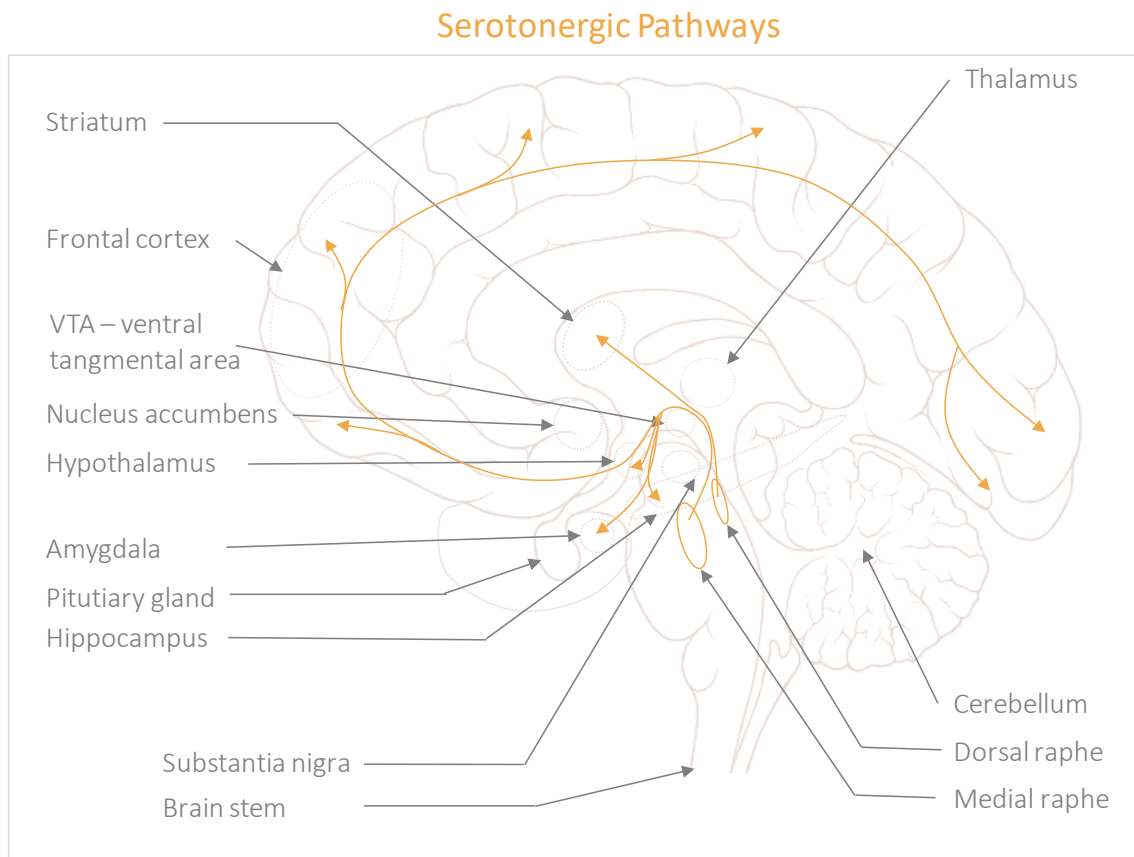


Fig. 3 The major serotonergic pathways in the human brain. The dorsal raphe, marked in orange circle projects mainly to the thalamus, striatum and cerebral cortex, marked in grey. The medial raphe, marked in orange projects to the frontal cortex and the hippocampus, marked in grey. The direction of projections is indicated by orange arrows. Adapted from (Barth, Villringer and Sacher, 2015).

The glutamate hypothesis

The glutamate hypothesis is the next step in understanding altered neurotransmission in schizophrenia disease. It is based on the observation that glutamate NMDAR antagonists such as phencyclidine (PCP), ketamine and MK-801 induce schizophrenia-like positive symptoms, negative symptoms and cognitive deficits. The hypothesis proposes that hypofunction of NMDAR leads to decreased GABA transmission, increased glutamate and dopamine transmission and disrupted excitatory-inhibitory balance in the schizophrenic brain (Schmitt *et al.*, 2012).

Glutamate is the main excitatory neurotransmitter in the CNS. It is estimated that up to half of all synapses in the brain release glutamate (Newcomer, Farber and Olney, 2000). The glutamatergic neurons are connected in their pathway with GABA-ergic interneurons, which play a crucial role

in the glutamate hypothesis of schizophrenia. There are five main glutamatergic pathways in the human brain (Fig. 4). The cortical brainstem pathway originates in the PFC and projects to brain stem areas, such as medial and dorsal raphe, ventral tangmental area and substantia nigra. The corticostriatal pathway projects from the PFC to the striatum and nucleus accumbens. The thalamocortical pathway originates in the thalamus and innervates the cortex. The cortico-cortical pathway connects the cortical neurons (Schwartz, Sachdeva and Stahl, 2012).

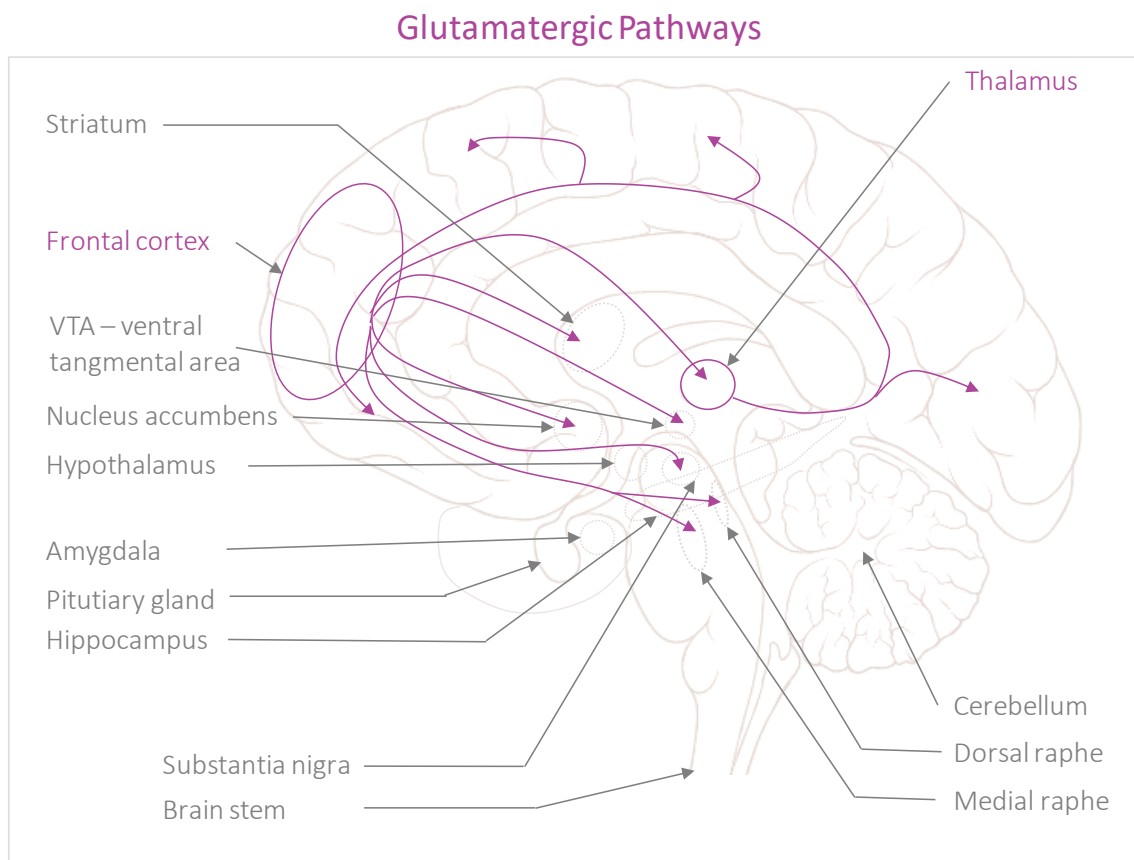


Fig. 4 The five major glutamatergic pathways in the human brain. The cortical brainstem pathway originates in PFC, marked in purple and projects to brain stem areas such as medial and dorsal raphe, ventral tangmental area and substantia nigra, marked in grey. The corticostriatal pathway projects from PFC to striatum and nucleus accumbens (in grey). The thalamocortical pathway originates in the thalamus, marked in purple and innervates cortex (in grey). The cortico-cortical pathway connects the cortical neurons. The direction of projections is marked with purple arrows. Adapted from (Barth, Villringer and Sacher, 2015).

Meanwhile, GABAergic neurons mostly project from the striatum to the substantia nigra, but also project from the hypothalamus to the occipital cortex and parietal cortex; from the hippocampus

to thalamus and striatum; and from the nucleus accumbens to thalamus. The cerebellum is also highly innervated by GABAergic projections (Fino and Venance, 2010) (Fig. 5).

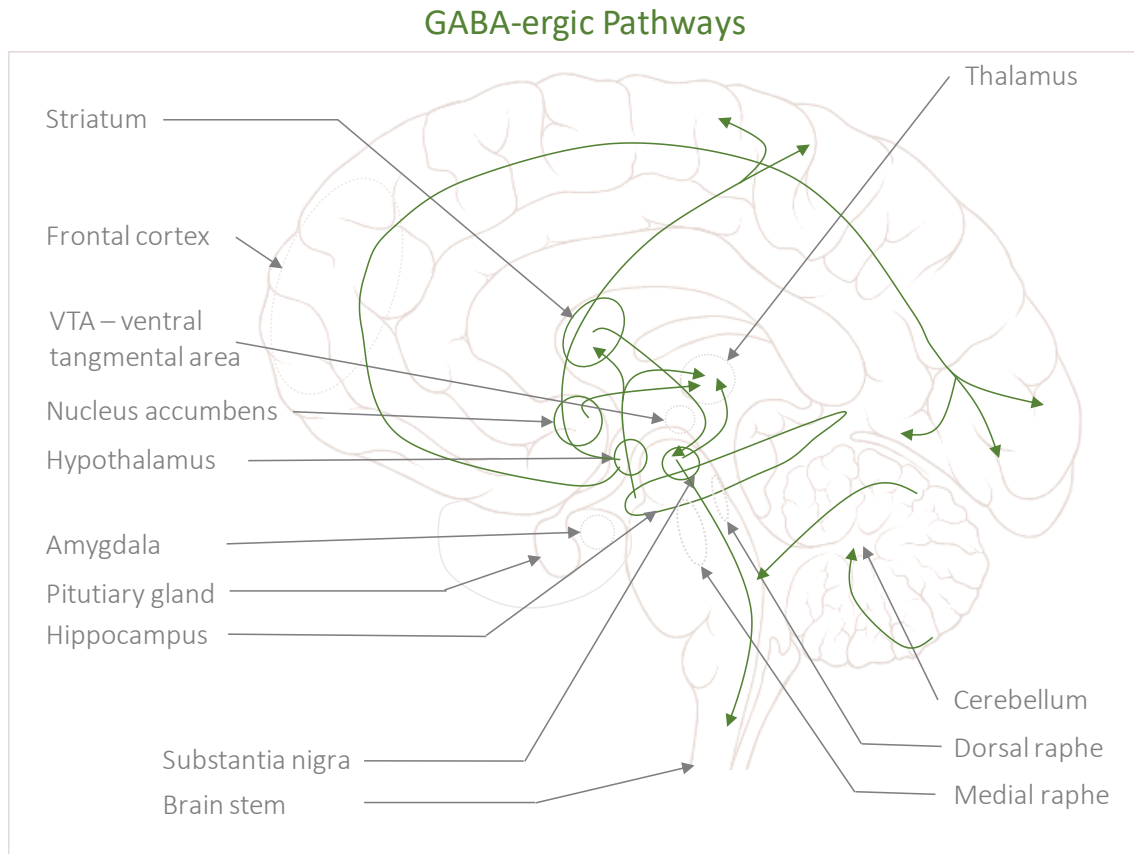


Fig. 5 The major GABAergic pathways in the human brain. The pathway from the striatum, marked in green to substantia nigra (in green) and brainstem (in grey). The pathway from the hypothalamus in green to the occipital cortex and parietal cortex and projects to brain steam areas such as medial and dorsal raphe, ventral tangmental area and substantia nigra, marked in grey. The corticostriatal pathway projects from PFC to striatum and nucleus accumbens (in grey). The thalamocortical pathway originates in the thalamus, marked in purple and innervates cortex (in grey). The cortico-cortical pathway connects the cortical neurons. The direction of projections is marked with green arrows. Adapted from (Barth, Villringer and Sacher, 2015).

Both positive and negative symptoms of schizophrenia may be explained on the cortical brainstem glutamatergic pathway. The first glutamatergic neuron originates in the PFC and fires upon a GABAergic interneuron, which in normal conditions reduces the firing rate of a secondary glutamatergic neuron, which then stimulates a dopaminergic neuron in the ventral tangmental area; resulting in normal dopamine transmission in the mesolimbic pathway. In schizophrenic

conditions, the hypofunction of the glutamate NMDA receptor in GABAergic interneurons results in the increased firing of secondary glutamatergic neurons, which overstimulate the dopaminergic neurons in the ventral tangmental area; causing an upregulation of the dopaminergic mesolimbic pathway (Schwartz, Sachdeva and Stahl, 2012) (Fig. 6).

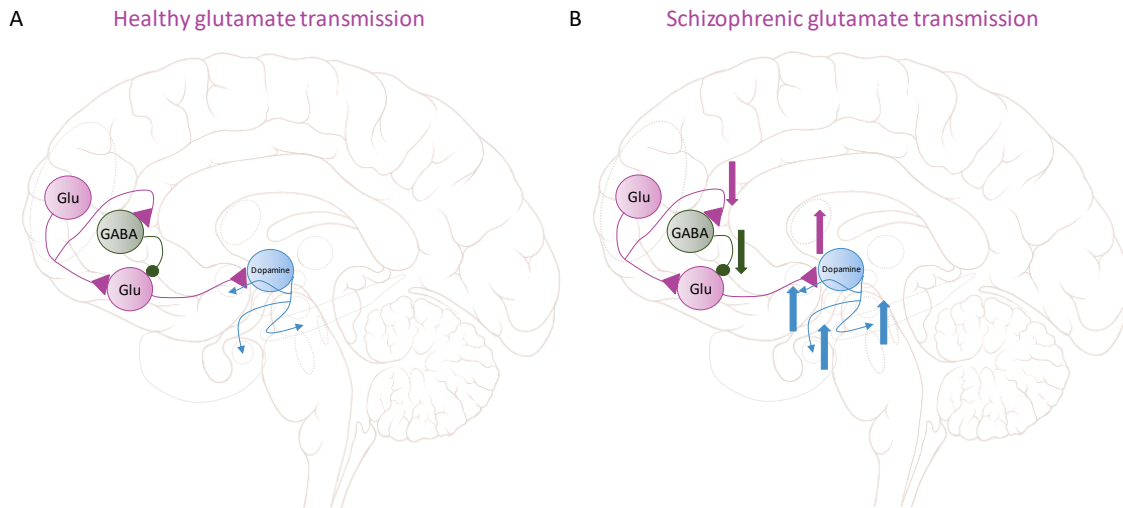


Fig. 6 Positive symptoms of schizophrenia according to glutamate hypothesis. (A) Healthy glutamate transmission in cortical brainstem pathway. (B) Schizophrenic glutamate transmission in cortical brainstem pathway. Glutamatergic neurons (Glu) are shown in purple, GABAergic neurons (GABA) shown in green, Dopaminergic neurons (Dopamine) shown in blue. Glutamatergic synapses are indicated as purple triangles. GABAergic synapses are indicated as green circles. Increased and decreased synaptic transmission are shown with arrows directed upwards and downwards respectively in colour specific to the neurotransmitter. Adapted from (Schwartz, Sachdeva and Stahl, 2012).

The negative symptoms can be explained with a slightly more complex system. The first cortical glutamatergic neuron is firing upon a GABAergic interneuron, which in normal conditions reduces the firing rate of a secondary glutamatergic neuron upon the second GABAergic neuron, which decreases the firing of a dopaminergic neuron projecting to the PFC. In schizophrenia, both GABAergic neurons are compromised due to the hypofunction of NMDAR receptors, causing increased transmission of the secondary glutamatergic neuron. This finally leads to overstimulation of the second GABAergic neuron and, in consequence, a decreased activity of dopaminergic neurons in the PFC (Schwartz, Sachdeva and Stahl, 2012) (Fig. 7).

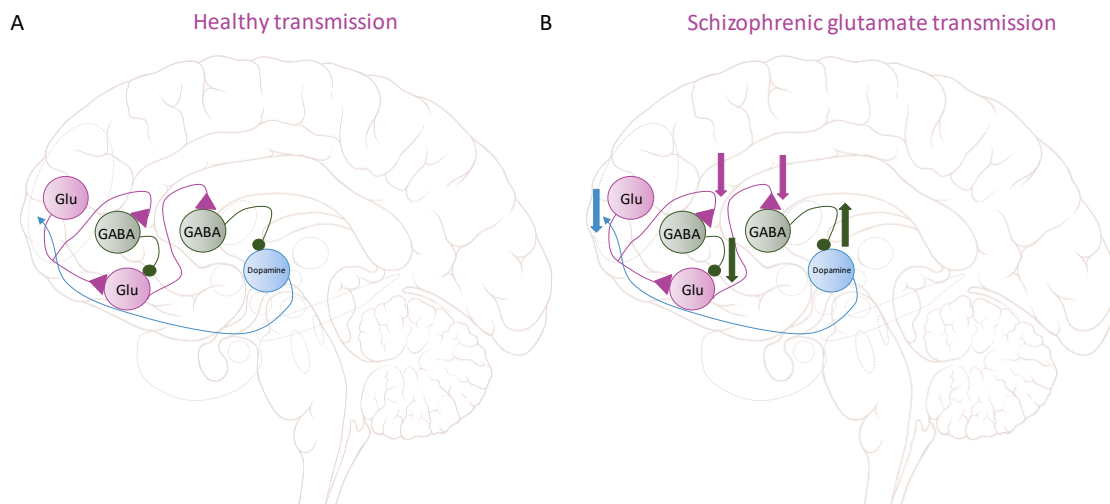


Fig. 7 Negative symptoms of schizophrenia according to glutamate hypothesis. (A) Healthy glutamate transmission in cortical brainstem pathway. (B) Schizophrenic glutamate transmission in cortical brainstem pathway. Glutamatergic neurons (Glu) are shown in purple, GABAergic neurons (GABA) shown in green, Dopaminergic neurons (Dopamine) shown in blue. Glutamatergic synapses are indicated as shown as purple triangles. GABAergic synapses are indicated as green circles. Increased and decreased synaptic transmission are shown with arrows directed upwards and downwards respectively in colour specific to the neurotransmitter. Adapted from (Schwartz, Sachdeva and Stahl, 2012).

Interestingly, NMDAR receptors located on GABA-ergic interneurons were described to be 10-fold more sensitive to NMDAR antagonists than NMDAR receptors located on pyramidal cells (Olney and Farber, 1995; Grunze et al., 1996). Moreover, the GRIN2A NMDAR subunit, which is associated with the disease and whose mRNA was reported to be decreased in GABAergic interneurons in schizophrenia patients (Woo, Walsh and Benes, 2004; Woo, Kim and Viscidi, 2008), is expressed five-fold higher in parvalbumin-expressing GABA-ergic interneurons than in pyramidal cells (Kinney et al., 2006). Those results give more insight into the biology of the disease and, considering the role of PV interneurons in the maturation of the mPFC, also in the development of schizophrenia.

1.3.5 The ECM alteration in schizophrenia

An increasing body of evidence shows ECM alteration in the schizophrenic brain. Human *post mortem* brain studies have reported reduced density of PNN in schizophrenia pathophysiology-related areas, such as the PFC (Enwright *et al.*, 2016), the entorhinal cortex, the amygdala

(Pantazopoulos *et al.*, 2010) and the hippocampus (Shah and Lodge, 2013). Moreover, decreased densities of aggrecan 3B3-immunoreactive PNN around parvalbumin neurons, CS56-immunoreactive glial form of PNN called dandelion-like structure (DACS) and aggrecan 3B3-immunoreactive glial form of PNN, were reported in the amygdala of *post mortem* schizophrenic brains (Pantazopoulos *et al.*, 2015). Additionally, reduced expression of chondroitin sulfate proteoglycans was shown in the olfactory epithelium of schizophrenic patients (Pantazopoulos *et al.*, 2013). Altogether those findings suggest that compromised ECM surrounding neurons and glia may play a role in schizophrenia pathophysiology.

In addition, 50% reduction of mRNA and protein levels of the ECM glycoprotein reelin, responsible for cell-cell interaction in cell migration and orientation process, were found in several brain areas of schizophrenia patients, including PFC and hippocampus (Impagnatiello *et al.*, 1998; Fatemi *et al.*, 1999; Guidotti *et al.*, 2000). Furthermore, expression levels of laminin - known to promote cell migration, differentiation, and axonal guidance- and collagen - known to regulate neuronal maturation- were reduced in human *post mortem* superior temporal cortex of schizophrenic patients (Schmitt *et al.*, 2012). Those deficits of the ECM may suggest its role in schizophrenia patients' early development changes in the brain.

Moreover, a massive increase in density of astrocyte-related forms of PNN was reported in the amygdala and entorhinal cortex of schizophrenic patients (Pantazopoulos *et al.*, 2010) suggesting a possible role of ECM in CNS inflammation responses during schizophrenia. However, a more recent study using human induced pluripotent stem cell-derived glial mouse chimeras reports schizophrenic glial progenitor cells induced changes in mice behavior, astrocytic morphology, electrophysiology and numerous glial progenitor cell gene expression including synapse-regulation-related ECM proteins TN-R and BCAN. In this study, Windren and colleagues used glial progenitor cells produced from induced pluripotent stem cells derived from patients with childhood-onset of schizophrenia and healthy individuals. The RNA sequencing of cultured schizophrenic human glial progenitor cells shows alteration in gene expression related to glial differentiation, synaptic transmission and ECM suggesting that glial pathology in those cases is cell-autonomous. The myelin wild-type mice which undergo neonatal implementation of human schizophrenic glial progenitor cells show the reduced threshold for hippocampal LTP, reduced PPI, excessive anxiety, antisocial traits and disturbed sleep, which can be considered as schizophrenia-like behavior in mice. Whereas myeline deficient schiverer mice, which undergo neonatal implementation of human schizophrenic glial progenitor cells show premature migration of glial progenitor cells into the cortex, resulting in hypomyelination as well as delayed astrocytic

differentiation and abnormal astrocytic morphologies suggesting a role of glial progenitor cells in hypomyelination and astrocytic abnormalities in childhood-onset of schizophrenia (Windrem *et al.*, 2017).

1.3.6 Treatment - typical and atypical antipsychotics

The first milestone in the pharmacological treatment of schizophrenia is a publication of Nobel prize winner Arvid Carlsson and Margit Lindqvist who reported in 1963 that small doses of two tranquillizers - chlorpromazine and haloperidol do not change dopamine levels in mice brains and probably inhibit neuronal transmission through blocking of the neurotransmitter receptor (Carlsson and Lindqvist, 1963). This finding initiated the shift in schizophrenia treatment from targeting neurotransmitters to targeting dopamine D2 receptors with the first generation of antipsychotics.

The first generation of antipsychotic drugs - called also typical antipsychotics - are dopamine D2 receptor antagonists. In this group, we can distinguish high potency antagonists such as Haloperidol, Fluphenazine, prochlorperazine and Trifluoperazine and low potency antagonists such as chlorpromazine. The high potency antagonists, due to strong binding with D2 receptor, acutely reduce psychosis in relatively low dosage, but also tend to cause more extrapyramidal side effects. On the other hand, low potency antagonists do not attach so strongly to D2 receptors and, therefore, induce a milder reduction in dopamine transmission; thus, causing milder extrapyramidal symptoms. However, they also have unspecific binding to other neurotransmitter receptors such as α -adrenergic, cholinergic and histamine receptors. This causes a variety of drug binding profile-specific side effects including sedation, weight gain, blurred vision, constipation and orthostatic hypotension. Although first generation antipsychotics reduce positive symptoms of the disease, they also tend to increase negative symptoms and cognitive deficits in the disease.

The second generation of antipsychotic drugs – called also atypical antipsychotics such as risperidone, olanzapine, clozapine and lurasidone, block dopamine D2 receptor as well as serotonin 5-HT_{2A} receptor. The 5-HT_{2A} receptor activation inhibits dopamine release. Therefore, blocking this receptor increase dopamine level, which is critical in brain areas that need it such as the prefrontal cortex or striatum. The atypical antipsychotics mechanism of action causes less extrapyramidal side effects as well as negative symptoms and impaired cognition side effects in comparison to typical antipsychotics. However, those drugs also have off-target binding partners and cause different side effects depending on the drug binding profile.

The introduction of aripiprazole in 2002 to schizophrenia treatment initiates the third generation of antipsychotic drugs. The third-generation antipsychotics are partial agonists of dopamine D2 receptor, antagonists of serotonin 5-HT_{2A} receptor and agonists of serotonin 5-HT_{1A} receptor. The partial agonists of the D2 receptor may act as receptor agonist or antagonist depending on endogenous receptor activation. This mechanism of action should theoretically reduce dopamine hyper-transmission in the mesolimbic pathway and increase dopamine hypo-transmission in the prefrontal cortex, allowing addressing both positive and negative symptoms of schizophrenia. Additional activation of serotonin 5-HT_{1A} receptor modulates motor function, mood and cognition. Although recent studies using the new third-generation drug cariprazine seem to confirm its effect against positive, negative and cognitive symptoms of schizophrenia, there is still heterogeneity in patient's response to the treatment and there is a strong need for a better understanding of the disease to develop a better treatment strategy.

1.4 The ketamine model of schizophrenia

Schizophrenia is a disorder of the human brain, although investigating this disorder in human individuals is extremely challenging. The limitation factors are the heterogeneity of genetic background, environmental factors, therapy and lack of brain samples. Therefore, there is a strong need for animal models of the disease. However, the potential of animal models is limited to certain aspects of the disease.

There are numerous animal models of schizophrenia, which can be divided into four categories: neurodevelopmental, pharmacological, lesion-based and genetic models. Each animal model can be validated using three criteria: the construct, the face and the predictivity. The animal model construct replicates the pathology and neurobiological rationale of schizophrenia. The animal model face shows the symptom homology with schizophrenic patients. Whereas, predictivity indicates the expected response or lack of response to pharmacological treatment used in schizophrenic patients (Jones, Watson and Fone, 2011).

Here we use a pharmacological rat model based on sub-chronic administration of NMDA receptor antagonist ketamine, based on the glutamate hypothesis of the disease. Ketamine, known under IUPAC name 2-(2-chlorophenyl)-2-(methylamino) cyclohexan-1-one, is a phencyclidine (PCP) derivative. It is primarily used as an anaesthetic in humans and animals, but it was also reported to have analgesic, anti-inflammatory and recently antidepressant properties. Due to its hallucinogenic and dissociative effects, ketamine is also used as a recreational drug (review by Frohlich and Van Horn, 2014).

Several studies on ketamine effect on healthy individuals have shown that already with the first intravenous administration of ketamine participants experience positive psychomimetic symptoms such as conceptual disorganization, hallucinations and suspiciousness, as well as negative psychomimetic symptoms such as blunted affect, emotional withdraw and motor retardation. Long-term ketamine abuse is associated with cognitive impairments (Krystal *et al.*, 1994; Morgan, Muetzelfeldt and Curran, 2009; Frohlich and Van Horn, 2014).

A magnetic resonance imaging study performed on recreational ketamine users reported cortical atrophy in the frontal, parietal and occipital lobes as well as a loss of frontal cortical white matter microstructure integrity (Edward Roberts *et al.*, 2014).

The previous studies using rat model sub-chronically treated with ketamine showed behavioural alterations that mimic schizophrenia-like negative symptoms such as the increase of aggressive behaviour and disrupted latent inhibition (Becker *et al.*, 2003). Latent inhibition is a phenomenon linked with the activity of the rat prefrontal cortex in which repeated preexposure of a conditioned stimulus that is not reinforced retards future association of this stimuli with an unconditioned stimulus. In humans, the disrupted latent inhibition is associated with the active phase of schizophrenia (Lubow *et al.*, 2000; Schmidt-Hansen, Killcross and Honey, 2009). The ketamine-induced changes in social behaviour were reported to be normalized by atypical antipsychotics such as diazepam, clozapine and risperidone (Keilhoff *et al.*, 2004).

The prepulse inhibition is linked with the activity of the rat hippocampus, in which exposition to weak prepulse stimuli reduces the startle reflex on following stronger stimuli. Disrupted prepulse inhibition shows a lack of ability to filter out non-important information and is strongly associated with schizophrenia disease. However, the rat model sub-chronically treated with ketamine showed no disruption of prepulse inhibition. The sub-chronic ketamine treatment did not affect locomotor activity, anxiety levels or social interaction time in rats (Becker *et al.*, 2003).

Previous studies using subchronically treated ketamine rat model show altered hippocampal expression of parvalbumin, neuronal nitric oxide synthase and cFOS similar to those found in human schizophrenia GABAergic interneurons in the hippocampus (Keilhoff *et al.*, 2004).

Although ketamine is primarily a ligand for NMDAR, it also has a varying degree of affinities for several other receptors (Kapur and Seeman, 2002; Hunt, Kessal and Garcia, 2005). An animal study using the rat ketamine model of schizophrenia shows dopamine D2, but not D1, receptor binding was increased in the hippocampus. Whereas glutamate binding was significantly reduced by 25% in the frontal cortex. The density of serotonin transporters increased in the striatum,

hippocampus and frontal cortex. Whereas dopamine transporter increased by 24% in stratum (Becker *et al.*, 2003).

1.5 The HAPLN1 protein

The HAPLN1 protein belongs to the hyaluronan and proteoglycan link proteins family containing four members: HAPLN1(Ctrl-1), HAPLN2 (Bral-1), HAPLN3 and HAPLN4 (Bral-2). Among those four members, three are predominantly expressed in CNS and brain. Those members are HAPLN1, HAPLN2 and HAPLN4. The HAPLN1 and HAPLN4 were reported to be part of PNNs and are expressed exclusively in neurons enwrapped in PNN. Whereas HAPLN2 was detected in myelinated fibre tracts in the adult brain and colocalized with the versican V2 isoform at the nodes of Ranvier (Oohashi *et al.*, 2002).

The HAPLN1 gene, as well as other link proteins, consists of an N-terminal signal sequence followed by the immunoglobulin domain and two consecutive link modules. The structure of HAPLN proteins is homologous to CSPGs N-terminal G1 domain responsible for binding to hyaluronan. The hyaluronan, CSPGs and HAPLN1 molecules form a tripartite complex in which HAPLN is suggested to stabilize noncovalent binding between CSPG and hyaluronan. The low level of sequence identity between the Ig domains of HAPLN members was suggested to affect HAPLN specificity. In the human genome, each HAPLN gene is colocalized with one of the four major CSPGs, suggesting that those paralogues can be expressed at the same time. Those paralogous are: HAPLN1 - versican, HAPLN2 - brevican, HAPLN3 - aggrecan and HAPLN4 - neurocan. However, HAPLN1 protein can be also co-expressed with aggrecan (Carulli *et al.*, 2010).

Most of the PNN components are expressed in the brain long before PNNs start to form, but link proteins and aggrecan are upregulated at the same time as PNN formation begins (Carulli *et al.*, 2010). *In vitro* experiments using HEK293T cells expressing the PNN molecules show that PNN formation requires a combination of HAS-3, HAPLN1 and aggrecan proteins (Kwok, Carulli and Fawcett, 2010). Moreover, animal studies using HAPLN1-deficient mice have shown strong attenuation of PNNs. The Wisteria floribunda staining has shown no PNN pattern around dendrites and a reduced amount of PNN around parvalbumin-positive interneuron somas.

Behavioural studies on mice lacking HAPN-1 in their CNS showed enhanced plasticity in the visual and somatosensory systems in the adult brain. Altogether, these results suggest that

HAPLN1 is necessary for the proper formation of PNNs and its deficiency compromises PNN regulatory function during the critical period (Carulli *et al.*, 2010).

Additionally, a recent study of the molecular signatures of ECM pathology in human schizophrenic *postmortem* brain samples shows increased mRNA levels of HAPLN1 and several hyaluronan synthesis and binding molecules such as HAS1, HAS2, HAS3, HABP2 and HABP4 across most of the investigated brain areas including PFC. The study also reports a decrease in mRNA levels of HAPLN2 and CD44 genes in the PFC of schizophrenic brain samples (Pantazopoulos *et al.*, 2021). Although this study cannot conclude if reported alterations are of disease or treatment origins it suggests that schizophrenic patients have altered gene expression of hyaluronan-related molecules which may lead to lower hyaluronan levels and deficits of hyaluronan interactions with cell membranes and proteoglycans.

2 Objectives of the thesis

As described above schizophrenia is a heterogeneous mental disorder characterized by the altered ratio of excitatory to inhibitory cortical activity and extracellular matrix deficits in several brain areas. The glutamate hypothesis of schizophrenia provides a plausible explanation of the role of the NMDA receptor hypofunction in generating the cortical excitatory and inhibitory imbalance leading to both positive and negative symptoms of the disease. This hypothesis also addresses the parvalbumin-expressing interneurons deficits in the schizophrenic brain as NMDA receptors composition on GABA-ergic interneurons were reported to be enriched in GRIN2A NMDAR subunit associated with the disease.

Interestingly several lines of evidence show that extracellular matrix might affect NMDAR-dependent glutamate transmission as well as GABA-ergic transmission.

Although schizophrenia is a disease of the human brain it is extremely difficult to obtain reliable data from schizophrenic patients post mortem brain samples due to heterogeneous genetic background, environmental factors treatments and sample processing. Therefore, there is a strong need to provide reliable animal models mimicking particular aspects of the disease.

Here we use a validated pharmacological model of schizophrenia targeting NMDA receptor to investigate NMDAR hypofunction effect on PV-expression interneurons in two disease-related brain areas, mPFC and hippocampus.

Using this model, we investigate if ketamine-induced glutamate hypofunction affects the density and fine structure of PNN surrounding those neurons.

Additionally, using rats treated with popular typical and atypical antipsychotics we investigated if those treatments might affect PNN around PV-expressing interneurons.

Moreover, we use a molecular model of mPFC HAPLN1 deficient mice to investigate if HAPLN1 deficits might affect excitatory-inhibitory balance in the cortical area.

3 Materials and methods

Parts of this section have already been published in (Matuszko *et al.*, 2017).

3.1 Animals

Sprague–Dawley (MolTac:SD, Taconic Denmark, SPD) male rats were used in all ketamine-induced schizophrenia model experiments. The animals were kept in controlled laboratory conditions: at $20 \pm 2^\circ\text{C}$, air humidity 55–60% and 12-h day/night cycle (lights on at 6 a.m.). The rats were housed in a group of five animals in Macrolon IV cages, with free access to food pellets (Altronim 1326) and tap water.

C57BL/6J mice were bred at the animal facility of DZNE Magdeburg and kept in standard laboratory conditions: at 20°C constant temperature, 12:12 h day/night cycle (lights on at 9 a.m.), tap water and food *ad libidum*. Littermate mice were housed with the mother first four weeks and later in groups of four to five animals. The father was removed from the cage before birth. After receiving the transcranial injection pups and mother was placed in inverted day/night cycle condition (lights on at 9 p.m.).

3.2 Hippocampal primary cell culture

Twelve-well cell culture plates (CellStar 666180) have been coated freshly before culture preparation with poly L-lysine hydrobromide (100 $\mu\text{g}/\text{ml}$, Sigma Aldrich 25988-63-0) and 25 $\mu\text{g}/\text{ml}$ laminin from Engellreth-Holm-Swarm murine sarcoma basement membrane (Sigma Aldrich L2020) for 1.5 h at RT, washed 3 times with distilled sterile water and kept with distilled water until use.

C57BL/6J female mice were sacrificed by spinal dislocation on the eighteenth day of pregnancy. Uteri were dissected and placed into ice-cold Hanks' Balanced Salt solution (HBSS) (Invitrogen 14175129). All the embryos were subsequently sacrificed. Hippocampi were dissected, cleaned from meninges and collected in a Petri dish with fresh ice-cold HBSS. Hippocampal tissue was chopped into approximately 1 mm^3 pieces and transported into Ca^{2+} and Mg^{2+} free PBS (Gibco 10010-015). Afterwards, the tissue was enzymatically digested using 0.25% trypsin-EDTA solution (Invitrogen 25200072) for 20 minutes at 37°C and triturated using a glass pipette. Cell debris was removed by centrifugation at 1500 g for 2 min. Cells were resuspended in PBS and counted manually under a light microscope using hemocytometer C-Chip (NanoEnTek DHC-

N01). Cells were plated at the density of 200 000 cells per one well in Dulbecco's Modified Eagle Medium (DMEM, Gibco 41965-039) supplemented by L-glutamine (20 mM, Gibco 25030-024), 1x B-27 (Gibco 17504-044) and penicillin and streptomycin (100 units/ml and 100 ng/ml, respectively, Pen Strep, Gibco 15140-122) called later DMEM⁺⁺⁺. After 3 h media was changed to Neurobasal medium (Gibco 21103049) supplemented with L-glutamine (20 mM), 1x B-27 (Gibco 17504-044) and penicillin and streptomycin (100 units/ml and 100 ng/ml, respectively, Pen Strep, Gibco 15140-122) called later Neurobasal⁺⁺⁺ in 1:1 ratio with astrocyte conditioned Neurobasal medium. Cells were incubated at 37 °C, and 5% CO₂ and 90-95% air humidity. Additional 200 µl of Neurobasal⁺⁺⁺ medium was added to each well at the day *in vitro* (DIV) 10, 17 and 21 and astrocyte conditioned medium (see below) was added at DIV14 to restore the level of astrocyte-secreted trophic factors and increase the cell survival rate.

3.2.1 Astrocyte conditioned medium

Astrocyte primary cell cultures were prepared from the cortex of E18 C57BL/6J mice in the same way as a neuronal culture. Cells were plated in DMEM medium supplemented by penicillin (100 Units/ml), streptomycin (100 ng/ml), 10% fetal bovine serum (Gibco 10270-106) and 0.6% sucrose. After 3h, the medium was changed to Neurobasal medium supplemented by penicillin (100 Units/ml), streptomycin (100 ng/ml), 20 mM L-glutamine and 0.6% sucrose. Astrocytes were incubated at 37 °C, and 5% CO₂ and 90-95% air humidity for 2.5 weeks. Afterwards, the medium was removed and cells were washed twice with fresh and prewarmed Neurobasal medium supplemented by penicillin (100 units/ml), streptomycin (100 ng/ml), 200 mM L-glutamine and 0.6% sucrose and incubated with the same medium. After 48h, the conditioned medium was collected and frozen at -20 °C.

3.2.2 AAV infection of hippocampal primary cell culture

At DIV 7, each well was infected with AAV_U6_HAPLN1_shRNA1_GFP (titer 2.35x10⁸), or separately with AAV_U6_scramble_shRNA_GFP control virus (same titer), both in 10 µl of Neurobasal⁺⁺⁺ medium as a vehicle. Additionally, 10 µl of Neurobasal⁺⁺⁺ were added in 3 wells as a negative control.

3.3 AAV preparation and injection

3.3.1 Construct preparation

For the construction of the HAPLN1 knockdown viruses, 3 pairs of oligonucleotides were designed, each containing 19 nucleotides, using mouse HAPLN1 sense and antisense si-RNA sequences (according to Dharmacon pGIPZ/SMART vector sequences):

HAPLN1_1 (V3LMM_508283), forward 5'GATCCGAACTCTGTCTTGATCTGGATTCAAGAGATCCAGATCAAGACAGAGTTCTTTTTG-3' and reverse 3'GCTTGAGACAGAATA GACCTAAGTTCTCTAGGTCTAGTTCTGTCTCAAGAAAAAACTTAA-5';

HAPLN1_2 (V3SM7671-232950004), forward 5'GATCCGTTAAGATTGTAGCGTCCCATTC AAGAGATGGGACGCTACAATCTTAACTTTTTG-3' and reverse 3'GCAATTCTAACATC GCAGGGTAAGTTCTCTACCCTGCGATGTTAGAATTGAAAAAACTTAA5';

HAPLN1_3 (V3SM7671-235483348); forward 5'GATCCGTGACCAGGGAGGCATCAT TTTCAAGAGAAATGATGCCTCCCTGGTCACTTTTTTG-3' and reverse 3'GCACTGGT CCCTCCGTAGTAAAAGTTCTCTTTACTACGGAGGGACCAGTGAAAAAACTTAA-5'.

A pair of oligonucleotides containing sequence published by Mao and colleagues in 2009 (Mao et al., 2009) was used as a control: forward 5'GATCCGCGGCTGAAACAAGAGTTGGTT CAAGAGACCAACTCTTGTTTCAGCCGCTTTTTTG-3' and reverse 3'GCGCCGACTTT GTTCTCAACCAAGTTCTCTGGTTGAGAACAAAGTCGGCGAAAAAACTTAA-5'.

Each pair of oligonucleotides was phosphorylated and annealed by incubation with 5U polynucleotide kinase (T4 PNK) (NEB M0201S) for 30 min at 37 °C, followed by enzyme deactivation for 5 min at 95 °C, and cool down for 20 min. Annealed oligonucleotides were ligated with previously digested (using restriction sites BamHI and EcoRI), pAAV-U6-GFP plasmid (Cell Biolabs #VPK-413; Fig. 8). Ligation was done using T4 ligase (NEB M0202S) overnight at RT. Ligated constructs were multiplied in Stable 3 competent cells after heat shock transformation. Positive clones were selected using LB ampicillin agar plates. From each construct, 10 colonies were selected for liquid culture. Plasmid DNA was then isolated using GeneJET Plasmid Miniprep Kit (Thermo Fischer Scientific K0503). Next positive clones were validated using EcoRI and AgeI restriction enzymes and sequenced. Validated clones were multiplied in Stable 3 competent cells, plasmid DNA was isolated using GenElute™ HP Plasmid Maxiprep kit (Sigma NA0310) and used for AAV preparation.

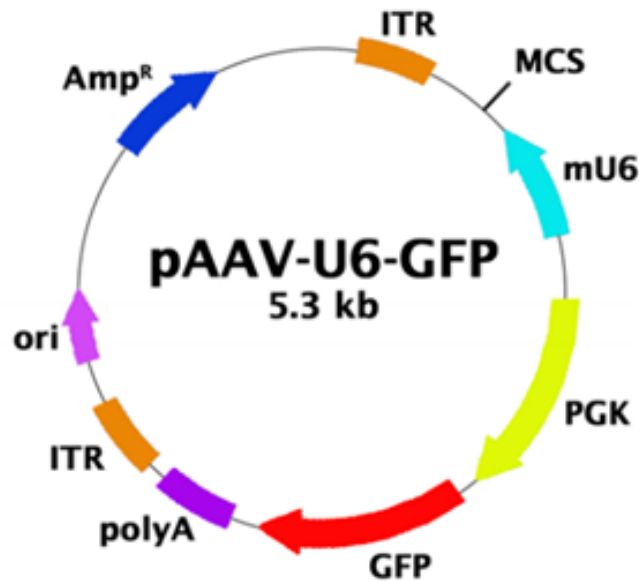


Fig. 8 pAAV_U6_GFP vector (Cell Biolabs #VPK-413). ShRNA oligonucleotide sequence was inserted in the multicistronic site (MCS), under universal promoter U6, marked in turquoise. The plasmid contains reporter gene coding green fluorescence protein (GFP) here marked in red, under separate universal promoter PGK marked in yellow. Also, selective gene sequence coding Ampicillin resistance, marked in blue, and origins of replication (*ori*) sequence marked in magenta, are under PGK promoter. hGH polyadenylation (polyA) and termination signal are shown in purple. Finally, the inverted terminal repeats (ITR) sequence, marked in orange, initiates viral DNA replication and is essential for successful virus packaging, integration and rescue. Adapted from *Cell Biolabs*.

3.3.2 HEK 293T culture

Human embryonic kidney cells HEK 293 T were cultured according to standard protocols in Iscove's modified Dulbecco's medium (IMDM) (Gibco 12440053) supplemented by penicillin (100 Units/ml), streptomycin (100 ng/ml), 10% fetal bovine serum at 37 °C, and 5% CO₂ and 90-95% air humidity.

3.3.3 Polyethylenimine Transfection

One day before transfection, cells were passage in a manner to reach on the next day 70-80% confluence on 140 mm Petri dish. Two dishes were prepared per each viral construct. 27 µg DNA of the plasmid of interest were mixed with pHelper, pDP1 and pDP2 plasmid in molar ratio 1:1:1:1 in IMDM media. Next, linear polyethylenimine (PEI) (Polysciences, Inc 23966-1) 1 mg/ml,

pH = 7, filtered using 0.22 μm filter was added in a 1:2 mass ratio. Then, the mixture was incubated for 15 min at RT and then half of it was added dropwise to each Petri dish. Cells were incubated overnight at 37 °C, 5% CO₂ and 90-95% air humidity. Next, 100% of the medium was exchanged for fresh IMDM media supplemented by penicillin (100 Units/ml), streptomycin (100 ng/ml), 10% fetal bovine serum and incubated for 48 h. Afterwards, cells were first washed with pre-warmed 10 ml PBS, then resuspended in 9 ml of warm PBS and centrifuged 10 min. at 1000 rpm at 4 °C. The collected cells in the cell pellet were frozen and kept at -80 °C.

3.3.4 Viral particle purification

Collected cells were lysed in 20 mM Tris (Sigma T6066) and 150 mM NaCl (Sigma S7653), at pH = 8 using 3 times freeze-thaw technique. Next, genomic DNA was digested using 50 U/mL benzonase nuclease in the same buffer at 37 °C for 1h. Afterwards, cell debris was separated by centrifugation at 4000 g for 30 min at 4 °C and filtrated using a 0.22 μm syringe filter (Carl Roth KH54.1). Viral particles were further purified using a HITRAP heparin column (VWR International 17-0406-01) according to the manufacturer's instruction. Contaminations were washed out using 20 ml of sterile 20 mM Tris, 100 mM NaCl buffer, pH = 8.0, and then with 5 ml of sterile buffer containing 20 mM Tris and 200 mM NaCl, pH = 8.0. Purified viral particles were eluted using 6 ml of sterile 20 mM Tris plus 500 mM NaCl solution, pH = 8.0. In order to exchange vehicle to biological neutral PBS solution, eluted viral particles were centrifuged with 100 kDa cut off Amicon ultra-4 centrifugal filter with stepwise-added PBS solution at 2000 rpm at 4 °C till volume reduction up to 50 μl . The purified and concentrated virus was next filtered using a 0.22 μm syringe filter and aliquoted in sterile conditions and frozen at -80 °C.

3.3.5 Viral titration

A sample of 3 μl was taken from each batch of the prepared virus, for titration. Viral capsid was digested using 5 mg/mL proteinase K (Sigma P2308) in Q5 buffer solution (BioLabs B9027S) for 1 hour at 50 °C followed by enzyme deactivation for 20 min at 95 °C and cooling down on the ice for 5 min. Digested samples were then diluted and quantified using quantitative polymerase chain reaction (QPCR) with QuantStudio 5 Real-Time PCR System device (Thermo Fischer Scientific). In order to recognize DNA construct FAM-tagged-hGH polyA, TaqMan fluorescent probe 5'AGTTGTTGGGATTCCAGGCATGCATGACCA with forward 5'TTCAAGCGATTCTCCTGCCTC and reverse 5'GAGATTAGGAGTTGGAGACCAGC

primers were used. Quantity of plasmid copies was calculated according to a calibration curve prepared using AAV1/2_U6_shRNA_scramble_GFP DNA described in Fig. 9: the viral titer in viral particles per mL was the result of interpolating the linear function derived from the calibration curve and multiplying by the dilution factor. All samples were measured from two technical replicates.

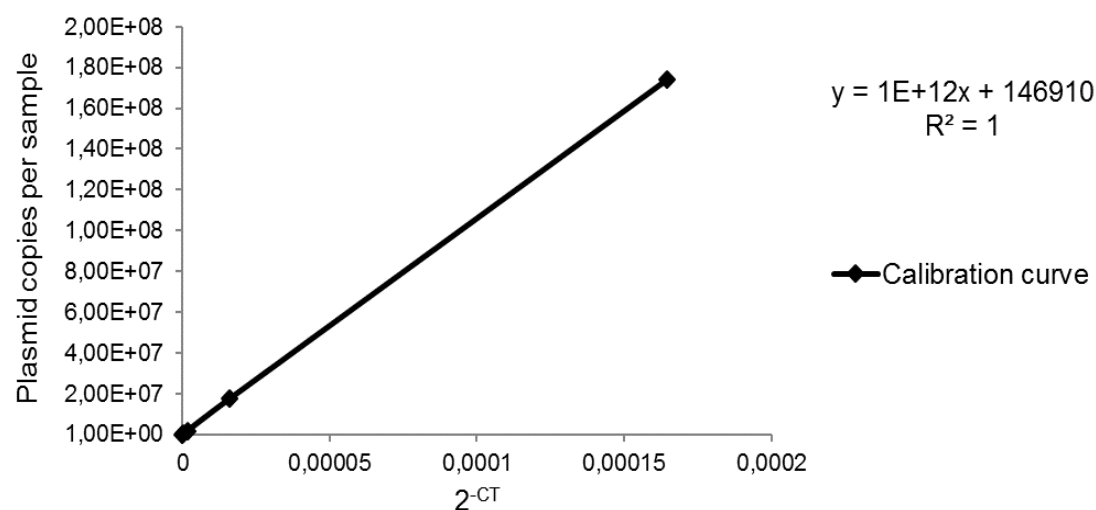


Fig. 9 QPCR calibration curve. The curve was calculated using AAV1/2_U6_shRNA_scramble_GFP DNA in concentrations: 1ng, 0.1ng, 0.01ng, 0.001ng and 0.0001ng per sample. The plasmid copies for these concentrations were calculated from DNA mass in gram and MW giving respectively 1.74×10^8 ; 1.74×10^7 ; 1.74×10^6 ; 1.74×10^5 ; 1.74×10^4 copies per sample. 2^{-CT} factors for each point respectively: 0.00016451; 0.00001593; 0.00000162; 0.00000011; 0.00000004 were calculated from the CT values generated automatically using QuantStudio™ Design and Analysis Software v1.4.3 respectively: 12.57; 15.94; 19.24; 23.08; 24.69.

3.3.6 Viral validation

HEK 293T cells were plated on 12-well cell culture plates (CellStar 666180), at a seeding density of 200 000 cells per well, and incubated in standard conditions. The next day, cultures were transfected with 1 μ g of pAAV_Syn1_HAPLN1_tagRFP vector and co-transfected in separate wells with 1 μ g of pAAV_U6_HAPLN1_shRNA1_GFP, 1 μ g of pAAV_U6_HAPLN1_shRNA2_GFP, 1 μ g of pAAV_U6_HAPLN1_shRNA3_GFP and 1 μ g of pAAV_U6_scramble_shRNA1_GFP control vector. Each of these four conditions was cultured in three biological replicates. Transfection was made using 150 μ l 500mM Ca sterile buffer A and 150 μ l sterile buffer B containing 140mM NaCl, 50mM HEPES, 1.5mM di-sodium hydrogen

phosphate, pH=7. The day after transfection, 100% medium was exchanged to fresh DMEM media supplemented by penicillin (100 Units/ml), streptomycin (100 ng/ml), 5% fetal bovine serum. Cells were collected forty-eight hours after transfection, and RNA was isolated using a universal RNA purification kit (ROBOKLON GmbH E3598-02) according to the manufacturer's instructions. The quality of the isolated RNA was validated through electrophoresis in 1% agarose gel for 20 min at 140 V. Next 500 ng of each RNA sample was converted into cDNA using a high capacity cDNA reverse transcription kit (Applied Biosystems 4368813). This cDNA was then used for qPCR using human HAPLN1 TaqMan® Gene Expression Assays (Hs01091999_m1) and control housekeeping human gene GAPDH 20× TaqMan® Gene Expression Assay (Hs03929097-g1) according to manufacturer's instructions. Each of the three biological replicates was measured with two technical replicates. Quantity of HAPLN1 cDNA was calculated using a difference between threshold cycle (CT) of housekeeping gene and gene of interest $\Delta\Delta CT$ and normalized for the scramble control. Results showed that shRNA1 was the most promising construct. This construct was used for viral preparation and tested in hippocampal primary cell cultures.

Hippocampal primary cells were cultured as described in part 3.2 and infected with viruses as described in part 3.2.2. At DIV 22 cells were collected and RNA was isolated using the universal RNA purification kit (ROBOKLON GmbH E3598-02), according to manufacture's instructions. The quality of samples was validated through electrophoresis as described in section 3.3.6. Afterwards, 300 ng of RNA were converted into cDNA using the high capacity cDNA reverse transcription kit (Applied Biosystems 4368813). Next, DNA was quantified using mouse HAPLN1 TaqMan® Gene Expression Assays (Mm00488952_m1) and control mouse GAPDH 20× TaqMan® Gene Expression Assay (Mm99999915_g1) according to manufacture instructions. The difference in HAPLN1 DNA quantity was calculated as described in HEK cells using $\Delta\Delta CT$. pAAV_U6_HAPLN1_shRNA1_GFP virus reduced HAPLN1 RNA by 90% and was qualified to be used in animal studies.

3.3.7 Viral injection

Twenty-one postnatal day 8 (P8) C57Bl6/J mice were used for viral injection. They were divided into two groups: 10 animals injected with HAPLN1 knocking down, and 11 with scramble control virus. The age of the animals was chosen based on previous studies showing PNN maturation in mice PFC between post-waving day 7 and 21 (Horii-Hayashi *et al.*, 2015). Shortly before surgery,

animals were separated from the mother, placed in a glass beaker containing bedding from the home cage, to preserve the mother's smell, and placed on a heating pad for body temperature stability. Next, mice were anaesthetized, one at a time, with isoflurane (4 vol%; Baxter, Germany). Cranial skin was locally disinfected with 70% EtOH and incised. Modest holes were drilled bilaterally in the skull above mPFC according to stereotaxic information with respect to external landmarks on the skull (ML=1 mm, DM=1 mm) and to other distinct landmarks such as characteristic blood vessels of the bone as shown in Fig. 10. Afterwards, 500 nl of pAAV_U6_HAPLN1_shRNA1_GFP (titer 7.26x10¹¹), or pAAV_U6_scramble_shRNA1_GFP (titer 7.26x10¹¹) were injected using Nanoliter injector (WPI Item#: NANOLITER2010) and 20 µm tip injection pipettes made from glass capillaries (WPI #504949). To avoid researcher bias during the injection virus samples were anonymized by a researcher noninvolved in the experiment. After injection skin was sutured with Perma Hand Suture size 6 (Johnson & Johnson k889), the animals were placed back into the beaker to recover. All animals were brought back to the home cage together in order to reduce mother stress.

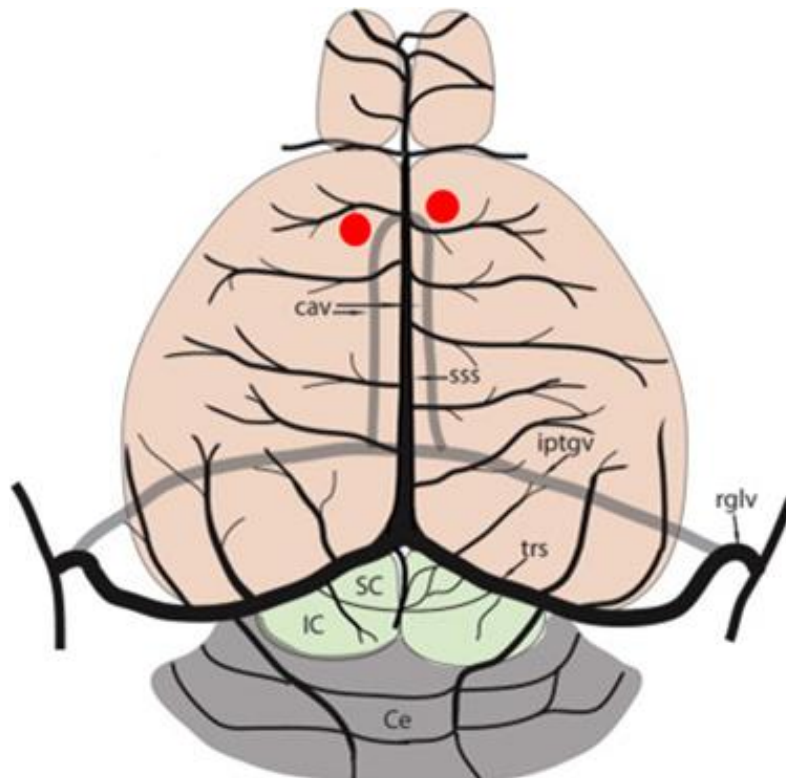


Fig. 10 Characteristic blood vessels used for determination of injection position. Blood vessels visible on the skull, including superior sagittal sinus (sss) used for coordination projected on brain view. Injection sites are marked with red dots. Adapted with modifications from (Scremin and Holschneider, 2012).

3.4 Ketamin treatment

Ketamine treatment was done according to the protocol of Becker and colleagues (Becker *et al.*, 2009). Eight-week-old rats were subjected to sub-chronic administration of ketamine (ketamine hydrochloride, Astrapin, Pfaffen- Schwabenhein, Germany). Ketamine (30 mg/kg b.w.) or 0.9% NaCl vehicle was injected in two sessions of 5 days, with daily injections separated by a 2-day break between sessions. Injections were made intraperitoneally (IP) at a volume of 1 ml/100 g of animal weight.

3.5 Social interaction test

Social interaction test was performed as described previously (Becker *et al.*, 2003; Becker *et al.*, 2009). Briefly, two days after the final injection, control rats and ketamine-treated rats were housed singly in Macrolon II cages with food and water ad libitum for 12 days. Two weeks after the last ketamine injection animals were familiarized with the open field arena (100 x 100 x 40 cm) in two trials of 7 min each two days prior to the social interaction test. The day prior to testing, rats were allocated with test partners based on pretreatment and body weight. The difference between the two partners was within 20 g. During the test, animal pairs were placed in the arena for 7 min. Total time of social interaction was measured and scored as nonaggressive (sniffing, following) or aggressive interactions (chasing, biting) between the two animals. Data are represented as the percentage of nonaggressive behaviour relative to the total social interaction time.

3.6 Acoustic startle reflex and pre-pulse inhibition

Four weeks after AAV injection, acoustic startle reflex (ASR) and pre-pulse inhibition (PPI) were tested with minor modifications as described previously (Valsamis & Schmid, 2011). Briefly, animals were placed in a mouse holder fixed on a motion sensor and housed within a padded soundproof chamber. Startle responses were registered using PHM-250 acoustic startle reflex equipment and analyzed using SOF-825 software (Med Associates, St. Albans, VT, USA). Both ASR and PPI measurements were performed on the same experimental day and the protocol lasted approximately 35 min. Throughout the experiment, sound stimuli were delivered with 10-30 seconds randomized inter-trial intervals.

The experiment consisted of 5 min of acclimation period followed by 50 ASR trials, where white noise pulses of 20 ms (1 ms rise) with five different sound pressure levels (0, 80, 90, 100 and 110

dB) were presented in a pseudo-randomized order. Ten measurements were taken for each pulse level and startle responses were recorded for 500 ms. The PPI trials consisted of 4 ms pre-pulses (white noise, 1 ms rise) of 0, 70, 75, 80 and 85 dB that preceded 20 ms pulses (white noise, 1 ms rise) of 110 dB in a pseudo-randomized order. The inter-stimulus interval was kept constant at 100 ms for all PPI trials. Ten measurements were taken for each pre-pulse level and data acquisition was made for 450 ms after the 110 dB pulse presentation.

Startle responses were quantified by the peak amplitudes reported by the SOF-825 software. The results from ASR trials were obtained by calculating the mean amplitudes of 10 trials for each pulse level. The mean amplitudes were then normalized to 0dB measurements and reported as the relative startle amplitudes. The results from the PPI trials were reported as the average percentage of PPI values of ten trials per pre-pulse level. The percentage of PPI was calculated as follows: $[(\text{response to pulse alone} - \text{response to pre-pulse plus pulse}) / \text{response to pulse alone}] \times 100$.

3.7 Immunohistochemistry

3.7.1 Immunohistochemistry of ketamine-treated rats

Two days after the social interaction test, animals were deeply anaesthetized (400 mg/kg b.w. chloral hydrate injection) and perfused transcardially with 4 % PFA. Brains were incubated overnight in 4 % PFA PBS solution at +4 °C, cryoprotected in 30% sucrose PB solution for 48 h at +4 °C. Then, frozen in 100 % 2-methylbutan at -80 °C and sliced in 50- μ m-thick coronal sections. Floating sections were kept in a solution consisting of 1 part ethylenglycol, 1 part of glycerin, 2 parts of PBS, with pH = 7.2. For each staining condition, three sections per brain area of each animal were selected. All sections were washed in 120 mM phosphate buffer, pH = 7.2.

For double PV and WFA staining, the medial prefrontal cortex (mPFC) and dorsal hippocampal sections were permeabilized with PB containing 0.5 % Triton X-100 (Sigma T9284) for 10 min at RT, followed by application of blocking solution (PB supplemented with 0.1% Triton X-100 and 5 % normal goat serum (NGS) (Gibco 16210- 064) for 1 h at RT. Afterwards, sections were incubated for 48 h in the presence of primary reagents: biotinylated Wisteria floribunda agglutinin (WFA) and rabbit anti-parvalbumin antibody (staining conditions are described in Table 1). Sections were washed three times in PB followed by overnight incubation at 4 °C with secondary reagents, streptavidin-Alexa 488 conjugate and goat anti-rabbit Alexa 546-conjugated secondary antibodies. Sections were washed in PB and stained for 1h with Hoechst 3342 (1 mg/ml in DMSO, 1:500, Sigma B2261) and mounted on SuperFrost glasses with Fluoromount (Sigma F4680).

For triple PV, WFA and HNK-1 staining, mPFC sections were permeabilized with PB buffer containing 0.3 % Triton X-100 for 10 min and blocked in PB containing 0.1% Triton X-100 and 10 % NGS for in 1 h at RT. Afterwards, sections were incubated with primary reagents (Table 1). After three washes in PB, secondary reagents, namely streptavidin Alexa 488, goat anti-rabbit Alexa 647 and goat anti-mouse Alexa 546-conjugated antibodies, were applied overnight at +4 °C.

For triple WFA, S100b and CS56 staining, mPFC sections were treated with blocking solution (PB containing 0.3 % Triton-X 100, 5 % NGS and 25 mM glycine) for 1 h at RT. After incubation with primary reagents (Table 1), sections were washed three times with PB and streptavidin Alexa 488, goat anti-rabbit Alexa 546 and goat anti-IgM mouse Cy5-conjugated antibodies were applied for 3 h at RT. PV, WFA and HNK-1 as well as WFA, S100b and CS56 stained sections were washed in PB and stained with DAPI (Invitrogen 01306, 1 mg/ml, 1:1000) and mounted on SuperFrost Plus (Thermo Scientific J800AMNZ) glasses with Fluoromount (Sigma F4680).

Table 1 Primary and secondary reagents used for histochemistry.

Reagents	Supplier and catalogue number	Dilution and incubation time
<i>Primary reagents</i>		
Rabbit anti-Parvalbumin, whole serum	SWANT PV 25	1:300 36 h, +4 °C
Mouse anti-L2/HNK-1 carbohydrate epitope antibody [ZN-12]	Abcam ab174437	1:200 36 h, +4 °C
Rabbit Anti-S100 β , whole serum	Abcam ab868	1:200 60 h, +4 °C
Mouse IgM Anti-CS-56, ascites fluid	Sigma–Aldrich C8035	1:200 60 h, +4 °C
Biotinylated lectin from <i>Wisteria floribunda</i> (WFA) 1 mg/ml	Sigma–Aldrich L1516	1:500 36 h, +4 °C

Secondary reagents

Goat Anti-IgG rabbit Alexa 647, 2 mg/ml	Thermo Fisher Scientific (A21245)	1:1000 12 h, +4 °C
Goat Anti-IgG mouse Alexa 546, 2 mg/ml	Thermo Fisher Scientific (A11030)	1:1000 12 h, +4 °C
Goat Anti-IgG rabbit Alexa 546, 2 mg/ml	Thermo Fisher Scientific (A11035)	1:1000 3 h, RT
Goat Anti-IgG rabbit Alexa 546, 2 mg/ml	LifeSpan Biosciences (LS-C349700)	1:1000 3 h, RT
Streptavidin Alexa 488, 2 mg/ml	Thermo Fisher Scientific (S11223)	1:1000 12 h, RT

3.7.2 Immunohistochemistry of AAV-treated mice

Six weeks old, previously treated with described AAV mice, were anaesthetized with isoflurane (4 % vol; Baxter, Germany) and perfused transcardially with 4 % PFA. Brain fixation, cryoprotection, slicing and section storage were done the same way as described before for rat tissue. Two brain sections were chosen for each staining condition. To investigate excitatory synaptic markers and ECM in dendritic area, sections were washed three times in PB solution, next permeabilized using PB containing 0.3 % Triton X-100 (Sigma T9284) for 1 h at RT, followed by application of blocking solution (PB supplemented with 0.2% Triton X-100 and 5 % normal goat serum (NGS) (Gibco 16210- 064) for 1h at RT. Afterwards, sections were incubated for 36 h with primary antibody: guinea pig anti-VGLUT1, mouse anti-PSD95, rabbit anti-BCAN and chicken anti-GFP (staining conditions are described in Table 2). Sections were subsequently washed four times in PB solution, then three times for 10 min at RT and the last wash for 3 h was at RT. This was followed by incubation for 2h at RT with secondary antibodies: donkey anti-guinea pig Alexa 405, goat anti-mouse Alexa 546, goat anti-rabbit Alexa 647, goat anti-chicken Alexa 488-conjugated secondary antibodies. Sections were washed three times in PB and mounted on SuperFrost glasses with Fluoromount (Sigma F4680).

In order to quantify inhibitory markers and ECM around cell somata of CaMK2 positive neurons, sections were washed, permeabilised and their non-specific antigens' interactions were blocked as described before for excitatory markers in the dendritic area. Afterwards, the tissue was incubated with primary antibodies: guinea pig anti-VGAT, mouse anti-CaMK2, rabbit anti-BCAN and chicken anti-GFP (Table 2). Then, sections were washed in PB solution as described before for excitatory markers. Next, sections were incubated for 2 h at RT with secondary antibodies: donkey anti-guinea pig Alexa 405, goat anti-mouse Alexa 647, goat anti-rabbit Alexa 546, goat anti-chicken Alexa 488-conjugated secondary antibodies.

For quantification of inhibitory markers and ECM in cell somata of PV immunopositive interneurons, sections were washed, permeabilised and their non-specific antigens' interactions were blocked as described before for excitatory markers. After incubation with primary reagents - guinea pig anti-VGAT, rabbit anti-PV, chicken anti-GFP and biotinylated lectin from *Wisteria floribunda* - (Table 2) sections were washed as described before for excitatory markers. Next, they were incubated for 2h at RT with secondary antibodies - donkey anti-guinea pig Alexa 405, goat anti-rabbit Alexa 647, goat anti-chicken Alexa 488-conjugated secondary antibodies and streptavidin Alexa 546. Sections were washed in PB and mounted on SuperFrost glasses with Fluoromount (Sigma F4680).

Table 2 Primary and secondary reagents used for histochemistry.

Reagents	Supplier and catalogue number	Dilution and incubation time
<i>Primary reagents</i>		
Rabbit anti-BCAN polyclonal Ab	Abcam ab111719	1:1000 36 h, + 4 °C
Chicken anti-GFP polyclonal Ab	Abcam ab13970	1:1000 36 h, + 4 °C
Mouse anti- PSD95 monoclonal Ab	Abcam ab2723	1:200 36 h, + 4 °C

Mouse anti-CaMK2 monoclonal Ab	Abcam ab22609	1:300 36 h, + 4 °C
Biotinylated lectin from <i>Wisteria floribunda</i> (WFA) 1 mg/ml	Sigma–Aldrich L1516	1:500 36 h, + 4 °C
Guinea pig anti-VGAT antiserum	Synaptic systems 131002	1:1000 36 h, + 4 °C
Guinea pig anti-VGLUT1 antiserum	Synaptic systems 135304	1:1000 36 h + 4°C

Secondary reagents

Goat Anti-IgG rabbit Alexa 647, 2 mg/ml	Thermo Fisher Scientific A21245	1:1000 2 h, RT
Goat Anti-IgG mouse Alexa 546, 2 mg/ml	Thermo Fisher Scientific A11030	1:1000 2 h, RT
Streptavidin Alexa 546, 2 mg/ml	Thermo Fisher Scientific	1:1000 2 h, RT
Goat Anti-IgG rabbit Alexa 647, 2 mg/ml	Thermo Fisher Scientific A21236	1:1000 2 h, RT
Donkey Anti-IgG guinea pig Alexa 405, 2 mg/ml	Sigma-Aldrich SAB4600230	1:1000 2 h, RT
Goat Anti-IgG chicken Alexa 488, 2 mg/ml	Thermo Fisher Scientific A11039	1:1000 2 h, RT

3.8 Acquisition and image processing

3.8.1 Acquisition and image processing of rats samples

Images were acquired using Zeiss LSM 700 confocal microscope and EC Plan-Neofluar 20x/0.50 M27, or Plan-Apochromat 63x/1.40 Oil M27 objective for PNN fine structure analysis, while the experimenter was blinded to the treatment group. For each animal, three 50- μm -thick brain sections sampled with 200- μm distance were selected for counting.

In order to analyze cell density in mPFC and hippocampus as well as to perform dendrite analysis in the hippocampus for each section, two z-stack images (16-bit, 10 optical sections, 1.55 μm interval between sections, frame 2048 x 2048, pixel size 0.156 μm) were acquired. Images were processed using ImageJ software. For each z-stack, eight consequent optical sections were chosen to make a z maximum projection. In the hippocampal CA1 area, due to a high density of presynaptic PV⁺ terminals, PV⁺, WFA⁺, and double immunoreactive PV⁺WFA⁺ cells were counted manually. Dendrites from PV⁺ cells were tracked manually and the intensity of fluorescence along the traced line was measured using ImageJ. The obtained values were averaged with a 10- μm step and normalized per mean intensity of the somatic signal in the vehicle group. In the mPFC, the fluorescence detection threshold was adjusted manually to clearly detect PV⁺ cells and then cells were counted automatically using a custom-made ImageJ macro analyzing particles greater than 130 μm^2 (available on request).

To measure the intensity of fluorescence, z-stack images were acquired: six images with PV, WFA and HNK-1 labelling (16-bit, five optical sections, the 1.55- μm interval between sections, 2048 x 2048 pixels, pixel size of 0.156 μm) and six images with WFA, S100b and CS-56 labelling (16-bit, 18 optical sections, the 0.353- μm interval between sections, 512 x 512 pixels, pixel size of 0.625 μm). For mean fluorescence intensity measurements, WFA, HNK-1 and PV average projections of z-stacks were obtained using ImageJ software. Thresholds were adjusted manually. Cell bodies were recognized automatically as particles greater than 65 μm^2 in the PV channel. Three different sets of regions of interest (ROIs) were defined: “full-ROI” to measure mean intensity of signals from the whole PV cell body, a “donut-ROI” to measure WFA or HNK-1 signals from the 1- μm -thick rim around a cell body, as shown in figure 10, and 20.6 x 20.6 μm “square-ROI” (3 ROIs per image sampled as far as possible from cell somata) for measurements of neuropil signal between cell bodies.

For WFA, S100b and CS56 staining average projections of z-stacks (16-bit, 18 optical sections, 0.35- μm intervals between sections, 512 x 512 pixels, pixel size of 0.625 μm) were obtained using ImageJ software. The intensity of CS56 fluorescence was measured for the whole image. Due to variability of CS56 expression outside clusters they were counted and outlined manually (Fig. 13, marked by *).

For PNN fine structure analysis, 10 images of PV⁺WFA⁺ cells for each of the 4 animals per group were acquired as z-stacks (16-bit, 14 optical sections, 0.170 μm intervals between sections, 1024 x 1024 pixels, pixel size of 0.099 μm). Single optical sections were used for quantitative analysis of meshes, which were traced on PV⁺ cell somata using the FIJI Meshes plugin as described previously (Schindelin *et al.*, 2012; Arnst *et al.*, 2016). To define the meshes vertices, the Fiji Point Picker tool was used. Pixels belonging to a particular mesh were selected as a polygon based on the vertex coordinates and quantified using the getHistogram Fiji command. The area of the mesh was calculated as the sum of pixels counts for the whole range of intensity values.

In order to investigate the distribution of WFA intensity of fluorescence along the perimeter of single meshes, a polarity index was calculated. Meshes characterized by WFA signal enrichments at ventricles and lower intensity at the middles of the edges defined as polar. On contrary, meshes with a homogeneously distributed intensity of WFA was defined as nonpolar. Polarity index was calculated as mean intensity in vertices defined by three pixels in vertex divided by the mean intensity of edge middle area defined as three pixels in the middle of edge and indicates WFA signal enrichment at meshes vertices.

3.8.2 Acquisition and image processing of AAV treated mice samples

Images were acquired using Zeiss LSM 700 confocal microscope and Plan-Apochromat 63x/1.40 Oil M27 objective and double digital zoom, while the experimenter was blinded to the treatment group. For each animal, two 50- μm -thick brain sections sampled with 200- μm distance were selected for synaptic markers analysis. In order to quantify synaptic markers in the dendritic area, two 51 μm^2 z-stack images for each section, from AAV infected area were acquired (8 bit, 10 optical sections, 0.3 μm distance between sections, 1024x 1024 pixels, pixel size of 0.050 μm). Afterwards, the first optical section from each z-stack was chosen for further analysis. From each image four 10 μm^2 images were selected in a dendritic area free from cell bodies. Synaptic puncta quantification was conducted with minor modifications as described before by (Castillo-Gomez *et al.*, 2016). All analysis was done using FIJI software and custom made macros (available at

request). The background was subtracted automatically using the rolling ball method, with 50 pixels radius, Gaussian blur filter (1.5 sigma) was applied and 94% of the intensity of fluorescence was set as the threshold for each image. Pre- and postsynaptic puncta were defined as particles bigger than $0.1 \mu\text{m}^2$ and quantified automatically. Synapses were defined if $0.05\mu\text{m}$ -thick donut-like ROIs around presynaptic puncta overlapped with postsynaptic markers binary maps. Expression of ECM around synapses was calculated as intensity of BCAN immunofluorescence in $0.5\mu\text{m}$ -thick donut-like ROI around presynaptic puncta. Additionally, the intensity of BCAN fluorescence was measured in the maximum projection of 5 consecutive optical sections for the whole image.

In order to quantify inhibitory presynaptic puncta around cell bodies of CaMK2 positive cells for each animal, ten $50 \mu\text{m}^2$ z-stack images of infected and CaMK2 positive cells were selected (8-bit, 5 optical sections, $1 \mu\text{m}$ distance between sections, frame of 1024×1024 pixels, pixel size of $0.05 \mu\text{m}^2$). From each stack, the fourth optical section was selected for further analysis. The background was subtracted automatically using the rolling-ball option with a 50-pixel radius, Gaussian blur filter (sigma of 1.5 pixels) was applied and 94% of the intensity of fluorescence was set as the threshold for each image. Cell bodies were defined using GFP signal due to its strong intensity of fluorescence. Synaptic puncta were calculated as particles bigger than $0.1 \mu\text{m}^2$ and overlapping or in $0.5 \mu\text{m}$ donut-like ROI around cell bodies.

3.9 Statistics

Two-tailed t-test, one- and two-way repeated measures (RM) ANOVA were used as indicated in Results and figure legends. If the Shapiro–Wilk normality test failed, the Mann–Whitney test was used instead of the t-test. Differences between groups were considered as significant if the p-value was less than 0.05. The number of animals used, n, is given in figure legends and the results.

4 Results

Parts of this section have already been published in (Matuszko *et al.*, 2017).

4.1 Results for ketamine-treated rats

4.1.1 Social interaction test

In line with the previous studies (Becker *et al.*, 2003, 2009), ketamine treatment led to a reduction in non-aggressive social inter-action relative to aggressive behavior (Vehicle: $84 \pm 4\%$, $n = 7$, ketamine: $57 \pm 9\%$, $n = 5$; one-way ANOVA, $p = 0.03$), as shown in Fig. 11.

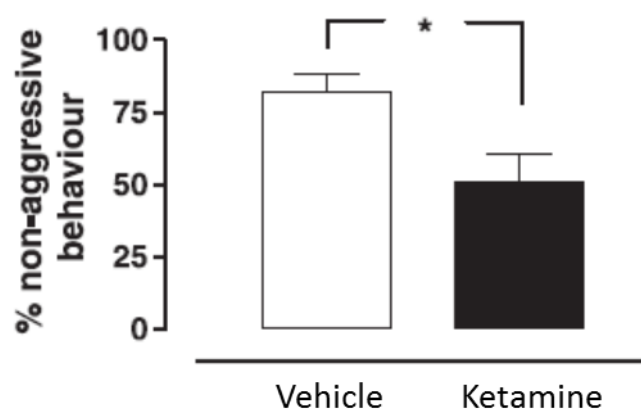


Fig. 11 Social interaction test. Non-aggressive interaction time shown as percentage of total interaction time. Mean \pm SEM, one-way ANOVA, $p = 0.03$, mean \pm SEM values are shown. Vehicle, $n = 5$; ketamine $n=7$. These experiments were performed in collaboration with Prof. Axel Becker from the Department of Pharmacology, University of Magdeburg. ⁺

4.1.2 Densities of PV and WFA positive cells in the hippocampal CA1 area of ketamine-treated rats

After confirmation of ketamine-induced changes in behaviour, I analyzed PNNs in the CA1 region of the hippocampus. This particular brain area was chosen because the majority of the available functional data demonstrating altered synaptic and cognitive functions upon ECM depletion were obtained for this brain region (Senkov *et al.*, 2014). In order to examine PNN expression changes

in the selected area, PV and WFA double staining was performed, and numbers of positive PV⁺, WFA⁺, PV-WFA⁺ and double-positive PV⁺WFA⁺ cells were quantified.

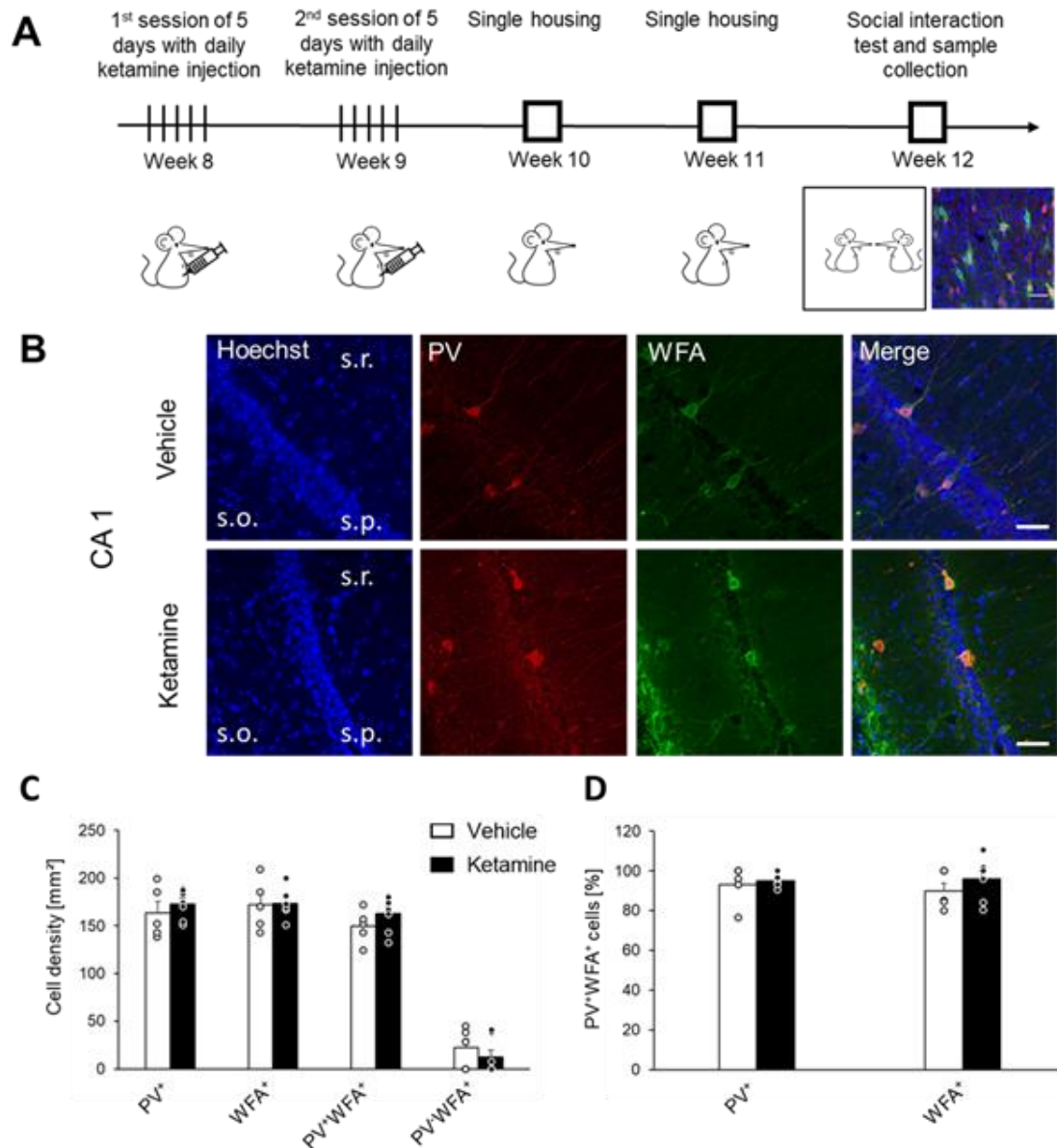


Fig. 12 Densities of PV and WFA positive cells in the hippocampal CA1 area of ketamine-treated rats. (A): The experiment timeline showing the scheme of ketamine treatment, single housing, behavioural test and sample collection. (B): Exemplary images of PV (in red) and WFA (in green) positive cells in the hippocampal CA1 area. Upper panels show vehicle-injected controls while the lower panels demonstrate ketamine-treated animal brains. Nuclei were visualized by the Hoechst reagent (in blue). Scale bar: 50 μ m. (C): PV⁺, WFA⁺, PV⁺WFA⁺ and PV⁻WFA⁺ cell density per μ m² in the hippocampal CA1 area. (D): PV⁺WFA⁺ double-positive

cells as a percentage of all PV⁺ and WFA⁺ cells in hippocampal CA1. (C,D): Mean ± SEM values are shown. Vehicle, n = 5; ketamine n = 7.

Cells densities analysis in the CA1 area shows no statistically significant differences in densities of PV⁺, WFA⁺, PV⁺WFA⁺, or PV-WFA⁺ cells between ketamine- and vehicle-treated groups (Fig. 12 B, C). Furthermore, percentages of PV⁺WFA⁺ cells among all PV⁺ and all WFA⁺ were unchanged after ketamine treatment (Fig. 12 D). Altogether, the performed analysis failed to expose any alteration in the number of PNNs and PV⁺ interneurons in the CA1 region driven by ketamine treatment.

4.1.3 Expression of dendritic ECM in the hippocampal CA1 area of ketamine-treated rats

Previous studies have shown the importance of ECM in the dendritic area (Levy et al., 2014), which depends on the expression of important for inhibitory synaptic transmission tenascin-R (Morawski et al., 2014). For analysis of dendritic PNN expression in the hippocampal CA1 area, I manually tracked dendrites of PV⁺ interneurons and analyzed the profiles of WFA intensity of fluorescence. As verified by the two-way mixed ANOVA test, there are no statistically significant effect in dendritic WFA reactivity after ketamine treatment (treatment and distance from cell body interaction: $F(6, 60) = 1.039$, $p=0.4094$, distance from cell body: $F(1.242, 12.42) = 19.33$, $P=0.0005$, ketamine versus vehicle treatment: $F(1, 10) = 0.2473$, $p=0.6297$, Fig. 13).

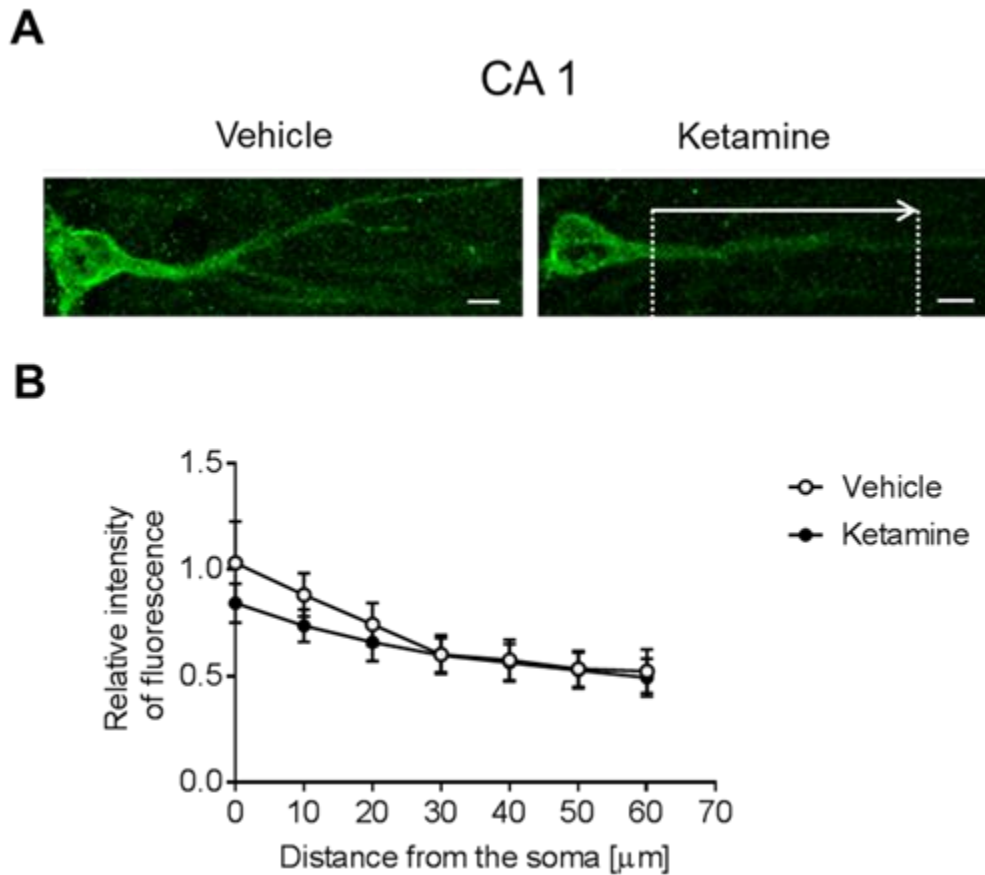


Fig. 13 Expression of dendritic ECM in the hippocampal CA1 area of ketamine-treated rats.

(A): Representative images of ECM visualized by WFA (in green) along dendrites of PV⁺ cells in the hippocampal CA1 area. The arrow indicates the beginning and the end of dendrite tracking. Scale bar: 10 μm . (B): Relative intensity of fluorescence was quantified as a function of distance from cell body [μm]. Mean \pm SEM values are shown relative to the mean value of vehicle control. Vehicle, $n = 5$; ketamine $n = 7$.

4.1.4 Densities of PV and WFA positive cells in the mPFC of ketamine-treated rats

The mPFC was then chosen for analysis due to its importance for the etiology of schizophrenia and because of previous human post mortem studies reporting a loss of PNNs around interneurons in this brain area (Mauney et al., 2013). I found a significant reduction of WFA⁺ cells density after ketamine treatment (vehicle: 108.4 ± 10 cells/ mm^2 ; ketamine: 80.7 ± 6 cells/ mm^2 ; $p = 0.04$, two-tailed t-test) and a strong tendency in reduction of double-positive PV⁺WFA⁺ cells (vehicle: 93 ± 9 cells/ mm^2 ; ketamine: 69 ± 6 cells/ mm^2 ; $p = 0.06$, two-tailed t-test). Furthermore, the percentage

of PV⁺WFA⁺ among all PV⁺ cells has a tendency to reduce after ketamine treatment ($p = 0.06$, two-tailed t-test, Fig. 14 C). Analysis of densities of PV⁺ and PV-WFA⁺ cells has shown no significant changes after ketamine treatment (Fig. 14 A, B). Percentages of PV⁺WFA⁺ among all PV⁺ cells and among all WFA⁺ cells were also not significantly different between ketamine- and vehicle-treated rats.

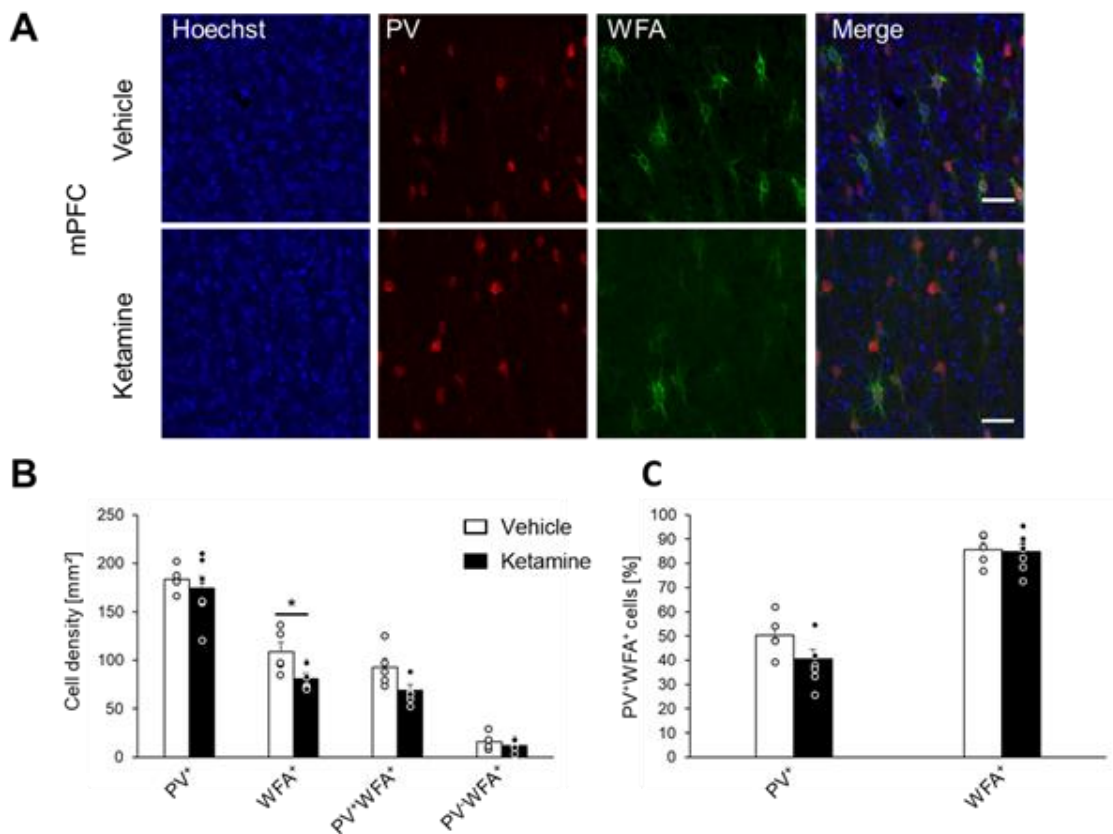


Fig. 14 Densities of PV- and WFA-positive cells in the mPFC of ketamine-treated rats. (A): Representative images of PV (in red) and WFA (in green) positive cells in mPFC. Upper panels show vehicle-injected controls, lower panels show ketamine-treated animal brains. Nuclei were visualized by Hoechst stain (in blue). Bar 50 μm . **(B):** PV⁺, WFA⁺, PV⁺WFA⁺ and PV⁻WFA⁺ cells density per mm² in mPFC. **(C):** PV⁺WFA⁺ double-positive cells as a percentage of all PV⁺ and WFA⁺ cells in mPFC (B, C). Mean \pm SEM values are shown. * $p = 0.04$, two-tailed t-test. Vehicle: $n=5$, ketamine: $n=7$.

4.1.5 Expression of PV, PNN marker and HNK-1 in the mPFC of ketamine-treated rats

Next, I decided to investigate HNK-1 carbohydrate expression because of previous studies showing its crucial role in regulating perisomatic GABAergic inhibition (Saghatelian *et al.*, 2000, 2001). The analysis was performed in the interneuronal perisomatic area due to its association with PNNs and the neuropil area because of its possible association with perisynaptic tenascin-R (Dityatev, Seidenbecher and Schachner, 2010) or with GluA2 subunit of glutamate receptors that may promote GluA2 cell surface expression (Morita *et al.*, 2009). In order to examine if reduction of PNNs in mPFC is associated with altered expression of PV immunofluorescence, I analyzed PV, WFA and HNK-1 triple stained brain section.

The results revealed a significant reduction of somatic PV fluorescence intensity after ketamine treatment (vehicle: 1 ± 0.02 ; ketamine: 0.59 ± 0.11 ; $p = 0.048$, Mann–Whitney test). In contrast, the perisomatic intensities of WFA and HNK-1 were unaffected by the treatment (Fig. 15 A, B).

Cell distribution of PV and WFA labelling in PV⁺ cells shows a small subpopulation of cells strongly expressing PV in the control group, which do not appear in ketamine-treated samples (Fig. 16). The cells with parvalbumin intensity over 20000 AU reach 6.6 % of all tested cells in vehicle-treated rats and 0.7 % of all tested cells in ketamine-treated rats. Distributions of WFA and HNK-1 intensities of fluorescent labelling across all PV⁺ cell shows no difference between both treatments (Fig. 16 and Fig. 17).

Neuropil expression of HNK-1 carbohydrate was not different between compared animal groups (Fig. 15 C). Altogether obtained results suggest that the loss of PNN is associated with the reduction of PV expression rather than altered HNK-1 expression.

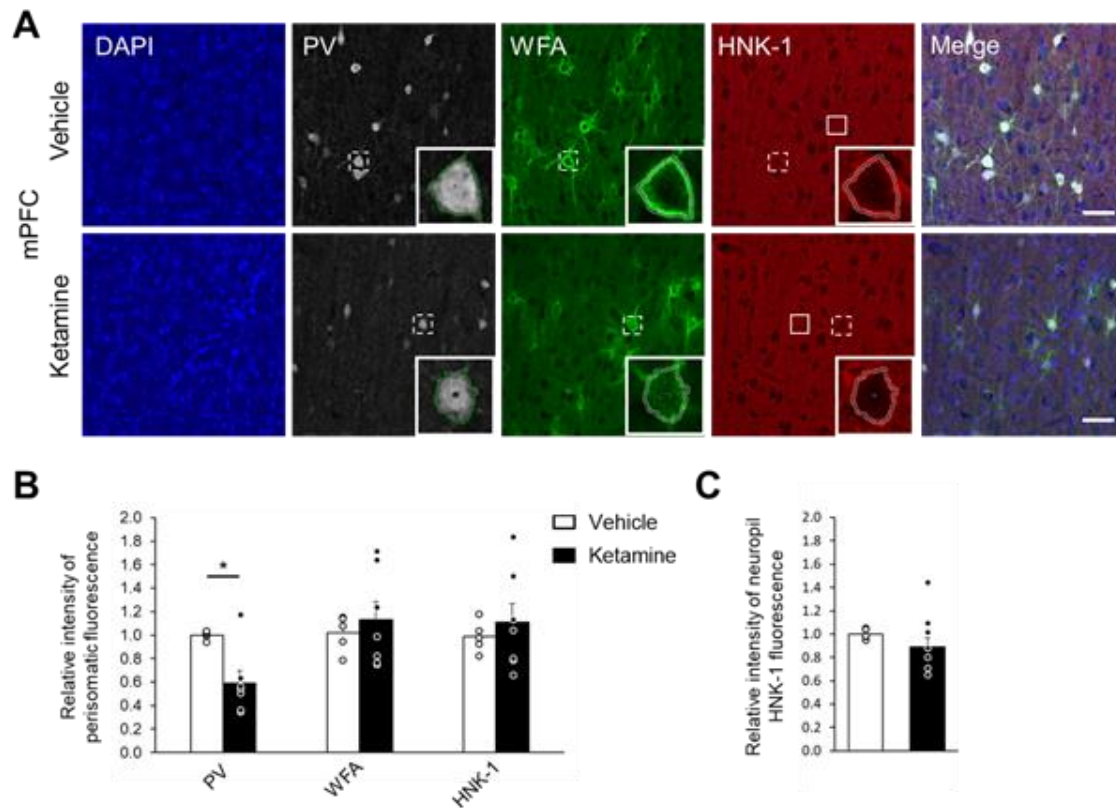


Fig. 15 Expression of PV, PNN marker and HNK-1 in the mPFC of ketamine-treated rats. (A): Representative images of PV (in grey), PNNs visualized by WFA (in green) and HNK-1 (in red) expression patterns in the mPFC. Nuclei were visualized by the Hoechst reagent (in blue). Picture inserts indicate different types of ROIs: full ROI for PV, „donut“ ROIs for WFA and HNK-1 signals around cell bodies, and rectangular ROIs for perisynaptic HNK-1. Scale bar: 50 μ m. (B): Relative intensity of fluorescence signal per cell body, normalized per mean value in the control group. Mean \pm SEM values are shown. * $p=0.048$, Mann-Whitney U-test; vehicle: $n = 5$, ketamine: $n = 7$. (C): Relative intensity of HNK-1 carbohydrate fluorescence in neuropil region normalized per mean value in the control group. Mean \pm SEM values are shown. Vehicle: $n = 5$, ketamine: $n = 7$.

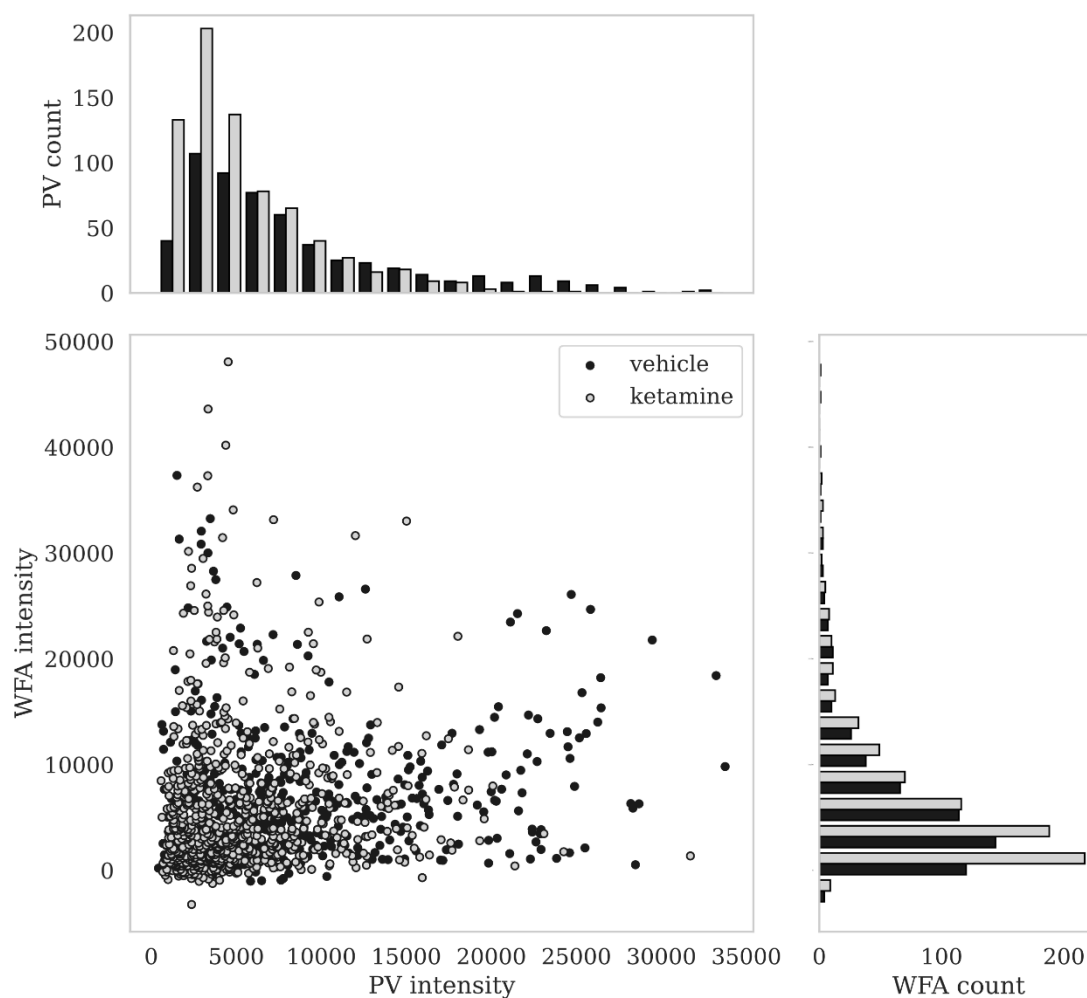


Fig. 16 Distribution of PV and WFA intensities of fluorescence in PV⁺ interneurons of ketamine treated rats. The upper panel shows frequencies of different intensities of PV in PV⁺ cell bodies. The lower left panel shows the distribution of intensity of fluorescence for both PV and WFA in PV⁺ cell bodies. The lower right panel shows frequencies of different intensities of WFA fluorescence around PV⁺ cell bodies. Bin = 2500, Vehicle in black (n = 5), ketamine in grey (n = 7).

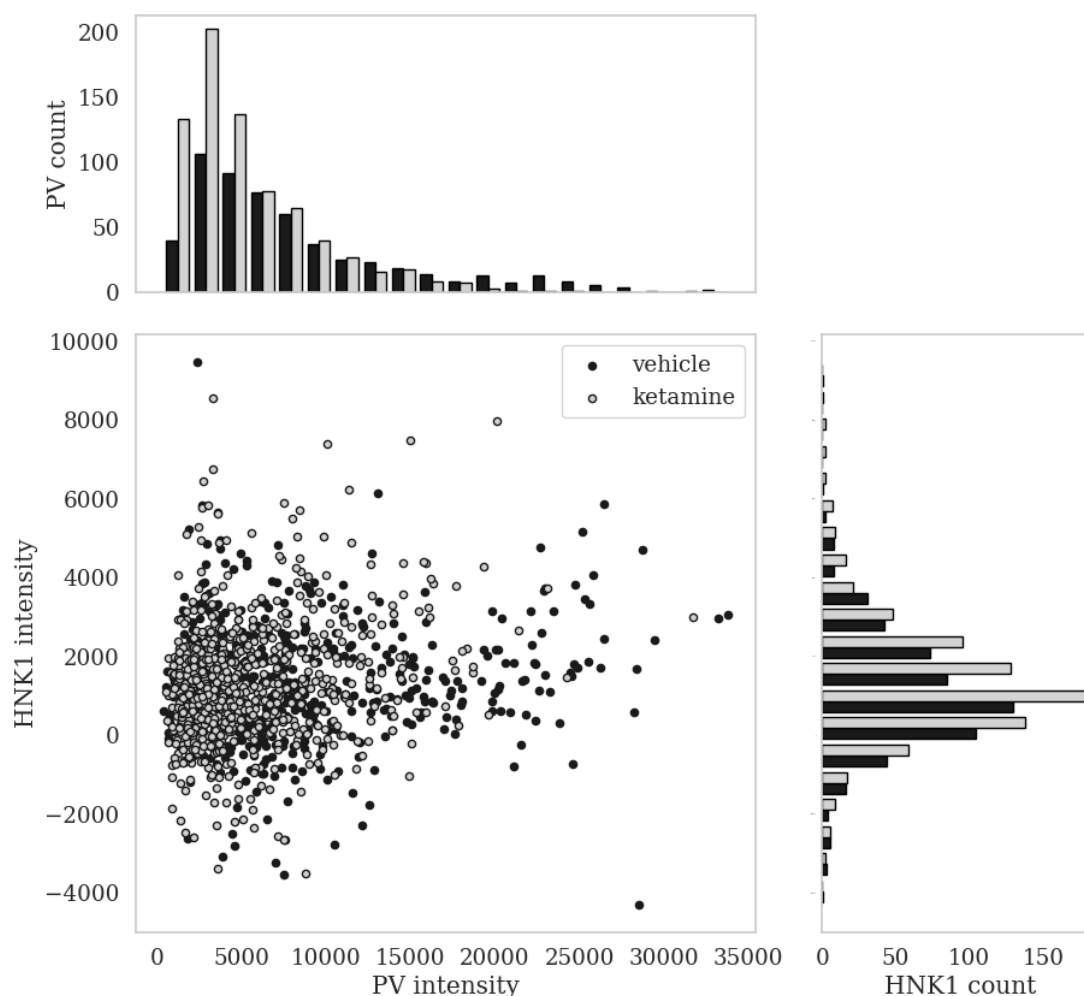


Fig. 17 Distribution of PV and HNK-1 intensities of fluorescence in PV⁺ interneurons of ketamine-treated rats. The upper panel shows frequencies of different intensities of PV in PV⁺ cell bodies. The lower left panel shows the distribution of intensity of fluorescence for both PV and HNK-1 in PV⁺ cell bodies. The lower right panel shows frequencies of different intensities of HNK-1 fluorescence around PV⁺ cell bodies. Bin = 2500, vehicle in black (n = 5), ketamine in grey (n = 7).

4.1.6 Dandelion Clock-like Structure (DACS) of glial ECM in the mPFC of ketamine-treated rats

As a previous study has shown, schizophrenia patients have an altered CS56⁺ immunoreactive form of ECM (Pantazopoulos *et al.*, 2015). Therefore, I analyzed CS56 labelling combined with WFA and astrocytic S100 β staining in mPFC (Fig. 18 A). The results reveal the increased intensity of CS56 immunolabeling within both CS56⁺ Dandelion Clock-like Structure (DACS) and in the

spaces between them (Fig. 18 B). WFA or S-100 β signals associated with CS56⁺ DACS clusters were not affected by ketamine treatment (Fig. 18 A, “Merge” panel). Quantitative analysis confirmed that the CS56 signal per image area was 1.4 ± 0.05 -fold increased in ketamine-treated rats ($p = 0.0005$, two-tailed t-test; Fig. 18 B). However, the spatial density of CS56⁺ clusters was unaltered (Fig. 18 B). Thus, there is an elevation of the CS56-immunoreactive form of ECM in ketamine-treated animals.

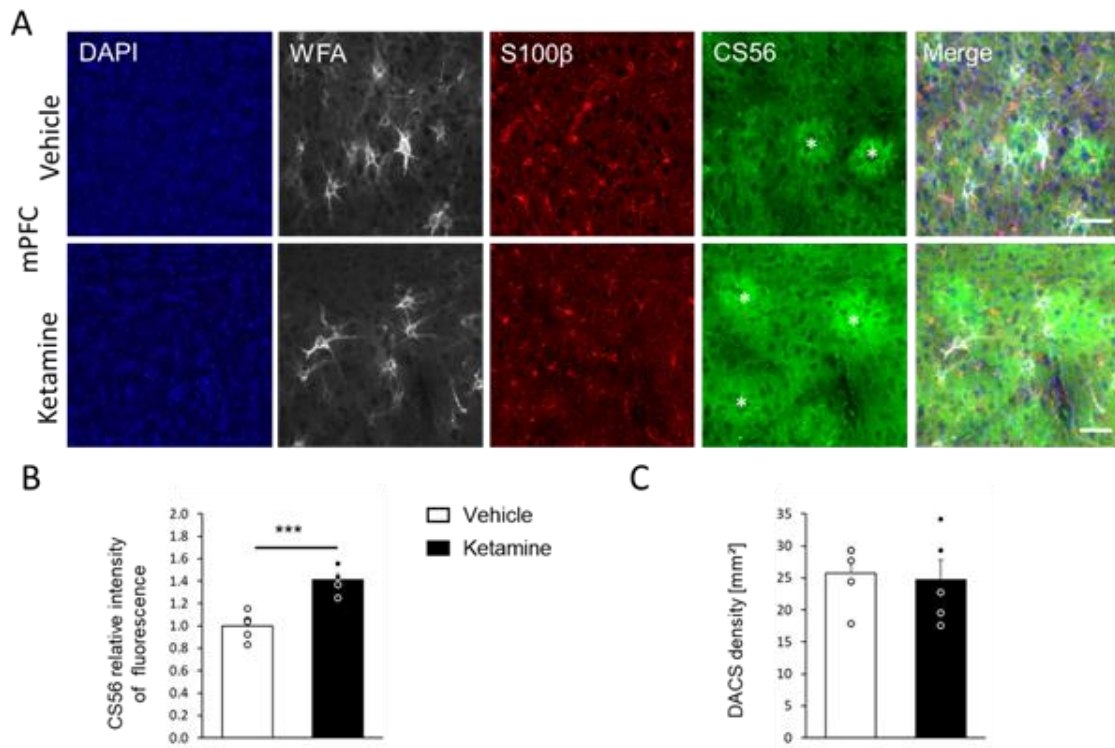


Fig. 18 Dandelion Clock-like Structure (DACS) of glial ECM in the mPFC of ketamine-treated rats. (A): Representative images of PNNs visualised by WFA (in green), astrocytes visualized by anti-S100 β (in red) and DACS visualized by anti-CS56. Nuclei were visualized by Hoechst stain (in blue). Scale bar, 50 μ m. (B): CS56 relative intensity of fluorescence per cell body normalized per mean value of vehicle control. (C) Densities of DACS⁺ structures (B,C) Mean \pm SEM are shown. *** $p = 0.0005$, two-tailed t-test. Vehicle: $n = 5$, ketamine: $n = 5$.

4.1.7 PNN fine structure analysis in the mPFC of ketamine-treated rats

In order to investigate ketamine-induced PNN structural alteration around PV interneurons, I performed an analysis of PNN structure in vehicle-treated (Fig. 19 A) and ketamine-treated rats (Fig. 19 B). The result revealed a small but statistically significant reduction of the number of

vertices in analyzed PNNs after ketamine treatment (vehicle 6.12 ± 0.06 ; ketamine 5.71 ± 0.13 ; $p = 0.03$; $F(1,6) = 7.5$, $n = 4$, one-way ANOVA; Fig. 19 C). Additionally, mesh area was significantly reduced in ketamine-treated samples (vehicle $1.25 \pm 0.06 \mu\text{m}$; ketamine $0.88 \pm 0.1 \mu\text{m}$; $p = 0.02$; $F(1,6) = 8.9$, $n = 4$, one-way ANOVA; Fig. 19 D) and polarity index analysis showed a trend for ketamine-induced reduction (vehicle: $1.24 \pm 0.01 \mu\text{m}$; ketamine: $1.2 \pm 0.01 \mu\text{m}$; $p = 0.08$; $F(1,6) = 4.6$, $n = 4$, one-way ANOVA; Fig. 19 E).

Altogether, those results suggest that ketamine treatment not only reduces the number of PV interneurons enwrapped with PNNs but also alters PNN architecture around interneurons, which might affect their function through modulation of somata surface accessibility for synaptic inputs.

4.1.8 Densities of PV- and WFA-positive cells in the mPFC of antipsychotics-treated rats

Human postmortem brain studies show a reduction of PNN in the brains of schizophrenic individuals, which we could also observe in ketamine-treated animals with schizophrenic-like behaviour. These results suggest that ECM deficits might be related to schizophrenic symptoms or etiology of disease. What remains to be, however, understand is the effect of antipsychotics on PNNs, which may bias PNN counts in schizophrenic patients. In order to investigate this issue, I analyzed total WFA⁺, PV⁺WFA⁺ and PV⁻WFA⁺ cells density in rat mPFC after subchronic oral treatment with typical antipsychotic haloperidol (0.075 mg/kg b.w.) and atypical antipsychotic risperidone (0.2 mg/kg b.w.) (Fig. 20).

The WFA⁺ cells density in was 123 ± 10 cells/mm² in control animals ($n = 7$), compared to 130 ± 16 cells/mm² in haloperidol-treated rats ($n = 8$, $p = 0.7$, t-test), and 137 ± 10 cells/mm² in risperidone-treated animals ($n = 7$, $p = 0.4$, t-test). Thus, there was no statistically significant effect of drugs on the density of WFA⁺ cells.

Also, the density of PV⁺WFA⁺ cells was not different between control animals (117 ± 12 cells/mm², $n = 7$) and haloperidol-treated rats (126 ± 16 cells/mm², $n = 8$, $p = 0.66$, t-test), or risperidone-treated animals (130 ± 12 cells/mm², $n = 7$, $p = 0.43$, t-test).

Furthermore, the PV⁻WFA⁺ cell density in control animals (8 ± 3 cells/mm², $n = 7$) was is not significantly altered compared to haloperidol-treated rats (4 ± 2 cells/mm², $n = 8$, $p = 0.4$, t-test), or risperidone-administrated animals (5 ± 3 cells/mm², $n = 7$, $p = 0.6$, t-test).

Additionally, percentage of double positive PV⁺WFA⁺ cells among all WFA⁺ cells show no statistically significant difference between control animals ($95\% \pm 3\%$, $n = 7$), haloperidol-treated group ($96\% \pm 2\%$, $n = 8$, $p = 0.6$, t-test) and risperidone-treated group ($94\% \pm 2\%$, $n = 7$, $p = 0.9$, t-test).

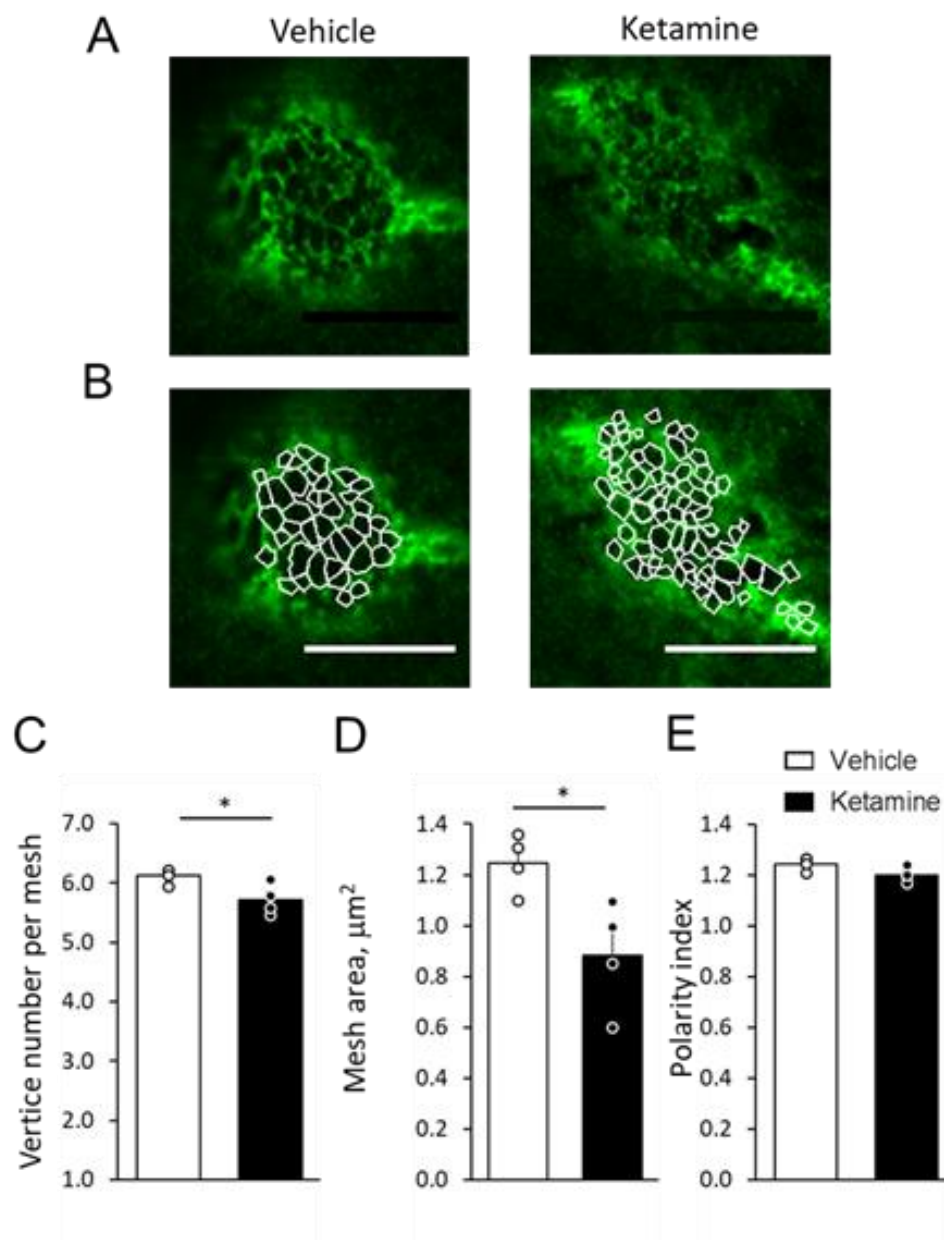


Fig. 19 PNN analysis in the mPFC of ketamine-treated rats. (A, B): Representative images of PNNs visualized by WFA (in green). (B): PNN vertices (in white). Scale bar, 10 μm. (C): Number of vertices per mesh. (D): Mesh area in μm². (E) Polarity index of singular meshes. (C, D, E): Mean ± SEM values are shown. * $p < 0.05$, One-way ANOVA. Vehicle: $n = 4$, ketamine: $n = 4$.

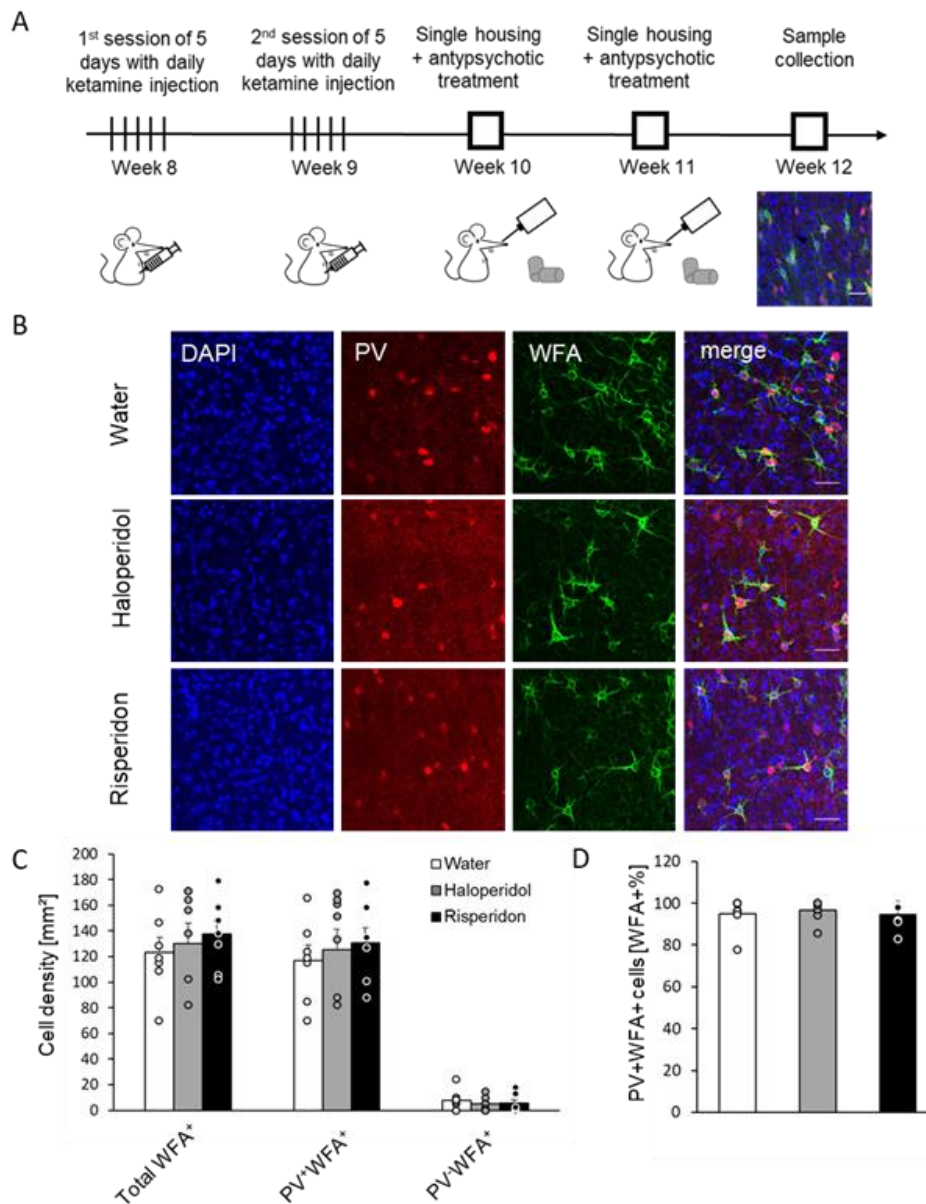


Fig. 20 WFA-positive cells after treatment with haloperidol and risperidone. (A): The experiment timeline showing the scheme of ketamine treatment, single housing and antipsychotic treatment, and sample collection. (B): Representative images of PV (in red) and WFA (in green) positive cells in mPFC. Upper panels show vehicle-injected controls, the middle panel shows haloperidol-treated and lower panels risperidone-treated animal brains. Nuclei were visualized with Hoechst (in blue). Bar 50 μ m. (C): Total WFA⁺, PV⁺WFA⁺ and PV⁻WFA⁺ cells density per mm² in mPFC. (D) PV⁺WFA⁺ double-positive cells as a percentage of all and WFA⁺ cells in mPFC. (C,D): Mean \pm SEM values are shown. Vehicle: n = 7, haloperidol: n = 8, risperidone: n = 7.

4.1.9 Glial ECM in the mPFC of antipsychotic-treated rats

Since my previous experiments revealed increased CS65 immunoreactivity after ketamine treatment, and human *post mortem* studies of schizophrenic patients detected changes in CS56 in the brain tissue (Pantazopoulos *et al.*, 2015), I analyzed immunohistochemically the total CS56 fluorescence in rat mPFC sections after subchronic oral treatment with haloperidol (0.075 mg/kg b.w.) or risperidone (0.2 mg/kg) (Fig. 21).

There were no statistically significant differences in CS56 immunoreactivity between haloperidol (0.92 ± 0.10), risperidone (1.05 ± 0.11) and vehicle-treated animal groups (1.0 ± 0.09), suggesting that the antipsychotic drugs used do not alter CS56 expression in the ECM. These results strengthen the interpretation of human postmortem studies, suggesting that reported CS56 alteration is indeed schizophrenia-related and not induced by treatment with antipsychotics.

4.2 Results for AAV treated mice

4.2.1 HAPLN1 shRNA constructs validation

Previous human *post-mortem* brain studies have shown a significant reduction of HAPLN1 RNA in pyramidal neurons from the superior temporal cortex of schizophrenia subjects (Pietersen *et al.*, 2014). Thus, I decided to knock down HAPLN1 in mice and study if this manipulation could result in changes in PNNs, as observed in patients and/or the ketamine model of schizophrenia. To find an efficient knockdown vector, I constructed three viral shRNA-expressing vectors containing different 19 base pairs (bp) of mice HAPLN1 sequence. I confirmed cloning results by restriction digestion with EcoRI and AgeI enzymes and electrophoresis in 1 % agarose gel supplemented by SYBR Green reagent. Fig. 22 shows the restriction pattern after this digestion. A negative control sample in lane N contains a 453 bp-long lower band (indicated by an asterisk). Positive samples in rows 1-8 contain insert visible as longer 514 bp-long lower bands. All samples confirmed by restriction digestion were reconfirmed by sequencing.

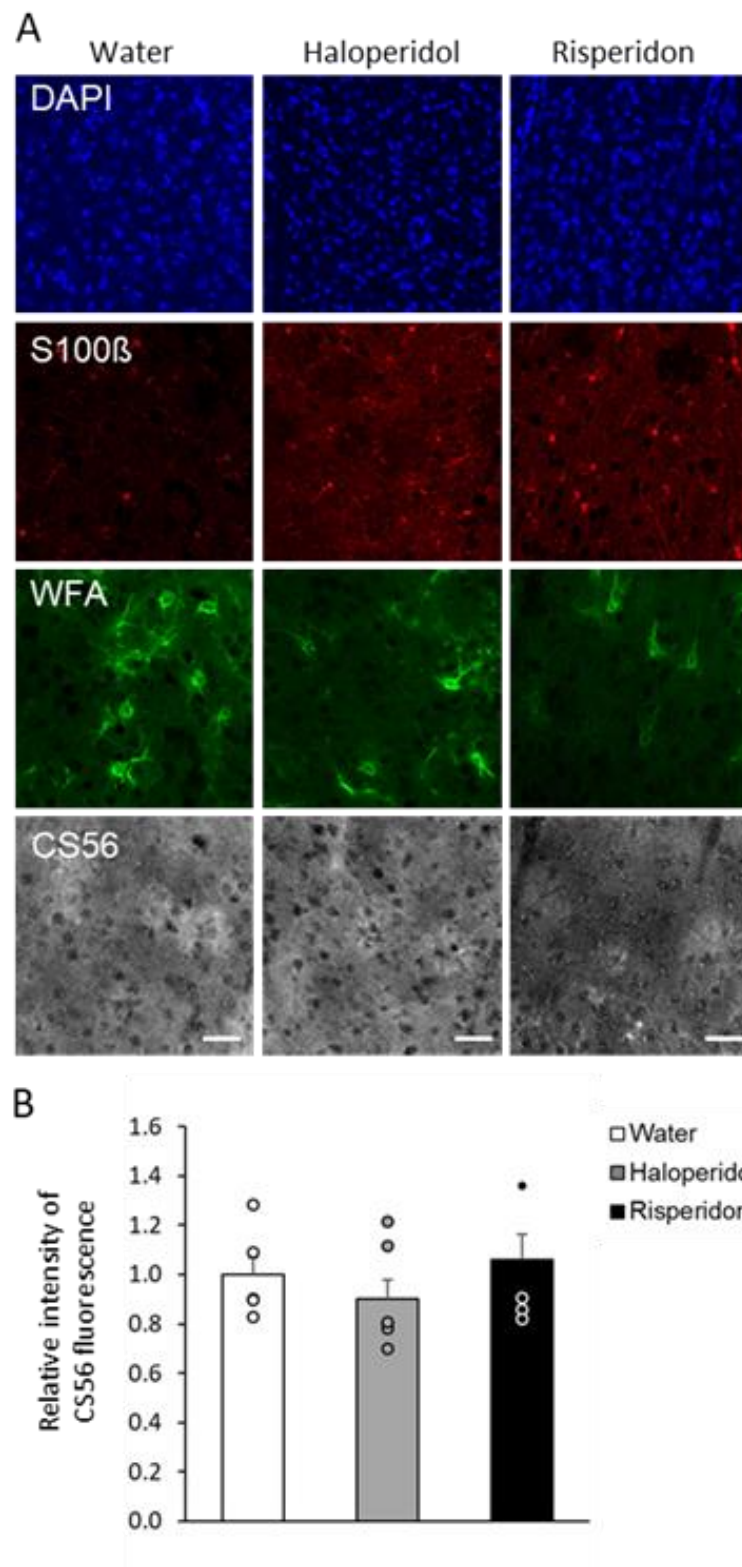


Fig. 21 Relative intensity of CS56 fluorescence in mPFC of antipsychotic treated rats. (A): Representative images of S100 β (in red), WFA (in green) and CS56 (in grey) in mPFC. The

left panels show vehicle-injected controls, the middle panel shows haloperidol-treated and the right panels show risperidone-treated animal brains. Nuclei were visualized with Hoechst (in blue). Bar 50 μm . (B): Relative intensity of total CS56 fluorescence normalized to vehicle control. Shown are mean \pm SEM values. Vehicle: n = 7, haloperidol: n = 8, risperidone: n = 7.

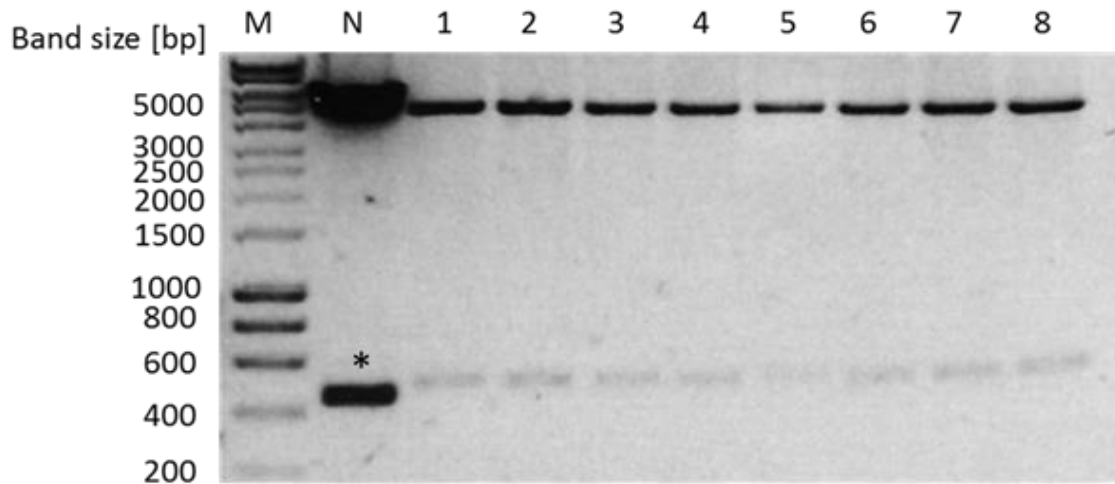


Fig. 22 Restriction digestion validation of cloned constructs. Lane M stands for the HyperLadder 1 marker. Lane N stands for the negative control pAAV_U6_GFP vector containing no insert digested with EcoRI and AgeI restriction enzymes indicating 453 bp lower band (*). Row 1-8 shows samples digested with EcoRI and AgeI restriction enzymes containing insert corresponding to the 514 bp lower band.

After sequencing confirmation of these three HAPLN1 shRNA constructs, I validated their knocking-down efficiency in HEK 293T cells (Fig. 23 C). First, I investigate the quality of RNA samples isolated from HEK293T cells treated with pAAV_Syn_HAPLN1_GFP overexpression vector together with pAAV_U6_control_shRNA_GFP or three different pAAV_U6_HAPLN1shRNA_GFP constructs by electrophoresis in 1 % agarose gel supplemented with SYBR green reagent (Fig. 23 A, B). I confirmed the good integrity of isolated samples through the lack of RNA degradation pattern (smears) upwards from the 28S rRNA band (Fig. 23 A) and, also with the 2:1 ratio between 28SrRNA and 18S rRNA band quantified in Fig. 23 B. qPCR analysis revealed that shRNA1 significantly reduced mRNA of HAPLN1 protein overexpressed in HEK 293T cells to $2\% \pm 2\%$ relative to a control shRNA ($100\% \pm 30\%$, t-test $p = 0.05$ Fig. 23 C), while the level after shRNA2 treatment was $150\% \pm 38\%$ and after shRNA3 treatment, it was $78\% \pm 38\%$.

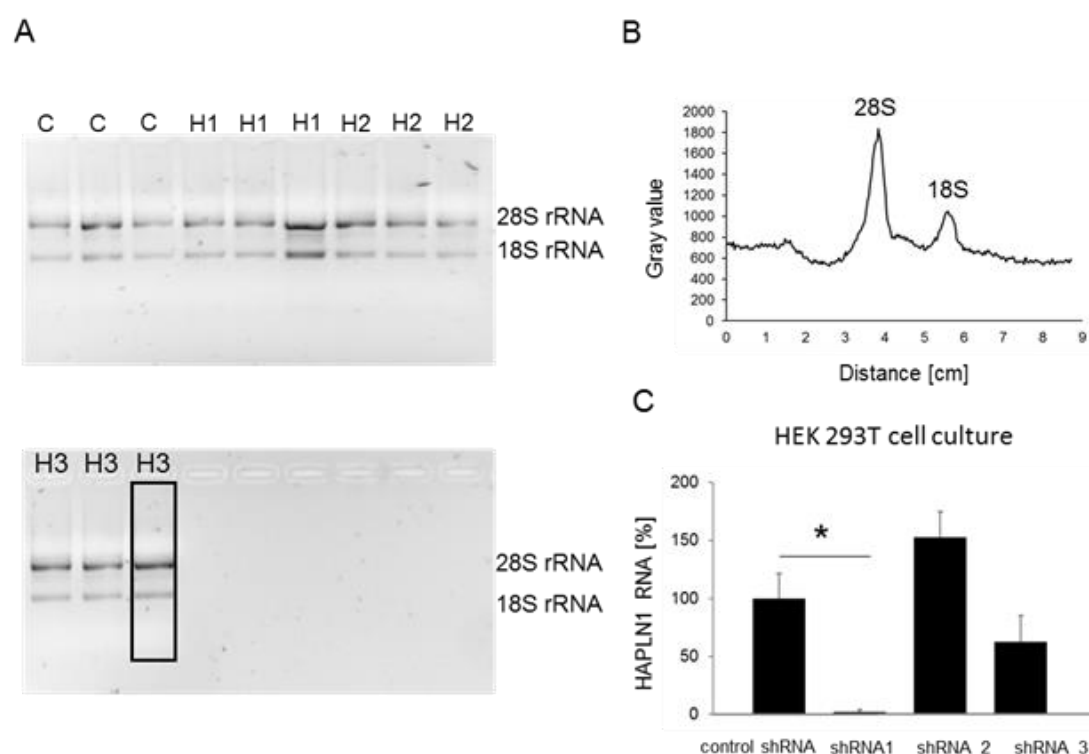


Fig. 23 Validation of pAAV_U6_HAPLN1shRNA_GFP vectors in HEK293T cell cultures.

(A): Quality control of isolated RNA samples validated by electrophoresis in 1 % agarose gel supplemented with SYBR Green reagent. Lane C indicates samples isolated from pAAV_Syn_HAPLN1_GFP overexpression and pAAV_U6_control_shRNA_GFP vector treated HEK293T cells. Lanes H1, H2 and H3 indicate samples isolated from pAAV_Syn_HAPLN1_GFP plus, respectively, pAAV_U6_HAPLN1shRNA1_GFP, pAAV_U6_HAPLN1shRNA2_GFP, or pAAV_U6_HAPLN1shRNA3_GFP co-treated HEK293T cells. (B): Quantification of 28S rRNA and 18S rRNA subunits bands' fluorescence intensity from the lane highlighted in the panel (A) by a rectangle, which is expressed as a function of gel distance in cm. (C): Validation of three HAPLN1 shRNA constructs in HEK 293T cells. Mean + SEM values for the effects of HAPLN1 shRNAs relative to the control shRNA are shown. * $p = 0.05$, t-test ($n = 3$).

Afterwards, I packed the selected construct into AAV1/2 viral capsid and validated its efficiency in mouse hippocampal primary cell culture (Fig. 24). First, I investigated the quality of RNA samples isolated from untreated hippocampal neurons, neurons treated with pAAV_U6_control_shRNA_GFP and neurons treated pAAV_U6_HAPLN1shRNA1_GFP virus. The electrophoresis in 1 % agarose gel supplemented with SYBR green reagent (Fig. 24 A, B) revealed a lack of RNA degradation pattern (smears) upwards the 28S rRNA band (Fig. 24 A) and proper 2:1 ratio between 28SrRNA and 18S rRNA band quantified in Fig. 24 B, which confirmed good integrity of isolated samples. Results of cDNA analysis show that the produced virus

significantly decreasing HAPLN1 RNA in treated culture two weeks after infection (untreated: $100 \% \pm 19 \%$, control shRNA: $82 \% \pm 21 \%$, HAPLN1 shRNA1: $7.5 \% \pm 4 \%$, different from untreated with $p = 0.01$ and from control shRNA with $p = 0.02$, t-test).

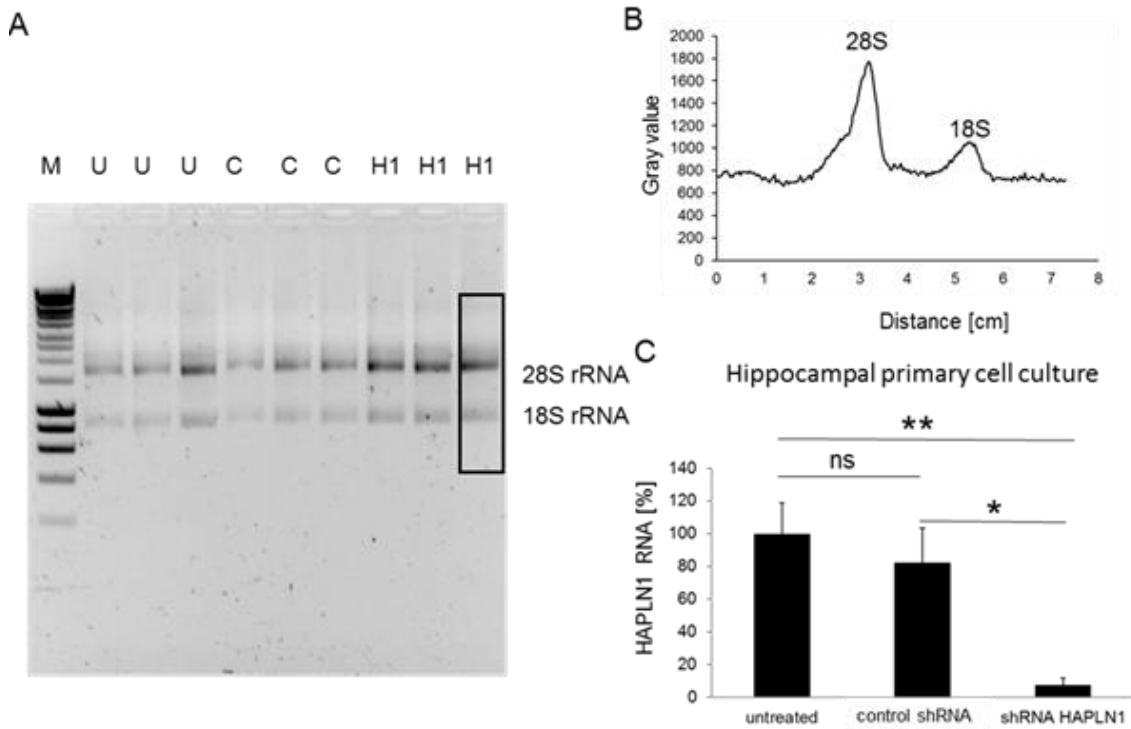


Fig. 24 Validation of pAAV_U6_HAPLN1shRNA_GFP vector in hippocampal primary cell cultures. (A): Quality control of isolated RNA samples validated by electrophoresis in 1 % agarose gel supplemented with SYBR Green reagent. Lane M indicates HyperLadder 1 DNA marker, Lane U represents samples isolated from uninfected hippocampal primary cell cultures. Lanes C and H1 indicate samples isolated from primary hippocampal cell cultures infected, respectively, with control shRNA AAV, or HAPLN1 shRNA1 AAV. (B): Quantification of 28S rRNA and 18S rRNA subunits bands intensity of fluorescence from a lane highlighted by a rectangle in (A) as a function of gel distance in cm. (C): Validation of AAV_U6_HAPLN1shRNA1 virus in hippocampal primary cell cultures. Results are shown as percentage relative to HAPLN1 RNA isolated from the untreated control sample. * $p = 0.02$; ** $p = 0.01$, t-test. Data represent mean + SEM values ($n = 3$).

4.2.2 Acoustic startle reflex and pre-pulse inhibition

To validate if reduction of HAPLN1 protein in mPFC may cause schizophrenia-like behaviour, I injected twenty-one P8 C57Bl6/J mice, divided into two groups: 10 animals injected with AAV1/2_U6_HAPLN1_shRNA, and 11 injected with AAV1/2_U6_control_shRNA virus and

after 4 weeks animals performed ASR and PPI behaviour tests (Fig. 25 A). The analysis of relative startle amplitude shows a significant increase of startle amplitude with increased pulse strength (two-way ANOVA $F(1,3) = 24.99$; $p = 2.3 \times 10^{-11}$). Therefore for PPI experiments, we use 110 dB pulse stimuli.

The two-way ANOVA analysis shows no statistical difference in relative startle amplitude between control and AAV1/2_U6_HAPLN1_shRNA injected animals ($F(1,3) = 0.18$, $p = 0.67$ for 80 dB, control shRNA: 259 ± 38 , HAPLN1 shRNA: 279 ± 43 ; for 90 dB, control shRNA: 651 ± 113 , HAPLN1 shRNA: 737 ± 106 ; for 100 dB, control shRNA: 1005 ± 100 , HAPLN1 shRNA: 1018 ± 143 ; for 110 dB, control shRNA: 1018 ± 84 , HAPLN1 shRNA: 1019 ± 132) suggesting that there is no treatment effect on motor responses to sensory information (Fig. 25 B).

The prepulse inhibition analysis shows no significant effect of prepulse strength on PPI (two-way ANOVA $F(1,3) = 2.4$; $p = 0.08$), however, the treatment with viruses significantly affects the PPI dependence on the prepulse strength (two-way ANOVA $F(1,3) = 15.25$; $p = 0.0002$), suggesting that the treatment affects sensorimotor gating (Fig. 25 B). The post hoc Bonferoni test shows HAPLN1 shRNA virus treatment-induced increased in PPI for prepulse 80 dB (control shRNA: $38 \% \pm 4 \%$, HAPLN1 shRNA: $54 \% \pm 3 \%$, $p = 0.01$) but no effect on treatment for prepulse 85 dB (control shRNA: $41 \% \pm 3 \%$, HAPLN1 shRNA: $50 \% \pm 3 \%$, $p = 0.08$), 70 dB (control shRNA: $35 \% \pm 4 \%$, HAPLN1 shRNA: $41 \% \pm 5 \%$, $p = 1$) and for prepulse 75 dB (control shRNA: $36 \% \pm 4 \%$, HAPLN1 shRNA: $44 \% \pm 3 \%$, $p = 0.47$). However Bonferoni corrections have the disadvantage of increasing the type 2 error rate and therefore falsely accept the null, and so neglect findings which might be theoretically or clinically relevant. Therefore we also use the false discovery rate post hoc test (FDR), which shows shows HAPLN1 shRNA virus treatment-induced increased in PPI for prepulse 80 dB and 85 dB ($p = 0.01$ and $p = 0.04$ respectively Fig. 25 C) as well as t-test which also shows significant increase of PPI after HAPLN1 shRNA treatment for prepulse 80 dB and 85 dB ($p = 0.003$ and $p = 0.02$ respectively).

Those results need to be interpreted with caution because of unusually weak increase of PPI with increased sound intensity in control animals.

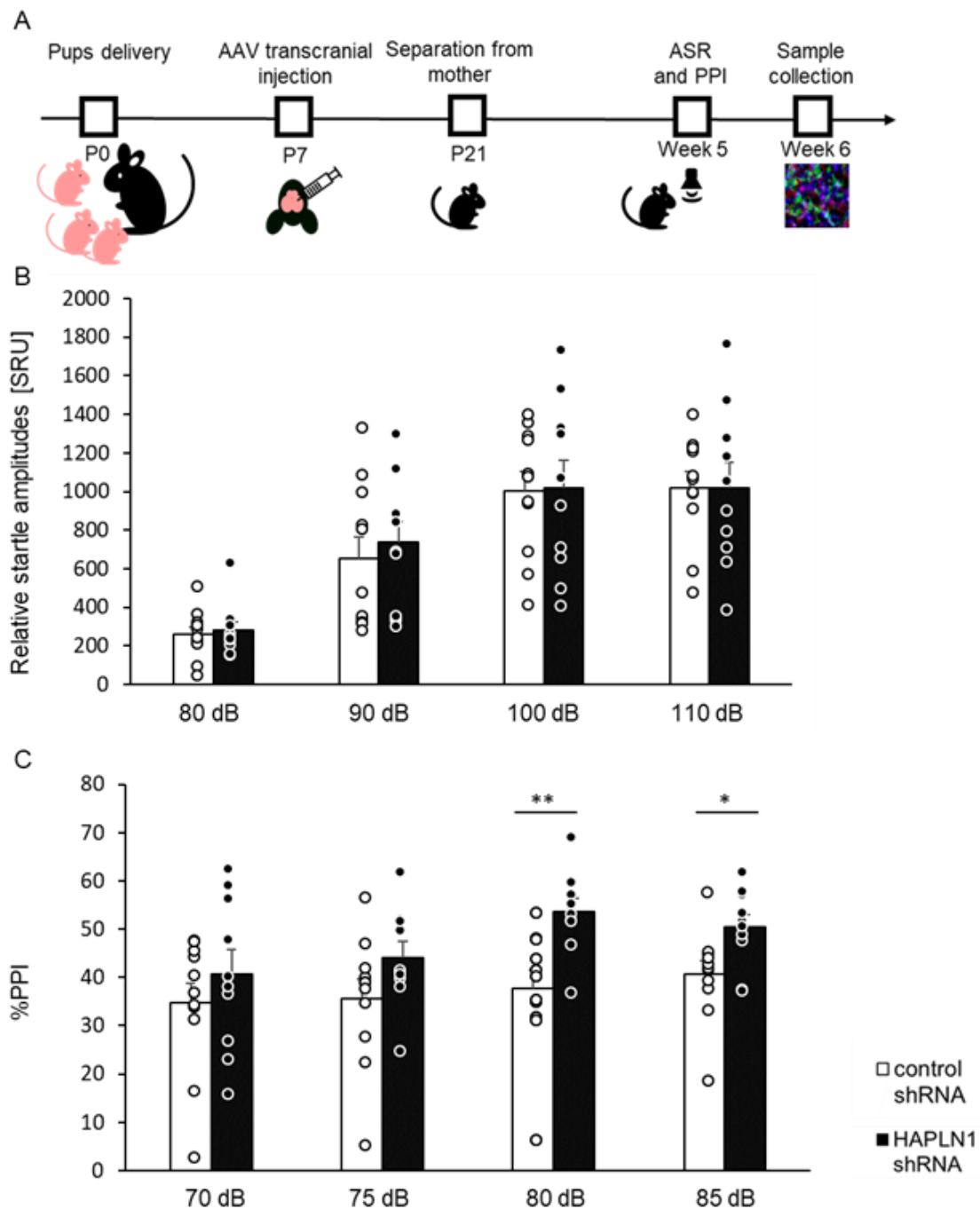


Fig. 25 Acoustic startle reflex and pre-pulse inhibition. (A): The timeline of the experiment showing transcranial injection, separation from the mother, behavioural test and sample collection (B): ASR is shown as relative startle amplitudes AVG ± SEM; N = 11 control shRNA, N = 10 HAPLN1 shRNA. (C): Percentage of PPI AVG ± SEM; N = 11 control shRNA, N = 10 HAPLN1 shRNA; two-way ANOVA, followed by FDR post hoc tests: * $p < 0.05$, ** $p < 0.005$.

4.2.3 Excitatory synaptic puncta and BCAN in the neuropil area

Based on previous human post mortem studies, which showed a decrease of dendritic spine density in the mPFC (Glantz and Lewis, 2000), and a decrease of excitatory synaptic marker VGLUT1 in the anterior cingulate cortex of schizophrenic patients (Barksdale, Lahti and Roberts, 2014), I performed an analysis of synaptic puncta and ECM in the neuropil and perisomatic area of CaMK2 positive neurons in AAV-infected mPFC. Two control animals were excluded from further analysis due to postinjection complications.

Immunohistochemistry analysis of excitatory presynaptic puncta visualized with VGLUT1 antibody in the mPFC neuropil revealed a dotted pattern shown in blue (upper panel of Fig. 26 A). After thresholding and applying a Gaussian filter, I created binary maps and analyzed puncta bigger than $0.1 \mu\text{m}^2$ marked as a region of interest with the yellow frame (right image Fig. 26 A). Those ROIs were used in further analysis of VGLUT1 synaptic puncta density (Fig. 26 B). I applied the same protocol to analyze the density of excitatory postsynaptic puncta visualized with PSD95 antibody marked as regions of interest in the green frame (lower panel Fig. 26 A).

The mPFC deep layers VGLUT1 density showed an average of 0.129 ± 0.002 puncta/ μm^2 in animals treated with pAAV_U6_control_shRNA_GFP virus, which corresponds to published data (Castillo-Gómez *et al.*, 2017). Therefore, I used VGLUT1 ROIs marked in blue in Fig. 26 B binary map and PSD95 merged image as the base for recognition of excitatory synapses. I measured grey values in $0.05 \mu\text{m}$ distance around VGLUT1 ROIs on PSD95 binary map shown as red circles in Fig. 26 B, left image. All values higher than zero were classified as synapses and marked with white asterisks (Fig. 26 B). Those VGLUT1 puncta, which have no PSD95 puncta in $0.05 \mu\text{m}$ proximity were not recognized as synapses.

In order to investigate changes in ECM in the neuropil area, I used an antibody against brevican, which expression was reported to be enriched in the neuropil area (Ajmo *et al.*, 2008) (Fig. 26 C in green). I used previously recognized synaptic puncta marked in red and blue and measured the intensity of BCAN fluorescence in $0.5 \mu\text{m}$ distance around each VGLUT1 and PSD95 synaptic puncta as well as total intensity from the whole image area.

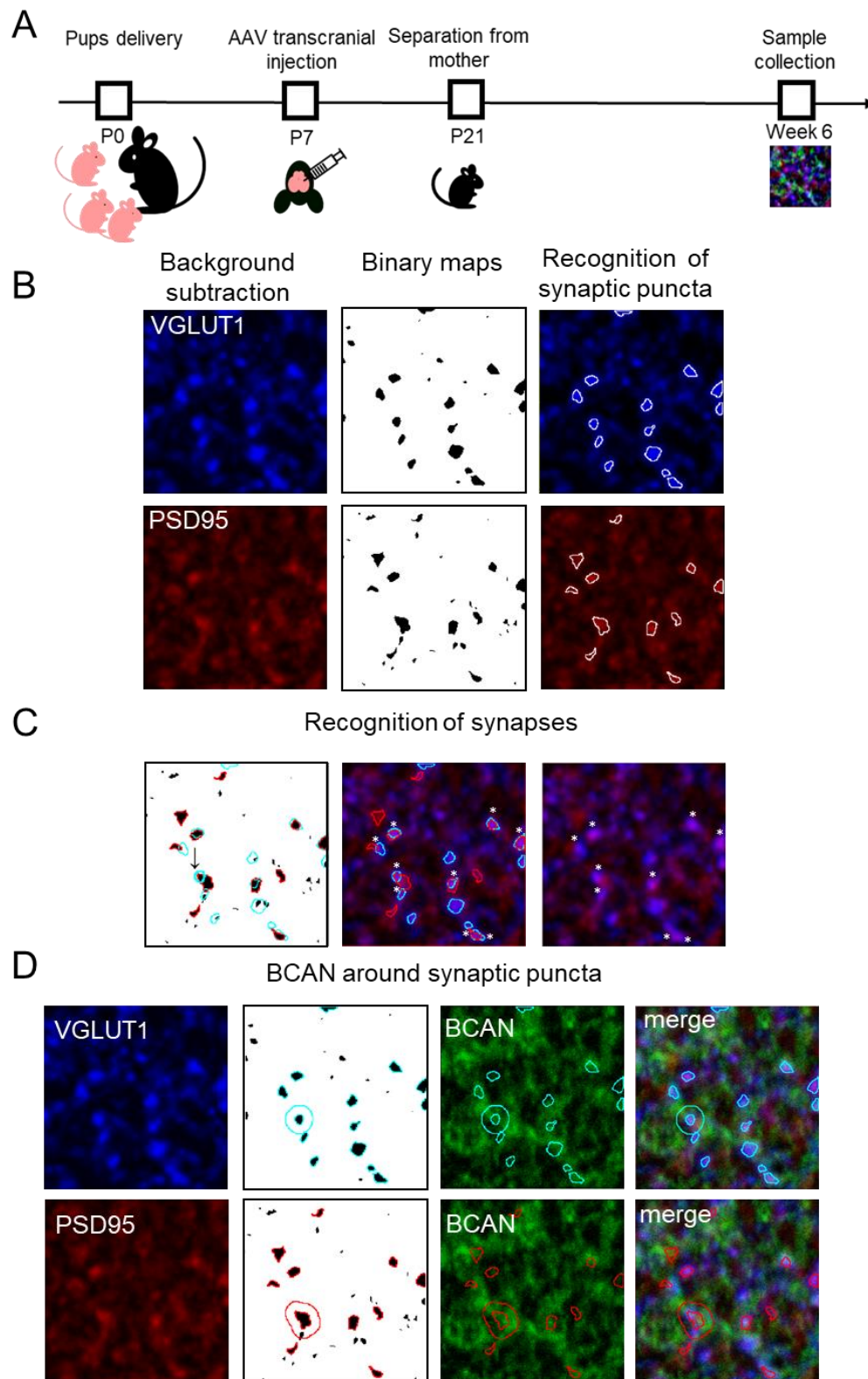


Fig. 26 Recognition of excitatory synaptic puncta, excitatory synapses and BCAN around them. (A): Left panel: representative images of excitatory synaptic markers VGLUT1 (in blue)

and PSD95 (in red). Center panel: binary maps after thresholding and Gaussian filtration. Right panel: Synaptic puncta bigger than 0.1 μm marked as ROIs in yellow. (B): Recognition of synapses shown on PSD95 binary map in the left panel, and PSD95 and VGLUT1 merged image in the right panel. VGLUT1 ROIs visualized in blue. 0.05 μm distance around VGLUT1 puncta marked in red circles. Recognized synapses are marked with red arrows. VGLUT1 puncta not recognized as synapses are marked by yellow arrows. (C): BCAN expression in green around excitatory synaptic puncta, VGLUT1 in blue and PSD95 in red. Synaptic puncta bigger than 0.1 μm are marked as ROIs in yellow on top of binary maps, BCAN and merge images 0.5 μm area around synaptic puncta is outlined in red.

There were no significant differences in VGLUT1⁺ densities of excitatory synaptic puncta between of AAV_U6_control_shRNA_GFP treated animals (0.129 ± 0.002 puncta/ μm^2 , N = 9) and AAV_U6_HAPLN1_shRNA1_GFP treated animals (0.125 ± 0.005 puncta/ μm^2 , N = 10, $p = 0.38$, t-test). Also the densities of PSD95⁺ puncta were very close (control: 0.103 ± 0.001 puncta/ μm^2 , N = 9; HAPLN1shRNA: 0.104 ± 0.001 puncta/ μm^2 , N = 10, $p = 0.28$, t-test; Fig. 27 B).

Excitatory synapses analysis revealed no significant differences ($p = 0.5$, t-test) between AAV_control_shRNA and AAV_HAPLN1_shRNA injected animals: 0.098 ± 0.002 synapses/ μm^2 , N = 9 and 0.101 ± 0.002 synapses/ μm^2 , N = 10, respectively (Fig. 27 C).

Additionally, the intensity of fluorescence of immunolabeled BCAN was not significant around both VGLUT1, (AAV_control_shRNA_GFP treated animals: 141 ± 6 AU; AAV_HAPLN1_shRNA1_GFP treated animals: 145 ± 12 AU, $p = 0.78$, t-test), and PSD95 (176 ± 11 AU versus 172 ± 8 AU, respectively, $p = 0.39$, t-test) immunopositive excitatory puncta, as well as in total image area (165 ± 13 AU versus 157 ± 13 AU, respectively, $p = 0.77$, t-test) (Fig. 27 D), suggesting that a deficit in HAPLN1 expression does not affect the expression of BCAN in the neuropil, possibly due to residual expression of HAPLN1 in uninfected cells or contribution of other members of HAPLN subfamily.

Altogether, these results suggest that knocking down HAPLN1 proteins in neurons does not affect excitatory synapses in neuropil area. The possible explanation could be due to the efficacy of neuronal AAV infection in tissue, which is not 100 % and non-infected cells might compensate for the deficiency of HAPLN1 protein in infected cells.

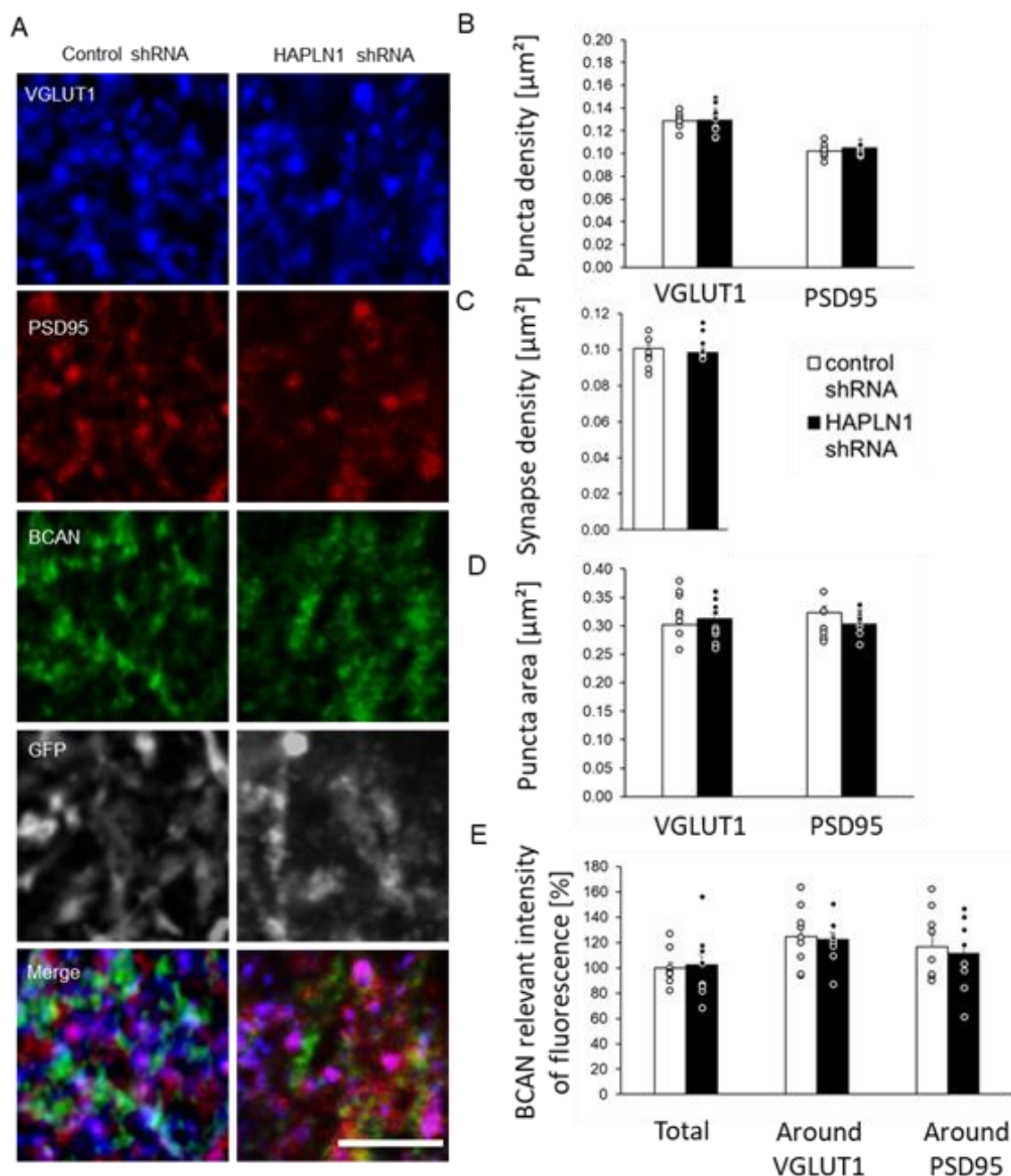


Fig. 27 Excitatory synaptic puncta and BCAN expression around excitatory synaptic puncta in the neuropil. (A): Representative images of excitatory synaptic markers VGLUT1 (in blue), PSD95 (in red) and BCAN (in grey). GFP (in green) indicates infected dendrites. The left panel shows the control-treated samples. The right panel shows the AAV_HAPLN1shRNA-treated samples. (B): Densities of excitatory synaptic puncta per μm^2 . (C): Densities of excitatory synapses per μm^2 . (D): Area of VGLUT1 and PSD95 synaptic puncta. (E): Expression of BCAN measured as intensity of fluorescence in the whole image and around VGLUT1 and PSD95

synaptic puncta; (B, C, D and E): Mean \pm SEM are shown; pAAV_control_shRNA_GFP: N = 9; AAV_HAPLN1shRNA1: N = 10.

4.2.4 Inhibitory presynaptic puncta and BCAN in perisomatic area of CaMK2 positive cells

Several studies reviewed by Gao and Penzes (Gao and Penzes, 2015) report excitatory-inhibitory imbalance in schizophrenia, suggested to be regulated by ECM molecules (Dityatev and Schachner, 2003; Faissner *et al.*, 2010). In order to investigate HAPLN1 function in the regulation of inhibitory input on excitatory cells, I performed a semiquantitative analysis of VGAT-positive (VGAT⁺) inhibitory presynaptic puncta (in blue) on CaMK2-positive (CaMK2⁺) excitatory perisomatic area (in grey) (Fig. 28 A, B). For this analysis, I used two methods. First, I investigated VGAT1 positive puncta bigger than 0.1 μm located in 1 μm proximity to CaMK2⁺ cells (marked as ROIs in yellow). I will refer to this method as method 1. Second, I investigated VGAT⁺ than 0.1 μm located in 0.75 μm band around CaMK2⁺ cell body in the art that 0.25 μm of the band is located inside cell body and 0.5 μm of the band is outside the cell body. I will refer to this method as method 2. Method 2 is more precise excluding puncta that have no direct contact with the cell body and including puncta that partially overlap with the cell body for measured signal strength for applied settings. BCAN immunostaining was used for the analysis of HAPLN1 knockdown-induced changes in ECM. In both methods, the BCAN signal was measured at 0.5 μm around the CaMK2⁺ cell body.

My analysis using method 1 revealed a reduced number of VGAT puncta on somata of CaMK2⁺ neurons infected with pAAV_U6_HAPLN1_shRNA virus (0.20 ± 0.01 puncta/ μm of the perimeter, N = 9, n = 95) versus pAAV_U6_control_shRNA virus (0.17 ± 0.01 puncta/ μm of the perimeter, N = 10, n = 108) (*p = 0.01, t-test, Fig. 22B Method 1). The analysis using method 2 also show a reduced number of VGAT⁺ puncta on CaMK2⁺ somata after pAAV_U6_HAPLN1_shRNA virus infection (0.15 ± 0.01 puncta/ μm of the perimeter, N = 9, n = 95) versus pAAV_U6_control_shRNA virus (0.13 ± 0.004 puncta/ μm of the perimeter, N = 10, n = 108) (**p = 0.002, t-test, Fig. 28 B Method 2).

The VGAT⁺ synaptic puncta area measured using method 1 shows no significant difference between the control group (0.34 ± 0.01 μm^2 , N = 9, n = 95) and pAAV_U6_HAPLN1_shRNA treated animals (0.34 ± 0.01 μm^2 , N = 10, n = 108, p = 0.8 control; t-test, Fig. 22D Method 1) as well as measured using method 2- the control group (0.32 ± 0.01 μm^2 , N = 9, n = 95) and

pAAV_U6_HAPLN1_shRNA treated animals ($0.33 \pm 0.01 \mu\text{m}^2$, $N = 10$, $n = 108$, $p = 0.8$ control; t-test, Fig. 28 2D Method 2).

The relative intensity of BCAN expression remained unaffected after treatment ($100 \pm 13\%$, $N = 9$, $n = 95$) in pAAV_U6_control_shRNA group versus ($115 \pm 20\%$, $N = 10$, $n = 108$) in pAAV_U6_HAPLN1_shRNA group ($p = 0.53$, t-test; Fig. 28 E) using both methods. These results suggest that the knockdown of HAPLN1 protein altered ECM around excitatory neurons in a manner that is not detectable using BCAN expression immunohistochemistry pattern. A possible explanation for this result is that expression of BCAN is too low to be accurately measured using applied methods.

Altogether, this data suggests that reduced neuronal expression of HAPLN1 protein might affect inhibitory input on CaMK2-positive cells.

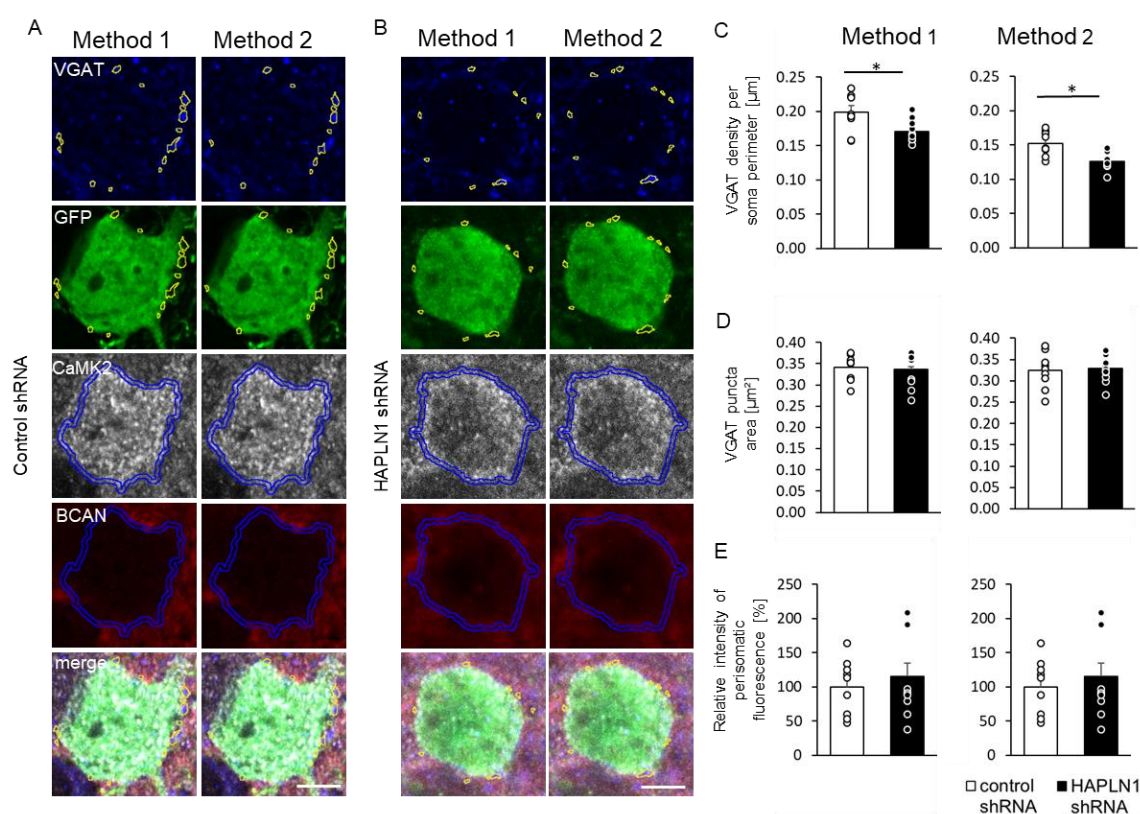


Fig. 28 Inhibitory presynaptic puncta and BCAN expression around CaMK2 positive cell soma. (A, B): Comparison of two approaches for automatic image analysis – Method 1, measuring VGAT puncta $> 0.1 \mu\text{m}$ inside $1 \mu\text{m}$ band around GFP marked cell body and Method 2 measuring VGAT puncta $> 0.1 \mu\text{m}$ inside $0.75 \mu\text{m}$ band around GFP marked cell body ($0.25 \mu\text{m}$ inside cell body and $0.5 \mu\text{m}$ outside cell body) - on top of representative images. The inhibitory presynaptic marker VGAT visualized in blue (selected puncta in method-dependent

cell body proximity marked in yellow). GFP (in green) indicates an infected cell body (the selected puncta in method-dependent cell body proximity marked in yellow). BCAN visualized in red in 0.5 μm distance around CaMK2 cell bodies visualized in grey (selected region marked in blue). The left panel (A): shows AAV_control_shRNA, right panel (B): shows AAV_HAPLN1_shRNA treated mice. (C): Densities of VGAT⁺ presynaptic puncta per soma perimeter μm^2 . (D): Relative intensity of BCAN perisomatic fluorescence. (E): VGAT⁺ synaptic puncta size around CaMK2⁺ cell bodies (B, C, D): Mean \pm SEM are shown. * $p = 0.01$, ** $p = 0.002$, t-test. Control_shRNA: N = 9, n = 95, HAPLN1_shRNA: N = 10, n = 108.

4.2.5 Inhibitory presynaptic puncta and WFA in perisomatic area of PV positive interneurons

To investigate HAPLN1 function in the regulation of inhibitory input on interneurons, I performed a semi-quantitative analysis of VGAT⁺ inhibitory presynaptic puncta (in blue) on the soma perimeter of PV⁺ interneurons (in grey) (Fig. 29 A, B). For this analysis, I use two methods. First, I investigate VGAT positive puncta bigger than 0.1 μm located in 1 μm proximity to PV⁺ (marked as ROIs in yellow). I will refer to this method as method 1. Second, investigated VGAT⁺ than 0.1 μm located in 0.5 μm band around PV⁺ cell body in the art that 0.35 μm of the band is located inside cell body and 0.15 μm of the band is outside the cell body. I will refer to this method as method 2. Method 2 is more precise excluding puncta that have no direct contact with the cell body and including puncta that partially overlap with the cell body for measured signal strength for applied settings. The band settings for PV⁺ cells are different than for CaMK2⁺ cells because the PV signal in my experiment was much stronger than the CaMK2 signal. WFA immunostaining (in red) was used for the analysis of HAPLN1 knockdown-induced changes in PNNs in 0.5 μm proximity of PV⁺ cell body.

Preliminary analysis of immunohistochemistry images revealed low efficacy of interneurons infection using both AAV_control_shRNA and AAV_HAPLN1_shRNA viruses. Therefore, for further analysis, I investigate only PV-positive interneurons expressing GFP (PV⁺ GFP⁺). As in immunohistochemistry analysis of the neuropil and CaMK2 positive cells two control mice were excluded from analysis due to injection complications. Two other control animals and two AAV_HAPLN1_shRNA-treated animals were excluded from further analysis due to the lack of PV⁺GFP⁺ cells in the infected area.

Analysis of VGAT⁺ inhibitory synaptic puncta on perisomatic area of PV⁺ GFP⁺ interneurons in mPFC show no effect of AAV_HAPLN1_shRNA treatment on puncta density (0.09 ± 0.01 puncta

per μm of soma perimeter, $N = 7$, total number of cells $n=27$) versus AAV_control_shRNA (0.10 ± 0.01 puncta per μm of soma perimeter, $N = 7$, total number of cells = 27; $p = 0.9$, t-test; Fig. 29 C Method 1). However, the analysis using method 2 shows significant reduction in perisomatic VGAT⁺ puncta density after AAV_HAPLN1_shRNA treatment (0.11 ± 0.02 puncta per μm of soma perimeter, $N = 7$, total number of cells $n = 27$) versus AAV_control_shRNA (0.07 ± 0.01 puncta per μm of soma perimeter, $N = 7$, total number of cells = 27; $p = 0.04$, t-test; Fig. 29 C Method 2). Those results suggest that HAPLN1 local deficits may affect inhibitory input on PV⁺ cells.

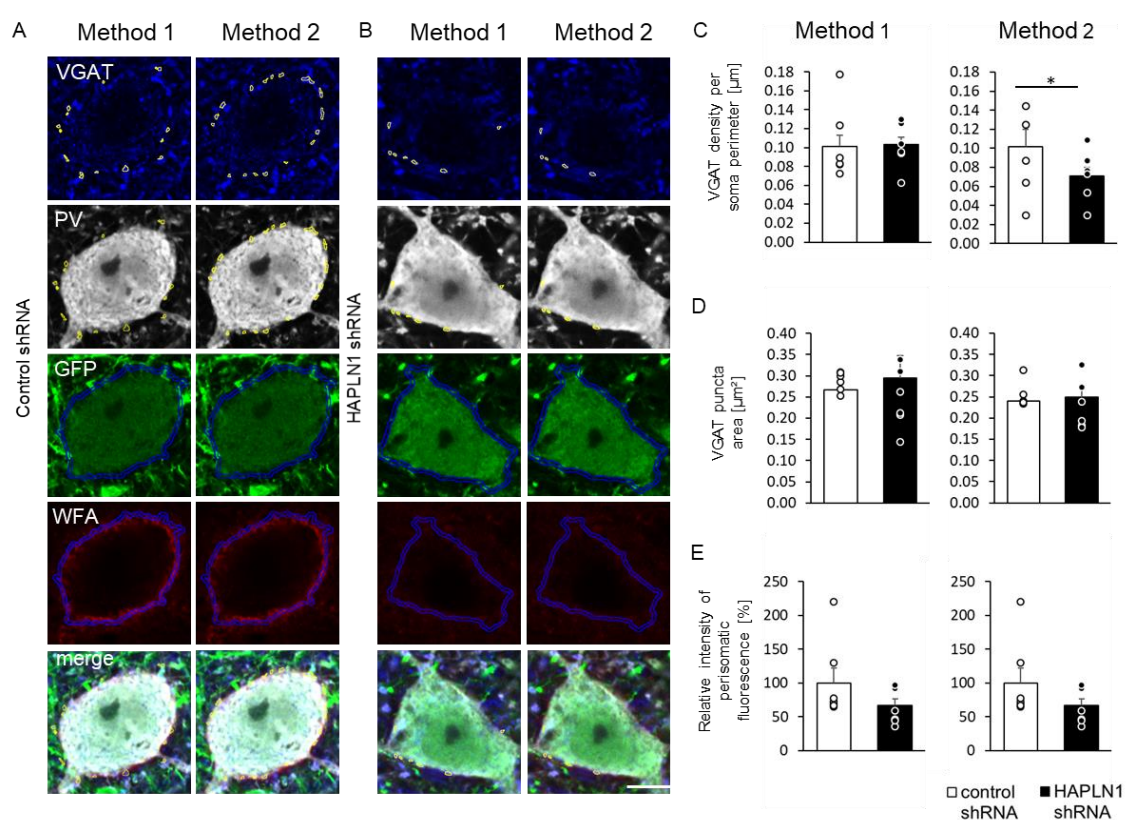


Fig. 29 Inhibitory presynaptic puncta and WFA expression around PV positive cell soma. (A, B): Comparison of two approaches for automatic image analysis – Method 1, measuring VGAT puncta $> 0.1 \mu\text{m}$ inside $1 \mu\text{m}$ band around GFP (in green) marked cell body and Method 2 measuring VGAT puncta $> 0.1 \mu\text{m}$ inside $0.75 \mu\text{m}$ band around GFP marked cell body ($0.25 \mu\text{m}$ inside cell body and $0.5 \mu\text{m}$ outside cell body) - on top of representative images. The inhibitory presynaptic marker VGAT visualized in blue, PV visualized in grey (selected puncta in method-dependent cell body proximity marked in yellow). WFA visualized in red around GFP⁺ infected cell body (in green). The $0.5 \mu\text{m}$ region around cell body marked in blue. The left (A): panel shows AAV_control_shRNA, right panel (B): shows AAV_HAPLN1_shRNA treated mice. (C): Densities of VGAT⁺ presynaptic puncta per soma perimeter μm^2 . (D): Relative

intensity of WFA perisomatic fluorescence. (E): VGAT⁺ synaptic puncta size around PV positive cell bodies (B, C, D): Mean \pm SEM are shown. * $p = 0.04$, t-test. Control_shRNA: N = 7, total number of cells n = 27, HAPLN1_shRNA: N = 7, total number of cells n = 27.

The analysis of VGAT puncta area using both methods shows no difference between control and HAPLN1shRNA viral treatment in PV⁺GFP⁺ cells for method 1 (AAV_control_shRNA: $0.28 \pm 0.01 \mu\text{m}^2$, control N = 7, total number of cells 27; AAV_HAPLN1_shRNA: $0.21 \pm 0.06 \mu\text{m}^2$, N = 7, total number of cells = 27; $p = 0.74$, t-test; Fig 24D Method 1) and for method 2 (AAV_control_shRNA: $0.25 \pm 0.01 \mu\text{m}^2$, control N = 7, total n = 27; AAV_HAPLN1_shRNA: $0.25 \pm 0.03 \mu\text{m}^2$, N = 7, n= 27; $p = 0.96$, t-test; Fig. 29 D Method 2).

Additionally, WFA relative intensity of fluorescence in $0.5 \mu\text{m}$ proximity around PV-positive interneurons soma revealed a tendency of reduction after AAV_HAPLN1_shRNA treatment ($67 \pm 10 \%$, N = 7, n = 27 versus $100 \pm 22 \%$, N = 7, n = 27 in control; $p = 0.1$, t-test; Fig. 29 B). This result is in the line with previous studies on the central nervous system of HAPLN1 knockout mice showing a diffuse pattern of PNN around PV⁺ cells. In this case, the diffused pattern of PNN may be less visible due to proximity to the cell body where the data was collected.

5 Discussion

Animal models of schizophrenia disease are an important tool to understand the cellular and molecular mechanisms behind the pathology of the disease. An increasing body of literature suggests that the extracellular matrix plays a significant role in the pathophysiology of the disease (Nacher, Guirado and Castillo-Gómez, 2013; Berretta *et al.*, 2015; Pantazopoulos *et al.*, 2015, 2021; Varbanov and Dityatev, 2016; Lepeta *et al.*, 2017). However, the exact mechanisms are still not well known.

In the first part of this thesis, I evaluated ECM alteration in rats sub-chronically treated with ketamine as a validated model of schizophrenia. The previous study using rats sub-chronically treated with ketamine shows behavioural alterations mimicking negative symptoms of schizophrenia, such as decreased latent inhibition and disrupted social interactions (Becker *et al.*, 2003). In Matuszko *et al.*, 2017 we show again disrupted social interaction, confirming that the applied protocol generates a schizophrenia-like phenotype.

The human post mortem brain studies show the reduced volume of several brain areas, including mPFC and hippocampus, in schizophrenic samples. Therefore, we chose those two brain areas to study ECM alterations in the ketamine model of schizophrenia and found new properties of this model. The results of the analysis of those two brain areas are discussed below.

5.1 Sub-chronic treatment with ketamine induces the reduction of WFA⁺ cells in rat mPFC

Image analysis of mPFC shows a significant reduction in the density of WFA⁺ cells in ketamine-treated rats. This is in line with human post-mortem brain studies reporting a reduction in density of PNN in PFC (Mauney *et al.*, 2013), entorhinal cortex and amygdala (Pantazopoulos *et al.*, 2010). However, the quantitative alteration in PNN density in PFC seems to be stronger in human samples, by 70 % (Mauney *et al.*, 2013), than in the ketamine-treated rat model, by 20 %. This difference can be explained due to the short duration of ketamine treatment and post-treatment time compared to the time course of the disease.

The ketamine-induced reduction of WFA⁺ cells in rat mPFC is probably a result of the ketamine blockade of the NMDA receptor since ketamine has the strongest binding affinity to the NMDA receptor (Becker and Grecksch, 2004). The *in vitro* study using hippocampal primary cell culture shows no effect of NMDA receptor agonist AP5 on the formation of PNN around interneurons.

However, those alterations might be brain area-specific. Moreover, the expression of ECM components and degradation enzymes is activity-dependent. Therefore, ketamine-induced alteration of PFC neural activity might affect the formation and degradation of local PNNs.

The reduced density of WFA⁺ cells in mPFC might affect the survival and function of PV⁺ interneurons. The human post-mortem studies of Alzheimer's subjects show PNNs' protective role against oxidative stress (Morawski *et al.*, 2004). Although my results show no decrease of PV⁺ cells density in mPFC, further analysis with a longer post-treatment interval might be necessary to show ketamine impact on PV⁺ cells survival. Animal studies show that the removal of PNNs with chondroitinase ABC reduces inhibition and increases gamma oscillation in the visual cortex (Lensjø *et al.*, 2017). Further analysis of gamma oscillation of ketamine-treated rats would give an interesting view on this animal model of schizophrenia disease.

Additionally, fine structure analysis of PNNs shows a significant reduction of the number of ventricles in PNN meshes as well as reduced mesh area surrounding interneurons in ketamine-treated rats mPFC. Those results show that not only the number of WFA⁺ cells but also the structure of PNNs can be affected by ketamine treatment. The reduced number of ventricles, as well as the reduced mesh area, might affect the accessibility of interneurons cell body surface for potential synaptic partners, leading to excitatory-inhibitory imbalance. However, further analysis of synaptic markers needs to be performed to confirm this hypothesis. The reduced mesh area might also implement further structural and functional changes in PNNs such as the GAG sulphation pattern associated with the maturation of PNNs.

5.2 Sub-chronic treatment with haloperidol and risperidone show no effects on the density of WFA⁺ cells in mPFC

My analysis of WFA⁺ cells shows no effect of common antipsychotic -haloperidol and atypical antipsychotic- risperidone schizophrenia treatment on WFA⁺ cells density in rat mPFC. Those results might suggest that observed in human post mortem brains reduction of PNNs is mostly driven by the disease not a side effect of used treatment. However, those results are limited to sub-chronic treatment, further long-term treatment studies might give a full view of the antipsychotic impact on WFA⁺ cells in mPFC.

5.3 Sub-chronic ketamine treatment show no effect on WFA⁺ cells in the hippocampal CA1 area

Image analysis of hippocampal CA1 area shows no ketamine-induced alteration of WFA⁺ cells density. These data might suggest that ketamine-induced WFA alterations are brain area-specific. Although the hippocampus is a schizophrenia-related brain area there is a lack of human post mortem brain studies showing reduction of PNN in schizophrenic brain hippocampus.

Additionally, our analysis of the intensity of WFA labelling along PV neurites shows no changes after ketamine treatment.

5.4 Sub-chronic ketamine treatment induces a significant reduction of parvalbumin expression in mPFC

The parvalbumin signal intensity analysis shows a significant reduction in rat mPFC after ketamine treatment. This is in line with human post mortem brain studies reporting reduced mRNA expression of parvalbumin and GAD 67 in schizophrenic PFC (Hashimoto *et al.*, 2003), as well as the reduced intensity of parvalbumin signal in DLPFC (Enwright *et al.*, 2016). Some of the human brain post mortem studies also report loss of parvalbumin-positive cells in schizophrenic PFC (Beasley and Reynolds, 1997; Reynolds, Beasley and Zhang, 2002; Sakai *et al.*, 2008), however, those reports do not include parvalbumin signal intensity analysis and it is possible that more sensitive methods would show rather a difference in parvalbumin expression level than decrease of relative parvalbumin cell density. In this regard, there are several human post mortem brain studies that report no difference in PV⁺ cell density in PFC of schizophrenic patients (Woo, Miller and Lewis, 1997; Tooney and Chahl, 2004; Alcaide *et al.*, 2019). These studies also show no signal intensity analysis; thus, it might be that in those studies even cells with low parvalbumin expression were included resulting in no cell loss.

Interestingly, parvalbumin deficits in PFC were also reported in several genetic and pharmacological animal models of schizophrenia (Abekawa *et al.*, 2007; Lodge, Behrens and Grace, 2009; Steullet *et al.*, 2017). A recent study comparing different animal models of schizophrenia and autism spectrum disorder suggests a link between PNN deficits, increased oxidative stress and decreased PV⁺ cells density in animals PFC (Steullet *et al.*, 2017), underlining the role of oxidative stress as a mechanism of the pathophysiology of schizophrenia. The PNN protective properties against oxidative stress were also shown in Alzheimer's patients' post mortem cerebral cortex samples (Morawski *et al.*, 2004). This study reports that PV⁺ cells without PNN were more sensitive to oxidative stress and that oxidative stress may compromise the PNN around PV cells. These results can help to understand the link between PNN deficits, oxidative stress and decreased PV⁺ cells density in PFC of schizophrenia and autism animal models. In the

context of these studies, it would be interesting to measure oxidative stress in ketamine-treated rats PFC in future experiments.

The animal studies on the differentiation of PV networks suggest that recent experience such as enriched environment or fear conditioning may modulate learning by targeting the differentiation state of PV⁺ neurons in adulthood. However, forced pharmacogenetic inhibition of PV neurons reverses the experience-induced PV neuron differentiation, leading to changes in parvalbumin expression, excitatory-inhibitory synaptic ratio, learning plasticity and processing of memories (Donato, Rompani and Caroni, 2013). In the context of this study, it would be interesting to investigate if ketamine-induced NMDA receptor block on PV⁺ cells may also alter the differentiation state of PV⁺ interneurons after PFC-related behavioural training. Further analysis of excitatory-inhibitory synaptic input on PV⁺ cells would bring more understanding of the WFA and PV deficits and their functional role in the ketamine model of schizophrenia.

5.5 Sub-chronic ketamine treatment shows no effect on HNK-1 expression in PFC

Although the ketamine treatment induces a decrease in WFA⁺ cell density, our analysis of tenascin-R-related HNK-1 expression shows no effect of the treatment. This result may be challenging taking into consideration that the general organization of neural ECM is similar in perisomatic and neuropil area. However, there are differences in the expression level of major ECM components such as chondroitin sulfate proteoglycans, tenascin-R and link proteins in both areas. Thus, alteration of one ECM molecule or ECM protease may differentially affect ECM associated with different cell types and subcellular domains.

Further high-resolution analysis of perisynaptic markers such as brevican and synaptic markers would give more understanding of ketamine-induced changes in neuropil ECM.

5.6 The decrease of WFA⁺ cells in PFC is accompanied by the upregulation of total CS56⁺ ECM

The CS56 antibody recognizes ECM of glial origins which forms a dandelion clock-like structure in non-GABAergic neurons neuropil. Those structures occurrence correlates with the maturation of different cortical areas and therefore is suggested to play a role in the regulation of synaptic plasticity parallel to PNN (Hayashi *et al.*, 2007).

The analysis of CS56⁺ ECM shows no alteration in the density of dandelion clock-like structures after ketamine treatment. However, the total intensity of CS56⁺ ECM is significantly increased in the PFC of ketamine treated rats. Previous human post mortem brain analysis of the amygdala

reported a decreased number of glial ECM clusters in schizophrenic patients; unfortunately, there are no data from PFC (Pantazopoulos *et al.*, 2015).

Currently available data are not sufficient to discuss the difference between those results. I can only speculate that the increased expression of CS56⁺ ECM might reflect the general state of glial cells. The increased activity of glia may suggest local inflammation. Human post mortem brain studies also reported a fraction of schizophrenic patients (38%) with increased expression levels of inflammatory markers such as interleukin-6, SERPINA3, interleukin-1 β and interleukin-8 as well as increased microglia density in dorsolateral PFC (Fillman *et al.*, 2013). However further analysis of inflammatory markers in the ketamine model of schizophrenia needs to be performed to confirm or reject this speculation.

However, astrocytes might be altered in schizophrenia as a result of disease pathology and not an inflammatory reaction. The human glial progenitor cells derived from patients with childhood-onset of schizophrenia showed an over two-fold increase in BCAN gene expression and over three-fold increase in TN-R gene expression suggesting a glial ECM-related mechanisms playing a role in the disease pathophysiology (Windrem *et al.*, 2017).

A recent study of ECM-related gene expression across several brain areas of *postmortem* brain samples from schizophrenic and healthy individuals shows alteration in expression of chondroitin sulphate synthesis genes in anterior PFC and dorsolateral PFC of schizophrenic brains. The study reports downregulation of crucial enzyme in the biosynthesis of chondroitin sulphate - chondroitin sulphate synthase 1 (CHSY-1) expression as well as an increase in mRNA levels of lysosomal exohydrolase (GALNS) involved in the degradation of keratan and chondroitin 6-sulphate in keratin and chondroitin sulphate chains and an increase in mRNA levels of in chondroitin 6-sulphate sulfotransferase (CHST3) in both PFC areas of schizophrenic brains (Pantazopoulos *et al.*, 2021). Those results suggest that genes relevant for ECM of glial origins are altered in the PFC of schizophrenic patients and may affect the formation of local dandelion clock-like structures and contribute to the modulation of synaptic plasticity.

5.7 The AAV-induced reduction of HAPLN1 protein in mouse mPFC

To better understand pathological mechanisms in the PFC of schizophrenic patients, in the second part of the thesis I created a new mouse model having AAV-induced reduction of HAPLN1 protein in mPFC to address the question of whether local acute deficits of one ECM protein can lead to an excitatory-inhibitory imbalance in the cortical area. The HAPLN1 protein was selected based on previous literature reporting that upregulation of HAPLN1 triggers PNN formation and mice lacking HAPN-1 in their CNS show enhanced plasticity in the visual and somatosensory systems in the adult brain, suggesting a role of the protein in the regulation of ECM and synaptic plasticity. The use of the acute AAV knockdown approach allows us to investigate the influence of protein deficit restricted to one brain area and avoid possible compensation mechanisms.

During the model preparation phase, the designed HAPLN1 shRNA constructs were validated in the HEK293T cell line co-transfected with HAPLN1 overexpressing construct using the qPCR approach. The most efficient shRNA construct was selected to be packed in AAV capsids. The functional AAV HAPLN1 shRNA virus was validated in mice primary hippocampal cell culture with qPCR. Afterwards, I validated the expression of the virus based on GFP fluorescence in five weeks old mice PFC after transcranial injection pups on day eight.

Nevertheless, this model has a few limitations. The use of only one knockdown virus does not allow us to exclude the possible off-target effect of the used construct in further experiments. Additionally, the use of qPCR technique only allows us to observe the virus effect on the RNA levels without allowing us to discard residual protein levels of HAPLN1. The use of additional techniques like Western blot or immunofluorescence targeting HAPLN1 protein would give a better overview of the effect on the protein level. Surprisingly, the analysis of GFP signal in mice PFC infected with the virus shows a lower infection rate of PV⁺ cells in comparison to CaMK2⁺ cells, suggesting that used AAV capsid packing system is more prone to infect excitatory cells. However, we were able to find a representative number of GFP⁺ PV⁺ cells to investigate the effect of the virus on interneurons.

Even though the AAV_HAPLN1_shRNA treated mice show promising results as a schizophrenia model, further validation needs to be performed in the future. And, very importantly, the obtained results need to be analysed very cautiously as a pilot experimental study.

5.8 Normal PPI in the AAV_HAPLN1_shRNA treated mice

The prepulse inhibition of startle is a cross-species measure of the ability of a non-startle stimulus to inhibit the animal response to a startle stimulus and it is used to validate sensorimotor gating, that is thought to test pre-attentional filtering mechanisms (Powell, Zhou and Geyer, 2009). Although PPI deficits were reported in many mental disorders, such as maniac bipolar disorder, autism, obsessive-compulsive disorder, Tourette's syndrome and Huntington's disease; the PPI deficits in schizophrenia patients are the best characterized and the most widely replicated. Therefore, we used PPI in order to validate if mPFC injection of AAV_HAPLN1_shRNA may induce schizophrenia-like behaviour in mice.

Interestingly, our analysis reveals that AAV_HAPLN1_shRNA treatment induces increased PPI response in comparison to control virus treated animals. However, those results need to be interpreted with caution because of weak increase of PPI with increased sound intensity in control animals comparing to the reported PPI response in 6 (70 dB > 50% PPI, 80 dB > 80% PPI, 85 dB > 80% PPI) and 9 weeks old C57/BL6 mice (69 dB ~ 20% PPI, 73 dB ~ 50% PPI, 77 dB ~ 70% PPI) (Brody *et al.*, 2004; Ouagazzal, Reiss and Romand, 2006). Although there are differences between PPI experimental protocols in the field including precise age of animals and intensity of sound, most studies share a common outcome of strong, significantly increased PPI response with

increased sound intensity. We could observe a similar response in our AAV_HAPLN1_shRNA treated mice but not control animals. Therefore, our results show normal PPI in AAV_HAPLN1_shRNA treated animals, suggesting that applied treatment is not generating schizophrenia-like behaviour in mice, possibly due to low levels of AAV infection of PV⁺ cells.

5.9 The AAV_HAPLN1_shRNA treatment does not affect neuropil density of excitatory puncta, synapses and surrounding BCAN

The analysis of neuropil excitatory puncta shows no effect of AAV_HAPLN1_shRNA treatment on the excitatory synaptic puncta area and density as well as density of excitatory synapses in mPFC. This result suggests that HAPLN1 deficits in our animal model may induce cell domain-specific changes.

Additionally, our analysis of BCAN expression in neuropil shows no alteration of total signal intensity as well as perisynaptic BCAN signal intensity after AAV_HAPLN1_shRNA treatment. This may suggest that the deficit in HAPLN1 expression does not affect the expression of BCAN in the neuropil, possibly due to residual expression of HAPLN1 in uninfected cells or due to a contribution of other members of HAPLN subfamily.

5.10 The inhibitory perisomatic input on CaMK2⁺ cells is decreased in mPFC of AAV_HAPLN1_shRNA treated mice

The analysis of VGAT perisomatic puncta around CaMK2⁺ positive cells shows a significant reduction in puncta density, but not puncta area, after AAV_HAPLN1_shRNA treatment. These results suggest that HAPLN1 deficits in close proximity to CaMK2⁺ cell bodies may affect the accessibility of cell body area due to possible structural changes of ECM.

These results are in line with human studies showing excitatory-inhibitory imbalance in schizophrenia (reviewed by Gao and Penzes, 2015). Several human *post mortem* studies reported inhibitory deficits in PFC of schizophrenic patients on genetic (Hashimoto *et al.*, 2003), protein (Volk *et al.*, 2002) and functional level (Haenschel *et al.*, 2009; Barr *et al.*, 2010). Volk and colleagues suggested that upregulated α_2 subunits of GABA_A receptor on pyramidal neurons is compensation mechanism on reduced GABA release. Those deficits could be a result of reduced mRNA levels of parvalbumin and GAD67 protein reported by Hashimoto and colleagues and in consequence could lead to reported disrupted gamma oscillations in PFC of schizophrenic

patients. Moreover, the inhibitory impairments were suggested to be regulated by ECM components based on observed deficits of PNN and ECM components in *post mortem* samples of schizophrenic patients (Mauney *et al.*, 2013; Berretta *et al.*, 2015).

5.11 The inhibitory perisomatic input on PV⁺ cells is decreased in mPFC of AAV_HAPLN1_shRNA treated mice

The analysis of inhibitory input on PV⁺ cells shows significantly reduced density of perisomatic VGAT puncta, but not puncta size, after AAV_HAPLN1_shRNA treatment. These results suggest that deficits of HAPLN1 may affect the inhibitory neurons transmission. The results are also in line with recent animal studies showing that PNN⁺ PV⁺ cells in mice PFC have higher excitatory and inhibitory puncta density onto their cell bodies than PV⁺ lacking PNN due to chondroitinase ABC treatment, suggesting that HAPLN1 deficits may compromise the local PNN (Carceller *et al.*, 2020). Also, animal studies using chondroitinase ABC treatment in hippocampal CA2 area show reduced synaptic input after treatment (Hayani, Song and Dityatev, 2018).

Additionally, the analysis of WFA signal intensity shows a weak tendency of signal reduction in close proximity to PV⁺ cell bodies in AAV_HAPLN1_shRNA treated mice suggesting that HAPLN1 deficits may affect the PNN of infected cells. This result is in line with a previous study on HAPLN1 KO mice showing structural changes in PNN in HAPLN1 deficient mice manifested as diffuse PNN.

For further investigation of the effect of the HAPLN1 protein deficits on PV⁺ interneurons a stronger model need to be applied. The biggest limitation of the current study regarding those interneurons is low infection rate. In order to improve this aspect without losing the advantage of acute effect, a tissue-specific and inducible knockout mice line can be generated using Cre/lox system. Such approach would allow us to specifically target cerebral PV⁺ interneurons upon chemical stimulation using cerebral Nes (Tronche *et al.*, 1999) and PV (Hippenmeyer *et al.*, 2005) promotor combined with exogenous tamoxifen-inducible Cre system such as CreER.

6 Conclusions

- Rats treated with 30 mg/kg of ketamine in a sub-chronic manner show a reduced density of WFA⁺ cells but not of PV⁺ cells in their mPFC. However, the same treatment does not affect the density of WFA⁺ cells in the rat's hippocampal CA1 area.
- Sub-chronic treatment with common antipsychotic haloperidol and atypical antipsychotic risperidone shows no effects on the density of WFA⁺ cells in mPFC of adult male rats.
- Rats treated with 30 mg/kg of ketamine in a sub-chronic manner show a significant reduction of parvalbumin expression in the cell bodies of their mPFC interneurons. However, the treatment shows no significant effect on the WFA signal in PNNs in the same brain area.
- Sub-chronic ketamine treatment shows no effect on HNK-1 expression in both perisomatic and neuropil areas of rats PFC.
- The decrease in the WFA⁺ cell density in the PFC is accompanied by the upregulation of total CS56⁺ ECM but is not affecting the density of glia-related DACs.
- Juvenile mice injected with the AAV_HAPLN1_shRNA in the PFC show normal PPI in their adulthood compared to the control virus injected mice.
- The AAV_HAPLN1_shRNA treatment does not affect density of excitatory puncta, synapses and surrounding them BCAN in the neuropil.
- The inhibitory perisomatic input on CaMK2⁺ cells is decreased in mPFC of AAV_HAPLN1_shRNA treated mice.
- The inhibitory perisomatic input on PV⁺ cells is decreased in mPFC of AAV_HAPLN1_shRNA treated mice.

References

- Abekawa, T., Ito, K., Nakagawa, S. and Koyama, T. (2007) 'Prenatal exposure to an NMDA receptor antagonist, MK-801 reduces density of parvalbumin-immunoreactive GABAergic neurons in the medial prefrontal cortex and enhances phencyclidine-induced hyperlocomotion but not behavioral sensitization to methamphetamine', *Psychopharmacology*, 192(3), pp. 303–316. doi:10.1007/s00213-007-0729-8.
- Aerts, J., Nys, J., Moons, L., Hu, T.-T. and Arckens, L. (2015) 'Altered neuronal architecture and plasticity in the visual cortex of adult MMP-3-deficient mice.', *Brain structure & function*, 220(5), pp. 2675–2689. doi:10.1007/s00429-014-0819-4.
- Ajmo, J.M., Eakin, A.K., Hamel, M.G. and Gottschall, P.E. (2008) 'Discordant localization of WFA reactivity and brevican/ADAMTS-derived fragment in rodent brain.', *BMC neuroscience*, 9, p. 14. doi:10.1186/1471-2202-9-14.
- Alcaide, J., Guirado, R., Crespo, C., Blasco-Ibáñez, J.M., Varea, E., Sanjuan, J. and Nacher, J. (2019) 'Alterations of perineuronal nets in the dorsolateral prefrontal cortex of neuropsychiatric patients', *International journal of bipolar disorders*, 7(1), p. 24. doi:10.1186/s40345-019-0161-0.
- Allen, M., Ghosh, S., Ahern, G.P., Villapol, S., Maguire-Zeiss, K.A. and Conant, K. (2016) 'Protease induced plasticity: matrix metalloproteinase-1 promotes neurostructural changes through activation of protease activated receptor 1.', *Scientific reports*, 6, p. 35497. doi:10.1038/srep35497.
- Andersen, S.L. (2003) 'Trajectories of brain development: point of vulnerability or window of opportunity?', *Neuroscience and biobehavioral reviews*, 27(1–2), pp. 3–18.
- Andreasson, S., Allebeck, P., Engstrom, A. and Rydberg, U. (1987) 'Cannabis and schizophrenia. A longitudinal study of Swedish conscripts.', *Lancet (London, England)*, 2(8574), pp. 1483–1486.
- Anvari, A.A., Friedman, L.A., Greenstein, D., Gochman, P., Gogtay, N. and Rapoport, J.L. (2015) 'Hippocampal volume change relates to clinical outcome in childhood-onset schizophrenia.', *Psychological medicine*, 45(12), pp. 2667–2674. doi:10.1017/S0033291715000677.
- Araque, A., Parpura, V., Sanzgiri, R.P. and Haydon, P.G. (1999) 'Tripartite synapses: glia, the unacknowledged partner.', *Trends in neurosciences*, 22(5), pp. 208–215. doi:10.1016/s0166-2236(98)01349-6.
- Arnst, N., Kuznetsova, S., Lipachev, N., Shaikhtudinov, N., Melnikova, A., Mavlikeev, M., Uvarov, P., Baltina, T. V, Rauvala, H., Osin, Y.N., Kiyasov, A.P. and Paveliev, M. (2016) 'Spatial patterns and cell surface clusters in perineuronal nets.', *Brain research*, 1648(Pt A), pp. 214–223. doi:10.1016/j.brainres.2016.07.020.
- Aujla, P.K. and Huntley, G.W. (2014) 'Early postnatal expression and localization of matrix metalloproteinases-2 and -9 during establishment of rat hippocampal synaptic circuitry.', *The Journal of comparative neurology*, 522(6), pp. 1249–1263. doi:10.1002/cne.23468.
- Axelrod, J. and Tomchik, R. (1958) 'Enzymatic O-methylation of epinephrine and other catechols.', *The Journal of biological chemistry*, 233(3), pp. 702–705. doi:10.1016/s0021-9258(18)64731-3.
- Barksdale, K.A., Lahti, A.C. and Roberts, R.C. (2014) 'Synaptic proteins in the postmortem anterior cingulate cortex in schizophrenia: relationship to treatment and treatment response.', *Neuropsychopharmacology: official publication of the American College of Neuropsychopharmacology*, 39(9), pp. 2095–2103. doi:10.1038/npp.2014.57.

- Barr, M.S., Farzan, F., Tran, L.C., Chen, R., Fitzgerald, P.B. and Daskalakis, Z.J. (2010) 'Evidence for excessive frontal evoked gamma oscillatory activity in schizophrenia during working memory.', *Schizophrenia research*, 121(1–3), pp. 146–152. doi:10.1016/j.schres.2010.05.023.
- Barth, C., Villringer, A. and Sacher, J. (2015) 'Sex hormones affect neurotransmitters and shape the adult female brain during hormonal transition periods', *Frontiers in Neuroscience*, p. 37. Available at: <https://www.frontiersin.org/article/10.3389/fnins.2015.00037>.
- Beasley, C.L. and Reynolds, G.P. (1997) 'Parvalbumin-immunoreactive neurons are reduced in the prefrontal cortex of schizophrenics.', *Schizophrenia research*, 24(3), pp. 349–355. doi:10.1016/s0920-9964(96)00122-3.
- Becker, A., Peters, B., Schroeder, H., Mann, T., Huether, G. and Grecksch, G. (2003) 'Ketamine-induced changes in rat behaviour: A possible animal model of schizophrenia', *Prog Neuropsychopharmacol Biol Psychiatry*. 2003/06/06, 27(4), pp. 687–700. doi:10.1016/s0278-5846(03)00080-0.
- Becker, A., Grecksch, G., Zernig, G., Ladstaetter, E., Hiemke, C. and Schmitt, U. (2009) 'Haloperidol and risperidone have specific effects on altered pain sensitivity in the ketamine model of schizophrenia', *Psychopharmacology*, 202(4), pp. 579–587. doi:10.1007/s00213-008-1336-z.
- Becker, A. and Grecksch, G. (2004) 'Ketamine-induced changes in rat behaviour: a possible animal model of schizophrenia. Test of predictive validity.', *Progress in neuro-psychopharmacology & biological psychiatry*, 28(8), pp. 1267–1277. doi:10.1016/j.pnpbp.2004.06.019.
- Begni, S., Popoli, M., Moraschi, S., Bignotti, S., Tura, G.B. and Gennarelli, M. (2002) 'Association between the ionotropic glutamate receptor kainate 3 (GRIK3) ser310ala polymorphism and schizophrenia.', *Molecular psychiatry*, 7(4), pp. 416–418. doi:10.1038/sj.mp.4000987.
- Berlucchi, G. and Buchtel, H.A. (2009) 'Neuronal plasticity: historical roots and evolution of meaning.', *Experimental brain research*, 192(3), pp. 307–319. doi:10.1007/s00221-008-1611-6.
- Beroun, A., Mitra, S., Michaluk, P., Pijet, B., Stefaniuk, M. and Kaczmarek, L. (2019) 'MMPs in learning and memory and neuropsychiatric disorders.', *Cellular and molecular life sciences: CMLS*, 76(16), pp. 3207–3228. doi:10.1007/s00018-019-03180-8.
- Berretta, S., Pantazopoulos, H., Markota, M., Brown, C. and Batzianouli, E.T. (2015) 'Losing the sugar coating: Potential impact of perineuronal net abnormalities on interneurons in schizophrenia', *Schizophrenia Research* [Preprint]. doi:10.1016/j.schres.2014.12.040.
- Bijoch, L., Borczyk, M. and Czajkowski, R. (2020) 'Bases of Jerzy Konorski's theory of synaptic plasticity.', *The European journal of neuroscience*. France, pp. 1857–1866. doi:10.1111/ejn.14532.
- Bilousova, T. V, Rusakov, D.A., Ethell, D.W. and Ethell, I.M. (2006) 'Matrix metalloproteinase-7 disrupts dendritic spines in hippocampal neurons through NMDA receptor activation.', *Journal of neurochemistry*, 97(1), pp. 44–56. doi:10.1111/j.1471-4159.2006.03701.x.
- Bitanirwe, B.K.Y. and Woo, T.-U.W. (2014) 'Transcriptional dysregulation of γ -aminobutyric acid transporter in parvalbumin-containing inhibitory neurons in the prefrontal cortex in schizophrenia.', *Psychiatry research*, 220(3), pp. 1155–1159. doi:10.1016/j.psychres.2014.09.016.
- Bourgeois, J.P., Goldman-Rakic, P.S. and Rakic, P. (1994) 'Synaptogenesis in the prefrontal cortex of rhesus monkeys.', *Cerebral cortex (New York, N.Y. : 1991)*, 4(1), pp. 78–96.

- Brody, S.A., Dulawa, S.C., Conquet, F. and Geyer, M.A. (2004) 'Assessment of a prepulse inhibition deficit in a mutant mouse lacking mGlu5 receptors', *Molecular Psychiatry*, 9(1), pp. 35–41. doi:10.1038/sj.mp.4001404.
- Brown, A.S., Cohen, P., Harkavy-Friedman, J., Babulas, V., Malaspina, D., Gorman, J.M. and Susser, E.S. (2001) 'A.E. Bennett Research Award. Prenatal rubella, premorbid abnormalities, and adult schizophrenia.', *Biological psychiatry*, 49(6), pp. 473–486.
- Brown, A.S., Begg, M.D., Gravenstein, S., Schaefer, C.A., Wyatt, R.J., Bresnahan, M., Babulas, V.P. and Susser, E.S. (2004) 'Serologic evidence of prenatal influenza in the etiology of schizophrenia.', *Archives of general psychiatry*, 61(8), pp. 774–780. doi:10.1001/archpsyc.61.8.774.
- Brown, A.S., Schaefer, C.A., Quesenberry, C.P.J., Liu, L., Babulas, V.P. and Susser, E.S. (2005) 'Maternal exposure to toxoplasmosis and risk of schizophrenia in adult offspring.', *The American journal of psychiatry*, 162(4), pp. 767–773. doi:10.1176/appi.ajp.162.4.767.
- Brown, A.S. and Susser, E.S. (2008) 'Prenatal nutritional deficiency and risk of adult schizophrenia.', *Schizophrenia bulletin*, 34(6), pp. 1054–1063. doi:10.1093/schbul/sbn096.
- Brown, R., Colter, N., Corsellis, J.A., Crow, T.J., Frith, C.D., Jagoe, R., Johnstone, E.C. and Marsh, L. (1986) 'Postmortem evidence of structural brain changes in schizophrenia. Differences in brain weight, temporal horn area, and parahippocampal gyrus compared with affective disorder.', *Archives of general psychiatry*, 43(1), pp. 36–42.
- Brückner, G., Brauer, K., Härtig, W., Wolff, J.R., Rickmann, M.J., Derouiche, A., Delpech, B., Girard, N., Oertel, W.H. and Reichenbach, A. (1993) 'Perineuronal nets provide a polyanionic, glia-associated form of microenvironment around certain neurons in many parts of the rat brain.', *Glia*, 8(3), pp. 183–200. doi:10.1002/glia.440080306.
- Cabungcal, J.-H., Steullet, P., Morishita, H., Kraftsik, R., Cuenod, M., Hensch, T.K. and Do, K.Q. (2013) 'Perineuronal nets protect fast-spiking interneurons against oxidative stress', *Proceedings of the National Academy of Sciences*, 110(22), pp. 9130 LP – 9135. doi:10.1073/pnas.1300454110.
- Cannon, T.D., van Erp, T.G.M., Bearden, C.E., Loewy, R., Thompson, P., Toga, A.W., Huttunen, M.O., Keshavan, M.S., Seidman, L.J. and Tsuang, M.T. (2003) 'Early and late neurodevelopmental influences in the prodrome to schizophrenia: contributions of genes, environment, and their interactions.', *Schizophrenia bulletin*, 29(4), pp. 653–669.
- Carceller, H., Guirado, R., Ripolles-Campos, E., Teruel-Martí, V. and Nacher, J. (2020) 'Perineuronal Nets Regulate the Inhibitory Perisomatic Input onto Parvalbumin Interneurons and γ Activity in the Prefrontal Cortex.', *The Journal of neuroscience : the official journal of the Society for Neuroscience*, 40(26), pp. 5008–5018. doi:10.1523/JNEUROSCI.0291-20.2020.
- Carlsson, A. and Lindqvist, M. (1963) 'Effect of Chlorpromazine or Haloperidol on Formation of 3-Methoxytyramine and Normetanephrine in Mouse Brain', *Acta Pharmacologica et Toxicologica*, 20(2), pp. 140–144. doi:10.1111/j.1600-0773.1963.tb01730.x.
- Carulli, D., Pizzorusso, T., Kwok, J.C.F.F., Putignano, E., Poli, A., Forostyak, S., Andrews, M.R., Deepa, S.S., Glant, T.T. and Fawcett, J.W. (2010) 'Animals lacking link protein have attenuated perineuronal nets and persistent plasticity.', *Brain : a journal of neurology*, 133(Pt 8), pp. 2331–2347. doi:10.1093/brain/awq145.
- Castillo-Gomez, E., Perez-Rando, M., Vidueira, S. and Nacher, J. (2016) 'Polysialic Acid Acute Depletion Induces Structural Plasticity in Interneurons and Impairs the Excitation/Inhibition Balance in Medial Prefrontal Cortex Organotypic Cultures.', *Frontiers in cellular neuroscience*, 10, p. 170. doi:10.3389/fncel.2016.00170.

- Castillo-Gómez, E., Pérez-Rando, M., Bellés, M., Gilabert-Juan, J., Llorens, J.V., Carceller, H., Bueno-Fernández, C., García-Mompó, C., Ripoll-Martínez, B., Curto, Y., Sebastián-Ortega, N., Moltó, M.D., Sanjuan, J. and Nacher, J. (2017) 'Early Social Isolation Stress and Perinatal NMDA Receptor Antagonist Treatment Induce Changes in the Structure and Neurochemistry of Inhibitory Neurons of the Adult Amygdala and Prefrontal Cortex', *eneuro* [Preprint]. doi:10.1523/ENEURO.0034-17.2017.
- Celio, M.R., Spreafico, R., De Biasi, S. and Vitellaro-Zuccarello, L. (1998) 'Perineuronal nets: past and present.', *Trends in neurosciences*, 21(12), pp. 510–515.
- Chang, M.C., Park, J.M., Pelkey, K.A., Grabenstatter, H.L., Xu, D., Linden, D.J., Sutula, T.P., McBain, C.J. and Worley, P.F. (2010) 'Narp regulates homeostatic scaling of excitatory synapses on parvalbumin-expressing interneurons', *Nature neuroscience*. 2010/08/22, 13(9), pp. 1090–1097. doi:10.1038/nn.2621.
- Chen, J., Lipska, B.K., Halim, N., Ma, Q.D., Matsumoto, M., Melhem, S., Kolachana, B.S., Hyde, T.M., Herman, M.M., Apud, J., Egan, M.F., Kleinman, J.E. and Weinberger, D.R. (2004) 'Functional Analysis of Genetic Variation in Catechol-O-Methyltransferase (COMT): Effects on mRNA, Protein, and Enzyme Activity in Postmortem Human Brain', *American Journal of Human Genetics*, 75(5), pp. 807–821. Available at: <http://www.ncbi.nlm.nih.gov/pmc/articles/PMC1182110/>.
- Cho, R.W., Park, J.M., Wolff, S.B.E., Xu, D., Hopf, C., Kim, J.-A., Reddy, R.C., Petralia, R.S., Perin, M.S., Linden, D.J. and Worley, P.F. (2008) 'mGluR1/5-dependent long-term depression requires the regulated ectodomain cleavage of neuronal pentraxin NPR by TACE', *Neuron*, 57(6), pp. 858–871. doi:10.1016/j.neuron.2008.01.010.
- Christopherson, K.S., Ullian, E.M., Stokes, C.C.A., Mallowney, C.E., Hell, J.W., Agah, A., Lawler, J., Moshier, D.F., Bornstein, P. and Barres, B.A. (2005) 'Thrombospondins are astrocyte-secreted proteins that promote CNS synaptogenesis.', *Cell*, 120(3), pp. 421–433. doi:10.1016/j.cell.2004.12.020.
- Consortium, S.P.G.-W.A.S. (GWAS) (2011) 'Genome-wide association study identifies five new schizophrenia loci', *Nature genetics*, 43(10), pp. 969–976. doi:10.1038/ng.940.
- Costa, E., Chen, Y., Davis, J., Dong, E., Noh, J.S., Tremolizzo, L., Veldic, M., Grayson, D.R. and Guidotti, A. (2002) 'REELIN and schizophrenia: a disease at the interface of the genome and the epigenome.', *Molecular interventions*, 2(1), pp. 47–57. doi:10.1124/mi.2.1.47.
- Dauth, S., Grevesse, T., Pantazopoulos, H., Campbell, P.H., Maoz, B.M., Berretta, S. and Parker, K.K. (2016) 'Extracellular matrix protein expression is brain region dependent.', *The Journal of comparative neurology*, 524(7), pp. 1309–1336. doi:10.1002/cne.23965.
- Devon, R.S., Anderson, S., Teague, P.W., Muir, W.J., Murray, V., Pelosi, A.J., Blackwood, D.H. and Porteous, D.J. (2001) 'The genomic organisation of the metabotropic glutamate receptor subtype 5 gene, and its association with schizophrenia.', *Molecular psychiatry*, 6(3), pp. 311–314. doi:10.1038/sj.mp.4000848.
- Dityatev, A., Brückner, G., Dityateva, G., Grosche, J., Kleene, R. and Schachner, M. (2007) 'Activity-dependent formation and functions of chondroitin sulfate-rich extracellular matrix of perineuronal nets', *Developmental Neurobiology*, 67(5), pp. 570–588. doi:10.1002/dneu.20361.
- Dityatev, A. and Rusakov, D.A. (2011) 'Molecular signals of plasticity at the tetrapartite synapse.', *Current opinion in neurobiology*, 21(2), pp. 353–359. doi:10.1016/j.conb.2010.12.006.
- Dityatev, A. and Schachner, M. (2003) 'Extracellular matrix molecules and synaptic plasticity.', *Nature reviews. Neuroscience*, 4(6), pp. 456–468. doi:10.1038/nrn1115.

- Dityatev, A., Seidenbecher, C.I. and Schachner, M. (2010) 'Compartmentalization from the outside: the extracellular matrix and functional microdomains in the brain.', *Trends in neurosciences*, 33(11), pp. 503–512. doi:10.1016/j.tins.2010.08.003.
- Dobbertin, A., Czvitkovich, S., Theocharidis, U., Garwood, J., Andrews, M.R., Properzi, F., Lin, R., Fawcett, J.W. and Faissner, A. (2010) 'Analysis of combinatorial variability reveals selective accumulation of the fibronectin type III domains B and D of tenascin-C in injured brain.', *Experimental neurology*, 225(1), pp. 60–73. doi:10.1016/j.expneurol.2010.04.019.
- Donato, F., Rompani, S.B. and Caroni, P. (2013) 'Parvalbumin-expressing basket-cell network plasticity induced by experience regulates adult learning', *Nature* [Preprint]. doi:10.1038/nature12866.
- Edward Roberts, R., Curran, H.V., Friston, K.J. and Morgan, C.J.A. (2014) 'Abnormalities in white matter microstructure associated with chronic ketamine use', *Neuropsychopharmacology: official publication of the American College of Neuropsychopharmacology*. 2013/08/09, 39(2), pp. 329–338. doi:10.1038/npp.2013.195.
- Elmer, B.M. and McAllister, A.K. (2012) 'Major histocompatibility complex class I proteins in brain development and plasticity.', *Trends in neurosciences*, 35(11), pp. 660–670. doi:10.1016/j.tins.2012.08.001.
- Enwright, J.F., Sanapala, S., Foglio, A., Berry, R., Fish, K.N. and Lewis, D.A. (2016) 'Reduced labeling of parvalbumin neurons and perineuronal nets in the dorsolateral prefrontal cortex of subjects with schizophrenia', *Neuropsychopharmacology* [Preprint]. doi:10.1038/npp.2016.24.
- Eroglu, Ç., Allen, N.J., Susman, M.W., O'Rourke, N.A., Park, C.Y., Özkan, E., Chakraborty, C., Mulinyawe, S.B., Annis, D.S., Huberman, A.D., Green, E.M., Lawler, J., Dolmetsch, R., Garcia, K.C., Smith, S.J., Luo, Z.D., Rosenthal, A., Mosher, D.F. and Barres, B.A. (2009) 'Gabapentin Receptor $\alpha 2\delta$ -1 Is a Neuronal Thrombospondin Receptor Responsible for Excitatory CNS Synaptogenesis', *Cell* [Preprint]. doi:10.1016/j.cell.2009.09.025.
- Evers, M.R., Salmen, B., Bukalo, O., Rollenhagen, A., Bösl, M.R., Morellini, F., Bartsch, U., Dityatev, A. and Schachner, M. (2002) 'Impairment of L-type Ca^{2+} Channel-Dependent Forms of Hippocampal Synaptic Plasticity in Mice Deficient in the Extracellular Matrix Glycoprotein Tenascin-C', *The Journal of Neuroscience*, 22(16), pp. 7177 LP – 7194. doi:10.1523/JNEUROSCI.22-16-07177.2002.
- Fagiolini, M. and Hensch, T.K. (2000) 'Inhibitory threshold for critical-period activation in primary visual cortex.', *Nature*, 404(6774), pp. 183–186. doi:10.1038/35004582.
- Faissner, A., Pyka, M., Geissler, M., Sobik, T., Frischknecht, R., Gundelfinger, E.D. and Seidenbecher, C. (2010) 'Contributions of astrocytes to synapse formation and maturation - Potential functions of the perisynaptic extracellular matrix.', *Brain research reviews*, 63(1–2), pp. 26–38. doi:10.1016/j.brainresrev.2010.01.001.
- Fatemi, S.H., Emamian, E.S., Kist, D., Sidwell, R.W., Nakajima, K., Akhter, P., Shier, A., Sheikh, S. and Bailey, K. (1999) 'Defective corticogenesis and reduction in Reelin immunoreactivity in cortex and hippocampus of prenatally infected neonatal mice', *Mol Psychiatry*. 1999/04/20, 4(2), pp. 145–154.
- Ferrer-Ferrer, M. and Dityatev, A. (2018) 'Shaping Synapses by the Neural Extracellular Matrix', *Frontiers in Neuroanatomy*, p. 40. Available at: <https://www.frontiersin.org/article/10.3389/fnana.2018.00040>.
- Fillman, S.G., Cloonan, N., Catts, V.S., Miller, L.C., Wong, J., McCrossin, T., Cairns, M. and Weickert, C.S. (2013) 'Increased inflammatory markers identified in the dorsolateral prefrontal cortex of individuals with schizophrenia.', *Molecular psychiatry*, 18(2), pp. 206–214.

doi:10.1038/mp.2012.110.

Fino, E. and Venance, L. (2010) 'Spike-timing dependent plasticity in the striatum', *Frontiers in synaptic neuroscience*, 2, p. 6. doi:10.3389/fnsyn.2010.00006.

Freeman, H. (1994) 'Schizophrenia and city residence.', *The British journal of psychiatry. Supplement*, (23), pp. 39–50.

Freitag, S., Schachner, M. and Morellini, F. (2003) 'Behavioral alterations in mice deficient for the extracellular matrix glycoprotein tenascin-R.', *Behavioural brain research*, 145(1–2), pp. 189–207. doi:10.1016/s0166-4328(03)00109-8.

Frischknecht, R., Heine, M., Perrais, D., Seidenbecher, C.I., Choquet, D. and Gundelfinger, E.D. (2009) 'Brain extracellular matrix affects AMPA receptor lateral mobility and short-term synaptic plasticity.', *Nature neuroscience*, 12(7), pp. 897–904. doi:10.1038/nn.2338.

Frohlich, J. and Van Horn, J.D. (2014) 'Reviewing the ketamine model for schizophrenia', *Journal of psychopharmacology (Oxford, England)*. 2013/11/20, 28(4), pp. 287–302. doi:10.1177/0269881113512909.

Fukata, Y., Adesnik, H., Iwanaga, T., Brecht, D.S., Nicoll, R.A. and Fukata, M. (2006) 'Epilepsy-related ligand/receptor complex LGI1 and ADAM22 regulate synaptic transmission.', *Science (New York, N.Y.)*, 313(5794), pp. 1792–1795. doi:10.1126/science.1129947.

GADDUM, J.H. and HAMEED, K.A. (1954) 'Drugs which antagonize 5-hydroxytryptamine', *British journal of pharmacology and chemotherapy*, 9(2), pp. 240–248. doi:10.1111/j.1476-5381.1954.tb00848.x.

Galtrey, C.M. and Fawcett, J.W. (2007) 'The role of chondroitin sulfate proteoglycans in regeneration and plasticity in the central nervous system.', *Brain research reviews*, 54(1), pp. 1–18. doi:10.1016/j.brainresrev.2006.09.006.

Gao, R. and Penzes, P. (2015) 'Common Mechanisms of Excitatory and Inhibitory Imbalance in Schizophrenia and Autism Spectrum Disorders', *Current molecular medicine*, 15(2), pp. 146–167. Available at: <http://www.ncbi.nlm.nih.gov/pmc/articles/PMC4721588/>.

Glantz, L.A. and Lewis, D.A. (2000) 'Decreased dendritic spine density on prefrontal cortical pyramidal neurons in schizophrenia.', *Archives of general psychiatry*, 57(1), pp. 65–73.

Glynn, M.W., Elmer, B.M., Garay, P.A., Liu, X.-B., Needleman, L.A., El-Sabeawy, F. and McAllister, A.K. (2011) 'MHCI negatively regulates synapse density during the establishment of cortical connections.', *Nature neuroscience*, 14(4), pp. 442–451. doi:10.1038/nn.2764.

Goddard, C.A., Butts, D.A. and Shatz, C.J. (2007) 'Regulation of CNS synapses by neuronal MHC class I.', *Proceedings of the National Academy of Sciences of the United States of America*, 104(16), pp. 6828–6833. doi:10.1073/pnas.0702023104.

Godwin, D., Alpert, K.I., Wang, L. and Mamah, D. (2018) 'Regional cortical thinning in young adults with schizophrenia but not psychotic or non-psychotic bipolar I disorder.', *International journal of bipolar disorders*, 6(1), p. 16. doi:10.1186/s40345-018-0124-x.

Goldman-Rakic, P.S. (1987) 'Development of cortical circuitry and cognitive function.', *Child development*, 58(3), pp. 601–622.

Gopnik, A., Meltzoff, A. and Kuhl, P. (2001) 'The Scientist in the Crib: Minds, Brains and How Children Learn', *Journal of Nervous and Mental Disease - J NERV MENT DIS*, 189. doi:10.1097/00005053-200103000-00011.

Gorkiewicz, T., Szczuraszek, K., Wyrembek, P., Michaluk, P., Kaczmarek, L. and Mozrzymas, J.W. (2010) 'Matrix metalloproteinase-9 reversibly affects the time course of NMDA-induced

- currents in cultured rat hippocampal neurons.’, *Hippocampus*, 20(10), pp. 1105–1108. doi:10.1002/hipo.20736.
- Gottesman, I.I. and Erlenmeyer-Kimling, L. (2001) ‘Family and twin strategies as a head start in defining prodromes and endophenotypes for hypothetical early-interventions in schizophrenia.’, *Schizophrenia research*, 51(1), pp. 93–102.
- Götz, M., Bolz, J., Joester, A. and Faissner, A. (1997) ‘Tenascin-C synthesis and influence on axonal growth during rat cortical development.’, *The European journal of neuroscience*, 9(3), pp. 496–506. doi:10.1111/j.1460-9568.1997.tb01627.x.
- Gu, Z., Kaul, M., Yan, B., Kridel, S.J., Cui, J., Strongin, A., Smith, J.W., Liddington, R.C. and Lipton, S.A. (2002) ‘S-nitrosylation of matrix metalloproteinases: signaling pathway to neuronal cell death.’, *Science (New York, N.Y.)*, 297(5584), pp. 1186–1190. doi:10.1126/science.1073634.
- Guidotti, A., Auta, J., Davis, J.M., Di-Giorgi-Gerevini, V., Dwivedi, Y., Grayson, D.R., Impagnatiello, F., Pandey, G., Pesold, C., Sharma, R., Uzunov, D. and Costa, E. (2000) ‘Decrease in reelin and glutamic acid decarboxylase67 (GAD67) expression in schizophrenia and bipolar disorder: a postmortem brain study’, *Arch Gen Psychiatry*. 2000/11/14, 57(11), pp. 1061–1069.
- Gundelfinger, E.D., Frischknecht, R., Choquet, D. and Heine, M. (2010) ‘Converting juvenile into adult plasticity: a role for the brain’s extracellular matrix.’, *The European journal of neuroscience*, 31(12), pp. 2156–2165. doi:10.1111/j.1460-9568.2010.07253.x.
- Haenschel, C., Bittner, R.A., Waltz, J., Haertling, F., Wibrall, M., Singer, W., Linden, D.E.J. and Rodriguez, E. (2009) ‘Cortical oscillatory activity is critical for working memory as revealed by deficits in early-onset schizophrenia.’, *The Journal of neuroscience : the official journal of the Society for Neuroscience*, 29(30), pp. 9481–9489. doi:10.1523/JNEUROSCI.1428-09.2009.
- Han, H., He, X., Tang, J., Liu, W., Liu, K., Zhang, J., Wang, X., Xu, Y. and Chen, X. (2011) ‘The C(-1562)T polymorphism of matrix metalloproteinase-9 gene is associated with schizophrenia in China.’, *Psychiatry research*. Ireland, pp. 163–164. doi:10.1016/j.psychres.2011.04.026.
- Hashimoto, T., Nishino, N., Nakai, H. and Tanaka, C. (1991) ‘Increase in serotonin 5-HT1A receptors in prefrontal and temporal cortices of brains from patients with chronic schizophrenia.’, *Life sciences*, 48(4), pp. 355–363. doi:10.1016/0024-3205(91)90556-q.
- Hashimoto, T., Volk, D.W., Eggan, S.M., Mirnics, K., Pierri, J.N., Sun, Z., Sampson, A.R. and Lewis, D.A. (2003) ‘Gene expression deficits in a subclass of GABA neurons in the prefrontal cortex of subjects with schizophrenia.’, *The Journal of neuroscience : the official journal of the Society for Neuroscience*, 23(15), pp. 6315–6326. doi:10.1523/JNEUROSCI.23-15-06315.2003.
- Hayani, H., Song, I. and Dityatev, A. (2018) ‘Increased Excitability and Reduced Excitatory Synaptic Input Into Fast-Spiking CA2 Interneurons After Enzymatic Attenuation of Extracellular Matrix.’, *Frontiers in cellular neuroscience*, 12, p. 149. doi:10.3389/fncel.2018.00149.
- Hayashi, N., Tatsumi, K., Okuda, H., Yoshikawa, M., Ishizaka, S., Miyata, S., Manabe, T. and Wanaka, A. (2007) ‘DACS, novel matrix structure composed of chondroitin sulfate proteoglycan in the brain.’, *Biochemical and biophysical research communications*, 364(2), pp. 410–415. doi:10.1016/j.bbrc.2007.10.040.
- Hensch, T.K., Fagiolini, M., Mataga, N., Stryker, M.P., Baekkeskov, S. and Kash, S.F. (1998) ‘Local GABA circuit control of experience-dependent plasticity in developing visual cortex.’, *Science (New York, N.Y.)*, 282(5393), pp. 1504–1508.
- Hippenmeyer, S., Vrieseling, E., Sigrist, M., Portmann, T., Laengle, C., Ladle, D.R. and Arber, S. (2005) ‘A developmental switch in the response of DRG neurons to ETS transcription factor signaling’, *PLoS Biology*, 3(5), pp. 0878–0890. doi:10.1371/journal.pbio.0030159.

- Hong, S.E., Shugart, Y.Y., Huang, D.T., Shahwan, S.A., Grant, P.E., Hourihane, J.O., Martin, N.D. and Walsh, C.A. (2000) 'Autosomal recessive lissencephaly with cerebellar hypoplasia is associated with human RELN mutations.', *Nature genetics*, 26(1), pp. 93–96. doi:10.1038/79246.
- Hor, K. and Taylor, M. (2010) 'Suicide and schizophrenia: a systematic review of rates and risk factors', *Journal of psychopharmacology (Oxford, England)*, 24(4 Suppl), pp. 81–90. doi:10.1177/1359786810385490.
- Horii-Hayashi, N., Sasagawa, T., Matsunaga, W. and Nishi, M. (2015) 'Development and Structural Variety of the Chondroitin Sulfate Proteoglycans-Contained Extracellular Matrix in the Mouse Brain.', *Neural plasticity*, 2015, p. 256389. doi:10.1155/2015/256389.
- Van Hove, I., Lemmens, K., Van de Velde, S., Verslegers, M. and Moons, L. (2012) 'Matrix metalloproteinase-3 in the central nervous system: a look on the bright side.', *Journal of neurochemistry*, 123(2), pp. 203–216. doi:10.1111/j.1471-4159.2012.07900.x.
- Howes, O.D. and Kapur, S. (2009) 'The dopamine hypothesis of schizophrenia: version III--the final common pathway', *Schizophrenia bulletin*. 2009/03/26, 35(3), pp. 549–562. doi:10.1093/schbul/sbp006.
- Hunt, M.J., Kessal, K. and Garcia, R. (2005) 'Ketamine induces dopamine-dependent depression of evoked hippocampal activity in the nucleus accumbens in freely moving rats.', *The Journal of neuroscience: the official journal of the Society for Neuroscience*, 25(2), pp. 524–531. doi:10.1523/JNEUROSCI.3800-04.2005.
- Ierusalimsky, V.N. and Balaban, P.M. (2013) 'Type 1 metalloproteinase is selectively expressed in adult rat brain and can be rapidly up-regulated by kainate.', *Acta histochemica*, 115(8), pp. 816–826. doi:10.1016/j.acthis.2013.04.001.
- Impagnatiello, F., Guidotti, A.R., Pesold, C., Dwivedi, Y., Caruncho, H., Pisu, M.G., Uzunov, D.P., Smalheiser, N.R., Davis, J.M., Pandey, G.N., Pappas, G.D., Tueting, P., Sharma, R.P. and Costa, E. (1998) 'A decrease of reelin expression as a putative vulnerability factor in schizophrenia', *Proc Natl Acad Sci U S A*. 1998/12/23, 95(26), pp. 15718–15723.
- Jones, C.A., Watson, D.J.G. and Fone, K.C.F. (2011) 'Animal models of schizophrenia.', *British journal of pharmacology*, 164(4), pp. 1162–1194. doi:10.1111/j.1476-5381.2011.01386.x.
- Kahler, A.K., Djurovic, S., Rimol, L.M., Brown, A.A., Athanasiu, L., Jonsson, E.G., Hansen, T., Gustafsson, O., Hall, H., Giegling, I., Muglia, P., Cichon, S., Rietschel, M., Pietilainen, O.P., Peltonen, L., Bramon, E., Collier, D., St Clair, D., Sigurdsson, E., *et al.* (2011) 'Candidate gene analysis of the human natural killer-1 carbohydrate pathway and perineuronal nets in schizophrenia: B3GAT2 is associated with disease risk and cortical surface area', *Biol Psychiatry*. 2010/10/19, 69(1), pp. 90–96. doi:10.1016/j.biopsych.2010.07.035.
- Kanda, H., Shimamura, R., Koizumi-Kitajima, M. and Okano, H. (2019) 'Degradation of Extracellular Matrix by Matrix Metalloproteinase 2 Is Essential for the Establishment of the Blood-Brain Barrier in Drosophila', *iScience*. 2019/05/27, 16, pp. 218–229. doi:10.1016/j.isci.2019.05.027.
- Kapur, S. and Seeman, P. (2002) 'NMDA receptor antagonists ketamine and PCP have direct effects on the dopamine D(2) and serotonin 5-HT(2) receptors-implications for models of schizophrenia.', *Molecular psychiatry*, 7(8), pp. 837–844. doi:10.1038/sj.mp.4001093.
- Katsel, P., Byne, W., Roussos, P., Tan, W., Siever, L. and Haroutunian, V. (2011) 'Astrocyte and glutamate markers in the superficial, deep, and white matter layers of the anterior cingulate gyrus in schizophrenia.', *Neuropsychopharmacology: official publication of the American College of Neuropsychopharmacology*, 36(6), pp. 1171–1177. doi:10.1038/npp.2010.252.

- Keilhoff, G., Becker, A., Grecksch, G., Wolf, G. and Bernstein, H.G. (2004) 'Repeated application of ketamine to rats induces changes in the hippocampal expression of parvalbumin, neuronal nitric oxide synthase and cFOS similar to those found in human schizophrenia', *Neuroscience* [Preprint]. doi:10.1016/j.neuroscience.2004.03.039.
- Knapp, M., Mangalore, R. and Simon, J. (2004) 'The global costs of schizophrenia.', *Schizophrenia bulletin*, 30(2), pp. 279–293. doi:10.1093/oxfordjournals.schbul.a007078.
- Krystal, J.H., Karper, L.P., Seibyl, J.P., Freeman, G.K., Delaney, R., Bremner, J.D., Heninger, G.R., Bowers, M.B.J. and Charney, D.S. (1994) 'Subanesthetic effects of the noncompetitive NMDA antagonist, ketamine, in humans. Psychotomimetic, perceptual, cognitive, and neuroendocrine responses.', *Archives of general psychiatry*, 51(3), pp. 199–214.
- Kucukali, C.I., Aydin, M., Ozkok, E., Bilge, E., Orhan, N., Zengin, A. and Kara, I. (2009) 'Do schizophrenia and bipolar disorders share a common disease susceptibility variant at the MMP3 gene?', *Progress in neuro-psychopharmacology & biological psychiatry*, 33(3), pp. 557–561. doi:10.1016/j.pnpbp.2009.02.012.
- Lachman, H.M., Papolos, D.F., Saito, T., Yu, Y.M., Szumlanski, C.L. and Weinshilboum, R.M. (1996) 'Human catechol-O-methyltransferase pharmacogenetics: description of a functional polymorphism and its potential application to neuropsychiatric disorders.', *Pharmacogenetics*, 6(3), pp. 243–250.
- Lambert de Rouvroit, C. and Goffinet, A.M. (1998) 'The reeler mouse as a model of brain development.', *Advances in anatomy, embryology, and cell biology*, 150, pp. 1–106.
- Laruelle, M., Abi-Dargham, A., Casanova, M.F., Toti, R., Weinberger, D.R. and Kleinman, J.E. (1993) 'Selective abnormalities of prefrontal serotonergic receptors in schizophrenia. A postmortem study.', *Archives of general psychiatry*, 50(10), pp. 810–818. doi:10.1001/archpsyc.1993.01820220066007.
- Lee, H.-K., Takamiya, K., Han, J.-S., Man, H., Kim, C.-H., Rumbaugh, G., Yu, S., Ding, L., He, C., Petralia, R.S., Wenthold, R.J., Gallagher, M. and Huganir, R.L. (2003) 'Phosphorylation of the AMPA receptor GluR1 subunit is required for synaptic plasticity and retention of spatial memory.', *Cell*, 112(5), pp. 631–643. doi:10.1016/s0092-8674(03)00122-3.
- Lensjø, K.K., Lepperød, M.E., Dick, G., Hafting, T. and Fyhn, M. (2017) 'Removal of Perineuronal Nets Unlocks Juvenile Plasticity Through Network Mechanisms of Decreased Inhibition and Increased Gamma Activity.', *The Journal of neuroscience : the official journal of the Society for Neuroscience*, 37(5), pp. 1269–1283. doi:10.1523/JNEUROSCI.2504-16.2016.
- Lepeta, K., Purzycka, K.J., Pachulska-Wieczorek, K., Mitjans, M., Begemann, M., Vafadari, B., Bijata, K., Adamiak, R.W., Ehrenreich, H., Dziembowska, M. and Kaczmarek, L. (2017) 'A normal genetic variation modulates synaptic MMP-9 protein levels and the severity of schizophrenia symptoms.', *EMBO molecular medicine*, 9(8), pp. 1100–1116. doi:10.15252/emmm.201707723.
- Li, H., Leung, T.C., Hoffman, S., Balsamo, J. and Lilien, J. (2000) 'Coordinate regulation of cadherin and integrin function by the chondroitin sulfate proteoglycan neurocan', *The Journal of cell biology*, 149(6), pp. 1275–1288. doi:10.1083/jcb.149.6.1275.
- Lodge, D.J., Behrens, M.M. and Grace, A.A. (2009) 'A loss of parvalbumin-containing interneurons is associated with diminished oscillatory activity in an animal model of schizophrenia', *The Journal of neuroscience : the official journal of the Society for Neuroscience*, 29(8), pp. 2344–2354. doi:10.1523/JNEUROSCI.5419-08.2009.
- Lonskaya, I., Partridge, J., Lalchandani, R.R., Chung, A., Lee, T., Vicini, S., Hoe, H.-S., Lim, S.T. and Conant, K. (2013) 'Soluble ICAM-5, a product of activity dependent proteolysis, increases

- mEPSC frequency and dendritic expression of GluA1.', *PloS one*, 8(7), p. e69136. doi:10.1371/journal.pone.0069136.
- Lu, Y.M., Jia, Z., Janus, C., Henderson, J.T., Gerlai, R., Wojtowicz, J.M. and Roder, J.C. (1997) 'Mice lacking metabotropic glutamate receptor 5 show impaired learning and reduced CA1 long-term potentiation (LTP) but normal CA3 LTP.', *The Journal of neuroscience : the official journal of the Society for Neuroscience*, 17(13), pp. 5196–5205. doi:10.1523/JNEUROSCI.17-13-05196.1997.
- Lubow, R.E., Kaplan, O., Abramovich, P., Rudnick, A. and Laor, N. (2000) 'Visual search in schizophrenia: latent inhibition and novel pop-out effects.', *Schizophrenia research*, 45(1–2), pp. 145–156. doi:10.1016/s0920-9964(99)00188-7.
- Magri, C., Gardella, R., Barlati, S.D., Podavini, D., Iatropoulos, P., Bonomi, S., Valsecchi, P., Sacchetti, E. and Barlati, S. (2006) 'Glutamate AMPA receptor subunit 1 gene (GRIA1) and DSM-IV-TR schizophrenia: a pilot case-control association study in an Italian sample.', *American journal of medical genetics. Part B, Neuropsychiatric genetics : the official publication of the International Society of Psychiatric Genetics*, 141B(3), pp. 287–293. doi:10.1002/ajmg.b.30294.
- Manchia, M., Piras, I.S., Huentelman, M.J., Pinna, F., Zai, C.C., Kennedy, J.L. and Carpiniello, B. (2017) 'Pattern of gene expression in different stages of schizophrenia: Down-regulation of NPTX2 gene revealed by a meta-analysis of microarray datasets.', *European neuropsychopharmacology : the journal of the European College of Neuropsychopharmacology*, 27(10), pp. 1054–1063. doi:10.1016/j.euroneuro.2017.07.002.
- Mateos-Aparicio, P. and Rodríguez-Moreno, A. (2019) 'The Impact of Studying Brain Plasticity', *Frontiers in Cellular Neuroscience*, p. 66. Available at: <https://www.frontiersin.org/article/10.3389/fncel.2019.00066>.
- Matuszko, G., Curreli, S., Kaushik, R., Becker, A. and Dityatev, A. (2017) 'Extracellular matrix alterations in the ketamine model of schizophrenia', *Neuroscience* [Preprint]. doi:10.1016/j.neuroscience.2017.03.010.
- Mauney, S.A., Athanas, K.M., Pantazopoulos, H., Shaskan, N., Passeri, E., Berretta, S. and Woo, T.U.W. (2013) 'Developmental pattern of perineuronal nets in the human prefrontal cortex and their deficit in schizophrenia', *Biol Psychiatry*. 2013/06/25, 74(6), pp. 427–435. doi:10.1016/j.biopsych.2013.05.007.
- McGregor, N., Thompson, N., O'Connell, K.S., Emsley, R., van der Merwe, L. and Warnich, L. (2018) 'Modification of the association between antipsychotic treatment response and childhood adversity by MMP9 gene variants in a first-episode schizophrenia cohort.', *Psychiatry research*, 262, pp. 141–148. doi:10.1016/j.psychres.2018.01.044.
- McRae, P.A., Rocco, M.M., Kelly, G., Brumberg, J.C. and Matthews, R.T. (2007) 'Sensory deprivation alters aggrecan and perineuronal net expression in the mouse barrel cortex.', *The Journal of neuroscience : the official journal of the Society for Neuroscience*, 27(20), pp. 5405–5413. doi:10.1523/JNEUROSCI.5425-06.2007.
- Meiners, S., Mercado, M.L., Nur-e-Kamal, M.S. and Geller, H.M. (1999) 'Tenascin-C contains domains that independently regulate neurite outgrowth and neurite guidance.', *The Journal of neuroscience : the official journal of the Society for Neuroscience*, 19(19), pp. 8443–8453. doi:10.1523/JNEUROSCI.19-19-08443.1999.
- Meiners, S. and Geller, H.M. (1997) 'Long and short splice variants of human tenascin differentially regulate neurite outgrowth.', *Molecular and cellular neurosciences*, 10(1–2), pp. 100–116. doi:10.1006/mcne.1997.0643.
- Meyer-Puttlitz, B., Junker, E., Margolis, R.U. and Margolis, R.K. (1996) 'Chondroitin sulfate

- proteoglycans in the developing central nervous system. II. Immunocytochemical localization of neurocan and phosphacan.’, *The Journal of comparative neurology*, 366(1), pp. 44–54. doi:10.1002/(SICI)1096-9861(19960226)366:1<44::AID-CNE4>3.0.CO;2-K.
- Michaluk, P., Mikasova, L., Groc, L., Frischknecht, R., Choquet, D. and Kaczmarek, L. (2009) ‘Matrix metalloproteinase-9 controls NMDA receptor surface diffusion through integrin beta1 signaling’, *The Journal of neuroscience: the official journal of the Society for Neuroscience*, 29(18), pp. 6007–6012. doi:10.1523/JNEUROSCI.5346-08.2009.
- Morawski, M., Brückner, M.K., Riederer, P., Brückner, G. and Arendt, T. (2004) ‘Perineuronal nets potentially protect against oxidative stress.’, *Experimental neurology*, 188(2), pp. 309–315. doi:10.1016/j.expneurol.2004.04.017.
- Morgan, C.J.A., Muetzelfeldt, L. and Curran, H.V. (2009) ‘Ketamine use, cognition and psychological wellbeing: a comparison of frequent, infrequent and ex-users with polydrug and non-using controls.’, *Addiction (Abingdon, England)*, 104(1), pp. 77–87. doi:10.1111/j.1360-0443.2008.02394.x.
- Morita, I., Kakuda, S., Takeuchi, Y., Itoh, S., Kawasaki, N., Kizuka, Y., Kawasaki, T. and Oka, S. (2009) ‘HNK-1 glyco-epitope regulates the stability of the glutamate receptor subunit GluR2 on the neuronal cell surface.’, *The Journal of biological chemistry*, 284(44), pp. 30209–30217. doi:10.1074/jbc.M109.024208.
- Morita, Y., Ujike, H., Tanaka, Y., Otani, K., Kishimoto, M., Morio, A., Kotaka, T., Okahisa, Y., Matsushita, M., Morikawa, A., Hamase, K., Zaitu, K. and Kuroda, S. (2007) ‘A genetic variant of the serine racemase gene is associated with schizophrenia.’, *Biological psychiatry*, 61(10), pp. 1200–1203. doi:10.1016/j.biopsych.2006.07.025.
- Mueser, K.T. and McGurk, S.R. (2004) ‘Schizophrenia.’, *Lancet (London, England)*, 363(9426), pp. 2063–2072. doi:10.1016/S0140-6736(04)16458-1.
- Mühleisen, T.W., Mattheisen, M., Strohmaier, J., Degenhardt, F., Priebe, L., Schultz, C.C., Breuer, R., Meier, S., Hoffmann, P., Rivandeneira, F., Hofman, A., Uitterlinden, A.G., Moebus, S., Gieger, C., Emeny, R., Ladwig, K.H., Wichmann, H.E., Schwarz, M., Kammerer-Ciernioch, J., *et al.* (2012) ‘Association between schizophrenia and common variation in neurocan (NCAN), a genetic risk factor for bipolar disorder’, *Schizophrenia Research*, 138(1), pp. 69–73. doi:10.1016/j.schres.2012.03.007.
- Muir, E.M., Adcock, K.H., Morgenstern, D.A., Clayton, R., von Stillfried, N., Rhodes, K., Ellis, C., Fawcett, J.W. and Rogers, J.H. (2002) ‘Matrix metalloproteases and their inhibitors are produced by overlapping populations of activated astrocytes’, *Molecular Brain Research*, 100(1), pp. 103–117. doi:https://doi.org/10.1016/S0169-328X(02)00132-8.
- Murase, S., Lantz, C.L. and Quinlan, E.M. (2017) ‘Light reintroduction after dark exposure reactivates plasticity in adults via perisynaptic activation of MMP-9.’, *eLife*, 6. doi:10.7554/eLife.27345.
- Nacher, J., Guirado, R. and Castillo-Gómez, E. (2013) ‘Structural Plasticity of Interneurons in the Adult Brain: Role of PSA-NCAM and Implications for Psychiatric Disorders’, *Neurochemical Research*, 38, pp. 1122–1133.
- Nakic, M., Manahan-Vaughan, D., Reymann, K.G. and Schachner, M. (1998) ‘Long-term potentiation in vivo increases rat hippocampal tenascin-C expression.’, *Journal of neurobiology*, 37(3), pp. 393–404.
- Newcomer, J.W., Farber, N.B. and Olney, J.W. (2000) ‘NMDA receptor function, memory, and brain aging’, *Dialogues in clinical neuroscience*, 2(3), pp. 219–232. Available at: <https://pubmed.ncbi.nlm.nih.gov/22034391>.

- Niedringhaus, M., Chen, X., Conant, K. and Dzakpasu, R. (2013) ‘Synaptic potentiation facilitates memory-like attractor dynamics in cultured in vitro hippocampal networks.’, *PloS one*, 8(3), p. e57144. doi:10.1371/journal.pone.0057144.
- Nikonenko, A., Schmidt, S., Skibo, G., Brückner, G. and Schachner, M. (2003) ‘Tenascin-R-deficient mice show structural alterations of symmetric perisomatic synapses in the CA1 region of the hippocampus’, *Journal of Comparative Neurology* [Preprint]. doi:10.1002/cne.10537.
- Ogier, C., Bernard, A., Chollet, A.-M., LE Diguardher, T., Hanessian, S., Charton, G., Khrestchatsky, M. and Rivera, S. (2006) ‘Matrix metalloproteinase-2 (MMP-2) regulates astrocyte motility in connection with the actin cytoskeleton and integrins.’, *Glia*, 54(4), pp. 272–284. doi:10.1002/glia.20349.
- Omori, W., Hattori, K., Kajitani, N., Tsuchioka, M.O.-, Boku, S., Kunugi, H., Okamoto, Y. and Takebayashi, M. (2020) ‘Increased matrix metalloproteinases in cerebrospinal fluids of patients with major depressive disorder and schizophrenia.’, *The international journal of neuropsychopharmacology* [Preprint]. doi:10.1093/ijnp/pyaa049.
- Oohashi, T., Hirakawa, S., Bekku, Y., Rauch, U., Zimmermann, D.R., Su, W.-D., Ohtsuka, A., Murakami, T. and Ninomiya, Y. (2002) ‘Brall, a brain-specific link protein, colocalizing with the versican V2 isoform at the nodes of Ranvier in developing and adult mouse central nervous systems.’, *Molecular and cellular neurosciences*, 19(1), pp. 43–57. doi:10.1006/mcne.2001.1061.
- Ouagazzal, A.M., Reiss, D. and Romand, R. (2006) ‘Effects of age-related hearing loss on startle reflex and prepulse inhibition in mice on pure and mixed C57BL and 129 genetic background’, *Behavioural Brain Research*, 172(2), pp. 307–315. doi:10.1016/j.bbr.2006.05.018.
- Palmer, B.A., Pankratz, V.S. and Bostwick, J.M. (2005) ‘The Lifetime Risk of Suicide in Schizophrenia: A Reexamination’, *Archives of General Psychiatry*, 62(3), pp. 247–253. doi:10.1001/archpsyc.62.3.247.
- Pantazopoulos, H., Woo, T.-U.U.W., Lim, M.P., Lange, N. and Berretta, S. (2010) ‘Extracellular matrix-glial abnormalities in the amygdala and entorhinal cortex of subjects diagnosed with schizophrenia’, *Archives of general psychiatry*, 67(2), pp. 155–166. doi:10.1001/archgenpsychiatry.2009.196.
- Pantazopoulos, H., Boyer-Boiteau, A., Holbrook, E.H., Jang, W., Hahn, C.-G., Arnold, S.E. and Berretta, S. (2013) ‘Proteoglycan abnormalities in olfactory epithelium tissue from subjects diagnosed with schizophrenia.’, *Schizophrenia research*, 150(2–3), pp. 366–372. doi:10.1016/j.schres.2013.08.013.
- Pantazopoulos, H., Markota, M., Jaquet, F., Ghosh, D., Wallin, A., Santos, A., Caterson, B. and Berretta, S. (2015) ‘Aggrecan and chondroitin-6-sulfate abnormalities in schizophrenia and bipolar disorder: a postmortem study on the amygdala’, *Transl Psychiatry*. 2015/01/21, 5, p. e496. doi:10.1038/tp.2014.128.
- Pantazopoulos, H., Katsel, P., Haroutunian, V., Chelini, G., Klengel, T. and Berretta, S. (2021) ‘Molecular signature of extracellular matrix pathology in schizophrenia’, *European Journal of Neuroscience*, 53(12), pp. 3960–3987. doi:10.1111/ejn.15009.
- Park, H.J., Kim, S.K., Kim, J.W., Kang, W.S. and Chung, J.-H. (2012) ‘Association of thrombospondin 1 gene with schizophrenia in Korean population.’, *Molecular biology reports*, 39(6), pp. 6875–6880. doi:10.1007/s11033-012-1513-3.
- Pauly, T., Ratliff, M., Pietrowski, E., Neugebauer, R., Schlicksupp, A., Kirsch, J. and Kuhse, J. (2008) ‘Activity-dependent shedding of the NMDA receptor glycine binding site by matrix metalloproteinase 3: a PUTATIVE mechanism of postsynaptic plasticity.’, *PloS one*, 3(7), p. e2681. doi:10.1371/journal.pone.0002681.

- Perea, G., Navarrete, M. and Araque, A. (2009) 'Tripartite synapses: astrocytes process and control synaptic information.', *Trends in neurosciences*, 32(8), pp. 421–431. doi:10.1016/j.tins.2009.05.001.
- Petit-Pedrol, M., Sell, J., Planagumà, J., Mannara, F., Radosevic, M., Haselmann, H., Ceanga, M., Sabater, L., Spatola, M., Soto, D., Gasull, X., Dalmau, J. and Geis, C. (2018) 'LGI1 antibodies alter Kv1.1 and AMPA receptors changing synaptic excitability, plasticity and memory', *Brain : a journal of neurology*, 141(11), pp. 3144–3159. doi:10.1093/brain/awy253.
- Pietersen, C.Y., Mauney, S.A., Kim, S.S., Lim, M.P., Rooney, R.J., Goldstein, J.M., Petryshen, T.L., Seidman, L.J., Shenton, M.E., McCarley, R.W., Sonntag, K.C. and Woo, T.U. (2014) 'Molecular profiles of pyramidal neurons in the superior temporal cortex in schizophrenia', *J Neurogenet.* 2014/04/08, 28(1–2), pp. 53–69. doi:10.3109/01677063.2014.882918.
- Pizzorusso, T., Medini, P., Berardi, N., Chierzi, S., Fawcett, J.W. and Maffei, L. (2002) 'Reactivation of ocular dominance plasticity in the adult visual cortex.', *Science (New York, N.Y.)*, 298(5596), pp. 1248–1251. doi:10.1126/science.1072699.
- Powell, S.B., Zhou, X. and Geyer, M.A. (2009) 'Prepulse inhibition and genetic mouse models of schizophrenia', *Behavioural brain research.* 2009/05/04, 204(2), pp. 282–294. doi:10.1016/j.bbr.2009.04.021.
- Qin, S., Zhao, X., Pan, Y., Liu, J., Feng, G., Fu, J., Bao, J., Zhang, Z. and He, L. (2005) 'An association study of the N-methyl-D-aspartate receptor NR1 subunit gene (GRIN1) and NR2B subunit gene (GRIN2B) in schizophrenia with universal DNA microarray.', *European journal of human genetics : EJHG*, 13(7), pp. 807–814. doi:10.1038/sj.ejhg.5201418.
- Reif, A., Herterich, S., Strobel, A., Ehrlis, A.-C., Saur, D., Jacob, C.P., Wienker, T., Töpner, T., Fritzen, S., Walter, U., Schmitt, A., Fallgatter, A.J. and Lesch, K.-P. (2006) 'A neuronal nitric oxide synthase (NOS-I) haplotype associated with schizophrenia modifies prefrontal cortex function.', *Molecular psychiatry*, 11(3), pp. 286–300. doi:10.1038/sj.mp.4001779.
- Reif, A., Schecklmann, M., Eirich, E., Jacob, C.P., Jarczok, T.A., Kittel-Schneider, S., Lesch, K.-P., Fallgatter, A.J. and Ehrlis, A.-C. (2011) 'A functional promoter polymorphism of neuronal nitric oxide synthase moderates prefrontal functioning in schizophrenia.', *The international journal of neuropsychopharmacology*, 14(7), pp. 887–897. doi:10.1017/S1461145710001677.
- Reynolds, G.P., Beasley, C.L. and Zhang, Z.J. (2002) 'Understanding the neurotransmitter pathology of schizophrenia: selective deficits of subtypes of cortical GABAergic neurons.', *Journal of neural transmission (Vienna, Austria: 1996)*, 109(5–6), pp. 881–889. doi:10.1007/s007020200072.
- Ripke, S., O'Dushlaine, C., Chambert, K., Moran, J.L., Kahler, A.K., Akterin, S., Bergen, S.E., Collins, A.L., Crowley, J.J., Fromer, M., Kim, Y., Lee, S.H., Magnusson, P.K., Sanchez, N., Stahl, E.A., Williams, S., Wray, N.R., Xia, K., Bettella, F., *et al.* (2013) 'Genome-wide association analysis identifies 13 new risk loci for schizophrenia', *Nat Genet.* 2013/08/27, 45(10), pp. 1150–1159. doi:10.1038/ng.2742.
- Roberts, D.J., Jenne, C.N., Léger, C., Kramer, A.H., Gallagher, C.N., Todd, S., Parney, I.F., Doig, C.J., Yong, V.W., Kubes, P. and Zygun, D.A. (2013) 'A prospective evaluation of the temporal matrix metalloproteinase response after severe traumatic brain injury in humans.', *Journal of neurotrauma*, 30(20), pp. 1717–1726. doi:10.1089/neu.2012.2841.
- Rogers, S.L., Rankin-Gee, E., Risbud, R.M., Porter, B.E. and Marsh, E.D. (2018) 'Normal Development of the Perineuronal Net in Humans; In Patients with and without Epilepsy.', *Neuroscience*, 384, pp. 350–360. doi:10.1016/j.neuroscience.2018.05.039.
- Rosso, I.M., Cannon, T.D., Huttunen, T., Huttunen, M.O., Lonnqvist, J. and Gasperoni, T.L.

- (2000) 'Obstetric risk factors for early-onset schizophrenia in a Finnish birth cohort.', *The American journal of psychiatry*, 157(5), pp. 801–807. doi:10.1176/appi.ajp.157.5.801.
- Rybakowski, J.K., Skibinska, M., Kapelski, P., Kaczmarek, L. and Hauser, J. (2009) 'Functional polymorphism of the matrix metalloproteinase-9 (MMP-9) gene in schizophrenia.', *Schizophrenia research*, 109(1–3), pp. 90–93. doi:10.1016/j.schres.2009.02.005.
- Saghatelyan, A.K., Gorissen, S., Albert, M., Hertlein, B., Schachner, M. and Dityatev, A. (2000) 'The extracellular matrix molecule tenascin-R and its HNK-1 carbohydrate modulate perisomatic inhibition and long-term potentiation in the CA1 region of the hippocampus', *European Journal of Neuroscience*, 12(9), pp. 3331–3342. doi:10.1046/j.1460-9568.2000.00216.x.
- Saghatelyan, A.K., Dityatev, A., Schmidt, S., Schuster, T., Bartsch, U. and Schachner, M. (2001) 'Reduced Perisomatic Inhibition, Increased Excitatory Transmission, and Impaired Long-Term Potentiation in Mice Deficient for the Extracellular Matrix Glycoprotein Tenascin-R', *Molecular and Cellular Neuroscience*, 17(1), pp. 226–240. doi:http://dx.doi.org/10.1006/mcne.2000.0922.
- Saghatelyan, A.K., Snapyan, M., Gorissen, S., Meigel, I., Mosbacher, J., Kaupmann, K., Bettler, B., Kornilov, A. V., Nifantiev, N.E., Sakanyan, V., Schachner, M. and Dityatev, A. (2003) 'Recognition molecule associated carbohydrate inhibits postsynaptic GABA_B receptors: a mechanism for homeostatic regulation of GABA release in perisomatic synapses', *Molecular and Cellular Neuroscience*, 24(2), pp. 271–282. doi:http://dx.doi.org/10.1016/S1044-7431(03)00163-5.
- Sakai, T., Oshima, A., Nozaki, Y., Ida, I., Haga, C., Akiyama, H., Nakazato, Y. and Mikuni, M. (2008) 'Changes in density of calcium-binding-protein-immunoreactive GABAergic neurons in prefrontal cortex in schizophrenia and bipolar disorder.', *Neuropathology : official journal of the Japanese Society of Neuropathology*, 28(2), pp. 143–150. doi:10.1111/j.1440-1789.2007.00867.x.
- Sbardella, D., Fasciglione, G.F., Gioia, M., Ciaccio, C., Tundo, G.R., Marini, S. and Coletta, M. (2012) 'Human matrix metalloproteinases: an ubiquitous class of enzymes involved in several pathological processes.', *Molecular aspects of medicine*, 33(2), pp. 119–208. doi:10.1016/j.mam.2011.10.015.
- Schindelin, J., Arganda-Carreras, I., Frise, E., Kaynig, V., Longair, M., Pietzsch, T., Preibisch, S., Rueden, C., Saalfeld, S., Schmid, B., Tinevez, J.-Y., White, D.J., Hartenstein, V., Eliceiri, K., Tomancak, P. and Cardona, A. (2012) 'Fiji: an open-source platform for biological-image analysis.', *Nature methods*, 9(7), pp. 676–682. doi:10.1038/nmeth.2019.
- Schmidt-Hansen, M., Killcross, A.S. and Honey, R.C. (2009) 'Latent inhibition, learned irrelevance, and schizotypy: assessing their relationship.', *Cognitive neuropsychiatry*, 14(1), pp. 11–29. doi:10.1080/13546800802664539.
- Schmitt, A., Steyskal, C., Bernstein, H.-G., Schneider-Axmann, T., Parlapani, E., Schaeffer, E.L., Gattaz, W.F., Bogerts, B., Schmitz, C. and Falkai, P. (2009) 'Stereologic investigation of the posterior part of the hippocampus in schizophrenia.', *Acta neuropathologica*, 117(4), pp. 395–407. doi:10.1007/s00401-008-0430-y.
- Schmitt, A., Leonardi-Essmann, F., Durrenberger, P.F., Wichert, S.P., Spanagel, R., Arzberger, T., Kretschmar, H., Zink, M., Herrera-Marschitz, M., Reynolds, R., Rossner, M.J., Falkai, P. and Gebicke-Haerter, P.J. (2012) 'Structural synaptic elements are differentially regulated in superior temporal cortex of schizophrenia patients.', *European archives of psychiatry and clinical neuroscience*, 262(7), pp. 565–577. doi:10.1007/s00406-012-0306-y.
- Schousboe, A., Scafidi, S., Bak, L.K., Waagepetersen, H.S. and McKenna, M.C. (2014) 'Glutamate metabolism in the brain focusing on astrocytes', *Advances in neurobiology*, 11, pp. 13–30. doi:10.1007/978-3-319-08894-5_2.

- Schulte, U., Thumfart, J.-O., Klöcker, N., Sailer, C.A., Bildl, W., Biniossek, M., Dehn, D., Deller, T., Eble, S., Abbass, K., Wangler, T., Knaus, H.-G. and Fakler, B. (2006) 'The epilepsy-linked Lgi1 protein assembles into presynaptic Kv1 channels and inhibits inactivation by Kvbeta1.', *Neuron*, 49(5), pp. 697–706. doi:10.1016/j.neuron.2006.01.033.
- Schwartz, T.L., Sachdeva, S. and Stahl, S.M. (2012) 'Glutamate neurocircuitry: theoretical underpinnings in schizophrenia', *Frontiers in pharmacology*, 3, p. 195. doi:10.3389/fphar.2012.00195.
- Scremin, O.U. and Holschneider, D.P. (2012) *Vascular Supply, The Mouse Nervous System*. Elsevier Inc. doi:10.1016/B978-0-12-369497-3.10014-7.
- Seigneur, E. and Südhof, T.C. (2018) 'Genetic Ablation of All Cerebellins Reveals Synapse Organizer Functions in Multiple Regions Throughout the Brain.', *The Journal of neuroscience: the official journal of the Society for Neuroscience*, 38(20), pp. 4774–4790. doi:10.1523/JNEUROSCI.0360-18.2018.
- Selemon, L.D. and Goldman-Rakic, P.S. (1999) 'The reduced neuropil hypothesis: a circuit based model of schizophrenia.', *Biological psychiatry*, 45(1), pp. 17–25.
- Senkov, O., Andjus, P., Radenovic, L., Soriano, E. and Dityatev, A. (2014) 'Neural ECM molecules in synaptic plasticity, learning, and memory.', *Progress in brain research*, 214, pp. 53–80. doi:10.1016/B978-0-444-63486-3.00003-7.
- Shah, A. and Lodge, D.J. (2013) 'A loss of hippocampal perineuronal nets produces deficits in dopamine system function: relevance to the positive symptoms of schizophrenia', *Translational psychiatry*, 3(1), pp. e215–e215. doi:10.1038/tp.2012.145.
- Sharpley, M., Hutchinson, G., McKenzie, K. and Murray, R.M. (2001) 'Understanding the excess of psychosis among the African-Caribbean population in England. Review of current hypotheses.', *The British journal of psychiatry. Supplement*, 40, pp. s60-8.
- Shatz, C.J. (2009) 'MHC Class I: an unexpected role in neuronal plasticity', *Neuron*, 64(1), pp. 40–45. doi:10.1016/j.neuron.2009.09.044.
- Sia, G.-M., Béïque, J.-C., Rumbaugh, G., Cho, R., Worley, P.F. and Huganir, R.L. (2007) 'Interaction of the N-terminal domain of the AMPA receptor GluR4 subunit with the neuronal pentraxin NP1 mediates GluR4 synaptic recruitment.', *Neuron*, 55(1), pp. 87–102. doi:10.1016/j.neuron.2007.06.020.
- Soleman, S., Filippov, M.A., Dityatev, A. and Fawcett, J.W. (2013) 'Targeting the neural extracellular matrix in neurological disorders.', *Neuroscience*, 253, pp. 194–213. doi:10.1016/j.neuroscience.2013.08.050.
- Spencer, K.M., Salisbury, D.F., Shenton, M.E. and McCarley, R.W. (2008) 'Gamma-band auditory steady-state responses are impaired in first episode psychosis.', *Biological psychiatry*, 64(5), pp. 369–375. doi:10.1016/j.biopsych.2008.02.021.
- Spencer, K.M., Niznikiewicz, M.A., Shenton, M.E. and McCarley, R.W. (2008) 'Sensory-evoked gamma oscillations in chronic schizophrenia.', *Biological psychiatry*, 63(8), pp. 744–747. doi:10.1016/j.biopsych.2007.10.017.
- Sternlicht, M.D. and Werb, Z. (2001) 'How matrix metalloproteinases regulate cell behavior.', *Annual review of cell and developmental biology*, 17, pp. 463–516. doi:10.1146/annurev.cellbio.17.1.463.
- Steullet, P., Cabungcal, J.-H., Coyle, J., Didriksen, M., Gill, K., Grace, A.A., Hensch, T.K., LaMantia, A.-S., Lindemann, L., Maynard, T.M., Meyer, U., Morishita, H., O'Donnell, P., Puhl, M., Cuenod, M. and Do, K.Q. (2017) 'Oxidative stress-driven parvalbumin interneuron

- impairment as a common mechanism in models of schizophrenia.’, *Molecular psychiatry*, 22(7), pp. 936–943. doi:10.1038/mp.2017.47.
- Strekalova, T., Sun, M., Sibbe, M., Evers, M., Dityatev, A., Gass, P. and Schachner, M. (2002) ‘Fibronectin domains of extracellular matrix molecule tenascin-C modulate hippocampal learning and synaptic plasticity.’, *Molecular and cellular neurosciences*, 21(1), pp. 173–187. doi:10.1006/mcne.2002.1172.
- Suttkus, A., Rohn, S., Weigel, S., Glöckner, P., Arendt, T. and Morawski, M. (2014) ‘Aggrecan, link protein and tenascin-R are essential components of the perineuronal net to protect neurons against iron-induced oxidative stress’, *Cell Death & Disease*, 5(3), p. e1119. doi:10.1038/cddis.2014.25.
- Suvisaari, J., Haukka, J., Tanskanen, A., Hovi, T. and Lonnqvist, J. (1999) ‘Association between prenatal exposure to poliovirus infection and adult schizophrenia.’, *The American journal of psychiatry*, 156(7), pp. 1100–1102. doi:10.1176/ajp.156.7.1100.
- Szepesi, Z., Hosy, E., Ruszczycki, B., Bijata, M., Pyskaty, M., Bikbaev, A., Heine, M., Choquet, D., Kaczmarek, L. and Wlodarczyk, J. (2014) ‘Synaptically released matrix metalloproteinase activity in control of structural plasticity and the cell surface distribution of GluA1-AMPA receptors’, *PLoS one*, 9(5), pp. e98274–e98274. doi:10.1371/journal.pone.0098274.
- Szklarczyk, A., Ewaleifoh, O., Beique, J.-C., Wang, Y., Knorr, D., Haughey, N., Malpica, T., Mattson, M.P., Haganir, R. and Conant, K. (2008) ‘MMP-7 cleaves the NR1 NMDA receptor subunit and modifies NMDA receptor function’, *FASEB journal : official publication of the Federation of American Societies for Experimental Biology*. 2008/07/21, 22(11), pp. 3757–3767. doi:10.1096/fj.07-101402.
- Titeler, M., Lyon, R.A. and Glennon, R.A. (1988) ‘Radioligand binding evidence implicates the brain 5-HT₂ receptor as a site of action for LSD and phenylisopropylamine hallucinogens.’, *Psychopharmacology*, 94(2), pp. 213–216. doi:10.1007/BF00176847.
- Tooney, P.A. and Chahl, L.A. (2004) ‘Neurons expressing calcium-binding proteins in the prefrontal cortex in schizophrenia.’, *Progress in neuro-psychopharmacology & biological psychiatry*, 28(2), pp. 273–278. doi:10.1016/j.pnpbp.2003.10.004.
- Torrey, E.F., Rawlings, R. and Waldman, I.N. (1988) ‘Schizophrenic births and viral diseases in two states.’, *Schizophrenia research*, 1(1), pp. 73–77.
- Trommsdorff, M., Gotthardt, M., Hiesberger, T., Shelton, J., Stockinger, W., Nimpf, J., Hammer, R.E., Richardson, J.A. and Herz, J. (1999) ‘Reeler/Disabled-like disruption of neuronal migration in knockout mice lacking the VLDL receptor and ApoE receptor 2.’, *Cell*, 97(6), pp. 689–701. doi:10.1016/s0092-8674(00)80782-5.
- Tronche, F., Kellendonk, C., Kretz, O., Gass, P., Anlag, K., Orban, P.C., Bock, R., Klein, R. and Schütz, G. (1999) ‘Disruption of the glucocorticoid receptor gene in the nervous system results in reduced anxiety.’, *Nature genetics*, 23(1), pp. 99–103. doi:10.1038/12703.
- Uhlhaas, P.J., Roux, F., Rodriguez, E., Rotarska-Jagiela, A. and Singer, W. (2010) ‘Neural synchrony and the development of cortical networks.’, *Trends in cognitive sciences*, 14(2), pp. 72–80. doi:10.1016/j.tics.2009.12.002.
- Ulrich, R., Gerhauser, I., Seeliger, F., Baumgärtner, W. and Alldinger, S. (2005) ‘Matrix metalloproteinases and their inhibitors in the developing mouse brain and spinal cord: a reverse transcription quantitative polymerase chain reaction study.’, *Developmental neuroscience*, 27(6), pp. 408–418. doi:10.1159/000088455.
- Valente, M.M., Allen, M., Bortolotto, V., Lim, S.T., Conant, K. and Grilli, M. (2015) ‘The MMP-

- 1/PAR-1 Axis Enhances Proliferation and Neuronal Differentiation of Adult Hippocampal Neural Progenitor Cells.’, *Neural plasticity*, 2015, p. 646595. doi:10.1155/2015/646595.
- Varbanov, H. and Dityatev, A. (2016) ‘Regulation of extrasynaptic signaling by polysialylated NCAM: Impact for synaptic plasticity and cognitive functions’, *Molecular and cellular neurosciences*, 81. doi:10.1016/j.mcn.2016.11.005.
- Volk, D.W., Pierri, J.N., Fritschy, J.-M., Auh, S., Sampson, A.R. and Lewis, D.A. (2002) ‘Reciprocal alterations in pre- and postsynaptic inhibitory markers at chandelier cell inputs to pyramidal neurons in schizophrenia.’, *Cerebral cortex (New York, N.Y. : 1991)*, 12(10), pp. 1063–1070. doi:10.1093/cercor/12.10.1063.
- Wiera, G., Nowak, D., van Hove, I., Dziegiel, P., Moons, L. and Mozrzymas, J.W. (2017) ‘Mechanisms of NMDA Receptor- and Voltage-Gated L-Type Calcium Channel-Dependent Hippocampal LTP Critically Rely on Proteolysis That Is Mediated by Distinct Metalloproteinases’, *The Journal of neuroscience: the official journal of the Society for Neuroscience*. 2017/01/09, 37(5), pp. 1240–1256. doi:10.1523/JNEUROSCI.2170-16.2016.
- Windrem, M.S., Osipovitch, M., Liu, Z., Bates, J., Chandler-Militello, D., Zou, L., Munir, J., Schanz, S., McCoy, K., Miller, R.H., Wang, S., Nedergaard, M., Findling, R.L., Tesar, P.J. and Goldman, S.A. (2017) ‘Human iPSC Glial Mouse Chimeras Reveal Glial Contributions to Schizophrenia.’, *Cell stem cell*, 21(2), pp. 195-208.e6. doi:10.1016/j.stem.2017.06.012.
- Wójtowicz, T. and Mozrzymas, J.W. (2014) ‘Matrix metalloprotease activity shapes the magnitude of EPSPs and spike plasticity within the hippocampal CA3 network.’, *Hippocampus*, 24(2), pp. 135–153. doi:10.1002/hipo.22205.
- Woo, T.U., Miller, J.L. and Lewis, D.A. (1997) ‘Schizophrenia and the parvalbumin-containing class of cortical local circuit neurons.’, *The American journal of psychiatry*, 154(7), pp. 1013–1015. doi:10.1176/ajp.154.7.1013.
- Woolley, D.W. and Shaw, E. (1954) ‘A BIOCHEMICAL AND PHARMACOLOGICAL SUGGESTION ABOUT CERTAIN MENTAL DISORDERS’, *Proceedings of the National Academy of Sciences of the United States of America*, 40(4), pp. 228–231. doi:10.1073/pnas.40.4.228.
- Yamaguchi, Y. (2000) ‘Lecticans: organizers of the brain extracellular matrix’, *Cell Mol Life Sci*. 2000/04/15, 57(2), pp. 276–289.
- Yang, N., Williams, J., Pekovic-Vaughan, V., Wang, P., Olabi, S., McConnell, J., Gossan, N., Hughes, A., Cheung, J., Streuli, C.H. and Meng, Q.J. (2017) ‘Cellular mechano-environment regulates the mammary circadian clock’, *Nature Communications* [Preprint]. doi:10.1038/ncomms14287.
- Ye, Q. and Miao, Q.-L. (2013) ‘Experience-dependent development of perineuronal nets and chondroitin sulfate proteoglycan receptors in mouse visual cortex.’, *Matrix biology: journal of the International Society for Matrix Biology*, 32(6), pp. 352–363. doi:10.1016/j.matbio.2013.04.001.
- Zhang, J.W., Deb, S. and Gottschall, P.E. (1998) ‘Regional and differential expression of gelatinases in rat brain after systemic kainic acid or bicuculline administration.’, *The European journal of neuroscience*, 10(11), pp. 3358–3368. doi:10.1046/j.1460-9568.1998.00347.x.
- Zhang, Y., Winterbottom, J.K., Schachner, M., Lieberman, A.R. and Anderson, P.N. (1997) ‘Tenascin-C expression and axonal sprouting following injury to the spinal dorsal columns in the adult rat.’, *Journal of neuroscience research*, 49(4), pp. 433–450.
- Zhou, X.H., Brakebusch, C., Matthies, H., Oohashi, T., Hirsch, E., Moser, M., Krug, M.,

-
- Seidenbecher, C.I., Boeckers, T.M., Rauch, U., Buettner, R., Gundelfinger, E.D. and Fässler, R. (2001) 'Neurocan is dispensable for brain development.', *Molecular and cellular biology*, 21(17), pp. 5970–5978. doi:10.1128/mcb.21.17.5970-5978.2001.
- Zhou, Y.-D., Lee, S., Jin, Z., Wright, M., Smith, S.E.P. and Anderson, M.P. (2009) 'Arrested maturation of excitatory synapses in autosomal dominant lateral temporal lobe epilepsy.', *Nature medicine*, 15(10), pp. 1208–1214. doi:10.1038/nm.2019.
- Zimmermann, D.R. and Dours-Zimmermann, M.T. (2008) 'Extracellular matrix of the central nervous system: from neglect to challenge', *Histochemistry and Cell Biology*, 130(4), pp. 635–653. doi:10.1007/s00418-008-0485-9.
- Zolkowska, K., Cantor-Graae, E. and McNeil, T.F. (2001) 'Increased rates of psychosis among immigrants to Sweden: is migration a risk factor for psychosis?', *Psychological medicine*, 31(4), pp. 669–678.

Declaration of Honour

“I hereby declare that I prepared this thesis without the impermissible help of third parties and that none other than the aids indicated have been used; all sources of information are clearly marked, including my own publications.

In particular, I have not consciously:

- fabricated data or rejected undesirable results,
- misused statistical methods with the aim of drawing other conclusions than those warranted by the available data,
- plagiarized external data or publications,
- presented the results of other researchers in a distorted way.

I am aware that violations of copyright may lead to injunction and damage claims by the author and also to prosecution by law enforcement authorities.

I hereby agree that the thesis may be electronically reviewed with the aim of identifying plagiarism.

This work has not been submitted as a doctoral thesis in the same or a similar form in Germany, nor in any other country. It has not yet been published as a whole.”

Braunschweig, 16.11.2021

Gabriela Matuszko